Evaluating soil and landscape models to predict liquefaction susceptibility in the Hinuera Formation, Hamilton Basin

A thesis
submitted in partial fulfilment
of the requirements for the degree
of
Master of Science in Earth Sciences
at
The University of Waikato

by

Aleesha McKay

THE UNIVERSITY OF
WAIKATO
Te Whare Wānanga o Waikato

University of Waikato
2017

Abstract

The Hinuera Formation, being an extensive alluvial deposit throughout the Hamilton Basin plains, has been identified by Kleyburg (2015) as being susceptible to liquefaction. As much of the infrastructure of the Hamilton Basin is based on the Hinuera Formation, liquefaction thus poses a risk to the population of the area. This research project aims to develop a susceptibility model for liquefaction within the Hinuera Formation.

Cone Penetration Test (CPT) data collected during investigation for the Hamilton Section of the Waikato Expressway were acquired from the NZ Geotechnical Database. CLiq™ software was used to analyse these data and determine the liquefaction potential index (LPI) of each CPT site. Soil map information (S-Map) was provided by Waikato Regional Council with the permission of Landcare Research, and Digital Elevation Data (DEM) by Waikato Regional Council. Parameters of slope, elevation, soil family and sibling number as well as the LPI derived from CLiq™ were input into STATISTICA™ and analysed using I-Tree analysis to determine the most influential factor to liquefaction. ArcGIS was then implemented to create landscape/soil models based on CLiq™ data as well as calculations identified by statistical analysis.

The Hinuera Formation was found to have an overall susceptibility to liquefaction, ranging from low to high LPI dependant on depth. At a depth of 10 m, liquefaction potential on average was high, when compared to 3 and 5 m depths that showed a low to moderate LPI. At 3 m depth, which is most likely to show surface manifestation, liquefaction potential was low to moderate with the majority being considered as having a low LPI.

Soil textures ranged from coarse sand, to silt, to clay with few organics. When LPI was related to soil behaviour index (Ic) soil that had a 'mixed' texture of silty sand/sandy silt were most susceptible to liquefaction (~1.8-2.4 Ic). Much of the calculated liquefaction occurrence within CLiq^{TM} directly correlated to these sand/silt soil textures. Soil that was nearer to granular (coarse sand) or clay–like in behaviour were shown to likely inhibit liquefaction occurrence.

Soil family, a pedological map (and taxonomic) class, was shown to provide a good initial indication of the physical conditions of the underlying liquefiable soil, and therefore in turn liquefaction potential of land on the plains within the Hamilton Basin. A correlation between soil family and topography was identified using statistical analysis showing Utuhina*f* and Kaipaki*f* as most susceptible. Both Utuhina*f* and Kaipaki*f* soil families are of an organic texture (associated with peat formation). This observation led to the conclusion that areas of peat formation are likely correlated to the underlying soils having a relatively high susceptibility to liquefaction. This correlation is based on the knowledge that for peat formation to occur the land must have little relief (flat to a slight depression) and a high water table, both of which are prerequisites for liquefaction.

Elevation was also shown as a good initial indicator of liquefaction potential where a range between 38–39 m showed the highest liquefaction potential. When compared to a digital elevation model (DEM) it was found that liquefaction potential was higher within interfluve and floodplain zones and lower in topography with a greater relief such as within the many paleo channels or low ridges of the Hamilton Basin. This is likely a result of the soil textures being finer with a higher silt component within the interfluve and floodplains due to the low energy depositional environment that is associated with these topographic features.

Based on the observations of soil family and topography being correlated to liquefaction susceptibility, two liquefaction susceptibility maps were developed to provide a preliminary assessment map

Acknowledgments

First of all I cannot thank my amazing supervisor Dr Vicki Moon enough for her support throughout this journey. Vicki not only pushed me beyond my limits, she was also there to always re-assure me when I doubted myself, which has always been greatly appreciated and often very much needed. Secondly I must express my gratitude to my secondary and equally as valuable supervisor Professor David Lowe, who is an absolute wealth of never ending knowledge and enthusiasm. A big thank you must also be made out to Cheryl Ward for all of her help with formatting.

I would like to say a huge thank you to Waikato Regional Council for the financial assistance I received which was greatly appreciated. I would also like to recognise and thank Landcare Research, AECOM and the Hamilton City Council for providing much needed data including soil maps, LIDAR imagery and of course the CPT data that made all of this possible. A thank you must also go out to the University of Waikato itself, for support in the form of a research scholarship, these extra funds were very much appreciated.

Thank you to those people in my life who were not related to the actual development of this thesis as without my friends and family this would not have been possible. Chaman Singh, a special shout out must go to you for always being there, whether it be to listen to my relentless stressing or just to make me laugh, you are one in a million. To Kelli Patterson, my time at university has been made by meeting you, and your support during the final few months of thesis was irreplaceable.

Yu-Shen, thank you for listening patiently to my never ending thesis rants. You are amazing and I am very lucky to have you.

Steve you are always someone I can go to and feel instantly lighter, thank you for always being there when I needed to laugh and forget my worries even if just for a moment. To my mum, you have always been my number one fan and my go to for everything and anything and during my thesis was no exception. Finally, an extra thank you to my mum and Steve for always believing in me even when did not believe in myself, without you two, I would not be where I am today.

Table of Contents

List of Figures

List of Tables

Chapter One

Introduction

1.1 Background and introduction to the problem

The Christchurch Earthquake in 2011 being a recorded Mw 6.3 (moment magnitude) was a pivotal moment for seismic research in relation to the potential risk that liquefaction events pose to infrastructure and human life (Ballegooy et al., 2015). It highlighted the extensive damage that can result in areas susceptible to liquefaction and gave rise to new evidence of the re-liquefaction phenomenon (Lees et al., 2015). Liquefaction is the process by which an increase in pore water pressure occurs from seismic stressors, resulting in the loss of shear strength and resultant fluid like behaviour of the affected soil (Obermeier, 2009). Liquefaction occurs in loosely–packed cohesionless soils, typically with a Plasticity Index (PI) below 5.5, with grain sizes predominantly of coarse silt to medium to fine sand (Robertson & Wride, 1998; Owen & Moretti, 2011; Eslami et al., 2014; Sağlam, 2015). These conditions generally occur on near to/horizontal ground where the susceptible soils lie below the water table (saturated soils). Upon significant seismic stresses (Mw >5.5) pore water pressures will build up and soils will move from a solid state to behave as a viscous fluid (Obermeier, 2009). Features deemed 'seismites' or paleo liquefaction features are the result of liquefied sediment (coarse silt to medium to fine sand) that has disrupted the original soil structure. Common seismites include dikes and sills (also known as fluidization features), sand boils (sand volcanoes) and sand craters from excessive sand and water expulsion (Bizhu & Xiufu, 2015). Ground displacement in the form of lateral spread is also a common problem and can be relatively large in scale (Obermeier, 2009). Soils of Holocene (<11,700 years old) to some cases late Pleistocene age are most susceptible to liquefaction if the conditions mentioned above are met, as weathering will typically increase the soil's resistance, to liquefaction as soils age.

1.2 **Current research**

Within the Hamilton Basin, which is the selected field area for this research (Figure 1.1), the Hinuera Formation is an extensive Late Pleistocene low angled fan deposit ≤ 90 m thick and covering ~2000 km^2 of the Hamilton Basin's alluvial plains (McCraw, 1967; Kamp & Lowe, 1981). The Hinuera Formation, an alluvially derived sedimentary deposit, consists predominantly of sandy gravels to gravelly sands and silty sands to sandy silts, with many interbedded clay horizons as well as peat that has developed locally. Characteristic features within the Hinuera Formation are its volcanogenic composition, being predominantly rhyolitic or pumiceous, as well as its extreme variability in stratigraphy including the tell-tale feature of cross bedding (Hume et al., 1975). Much of this stratigraphic variation within the Hinuera Formation can be attributed to the flow dynamics of paleo-river systems (Chapter Three).

Early research by Sherwood (1972) indicated that the Hamilton Basin, and in particular the Hinuera Formation, did have post depositional structures that were likely the result of liquefaction induced by a seismic event. Although liquefaction structures were scarce and when found were proximal to one another, Sherwood (1972) did observe that when liquefaction occurred it seemed restricted to individual horizons, leading to questions for further research. Due to the characteristics of the Hinuera Formation alongside a high water table and the earlier findings of Sherwood (1972), Hume et al (1975) undertook detailed analysis of the formation to determine whether liquefaction had occurred historically. Deformation structures of corregated laminations, injection and flame structures were all identified within the Hamilton Basin and were deemed as induced by seismic and therefore liquefaction processes. This led to the idea that liquefaction is a risk within the Hamilton Basin if a seismic event were to occur.

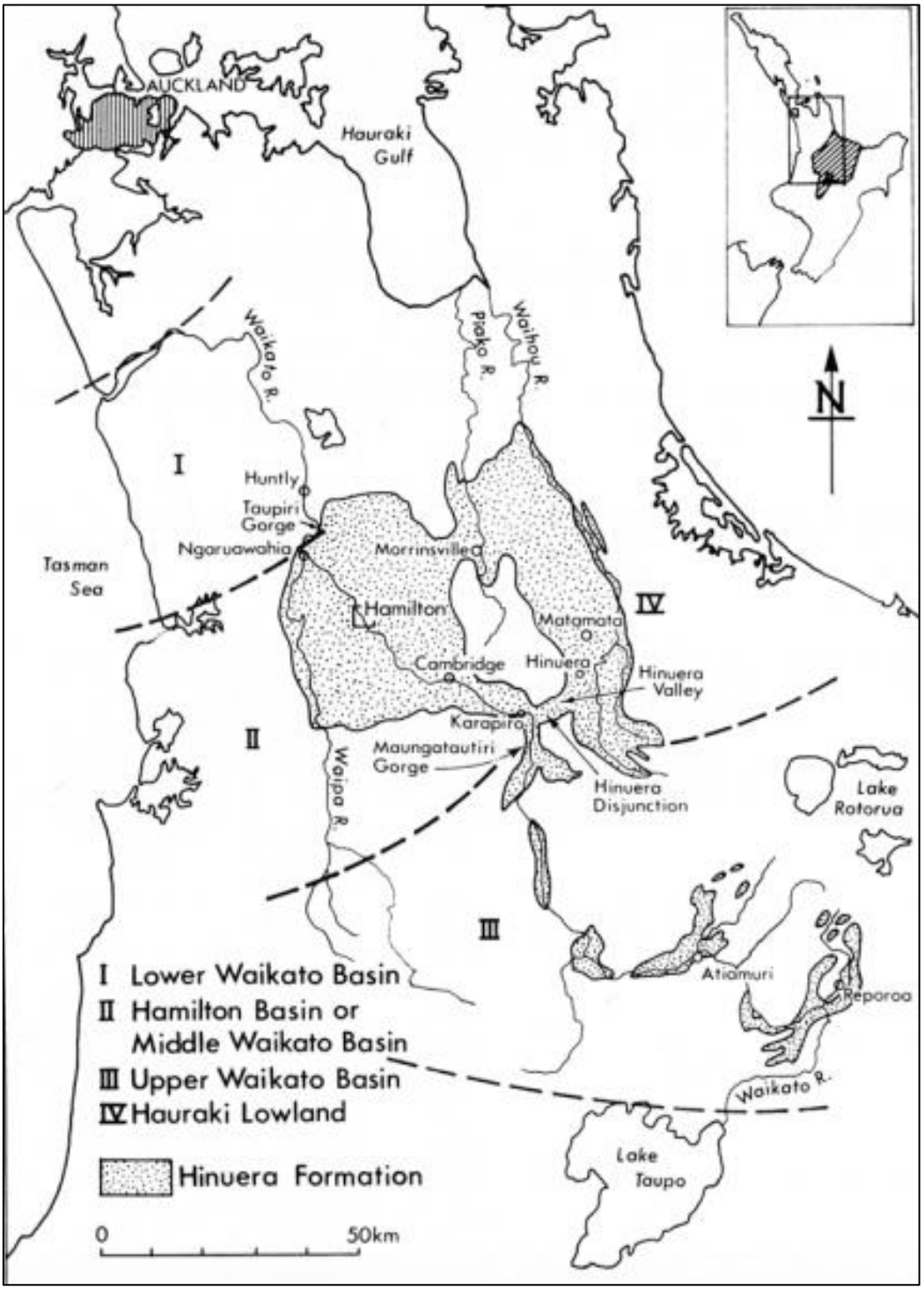

Figure 1.1 Aerial depiction of the extent of the Hinuera Formation as well as the basins and lowlands within the upper North Island including the Hamilton Basin and Hauraki Lowlands in which the Hinuera Formation resides (Hume et al., 1975).

The Hamilton Basin has since been suggested by Kleyburg (2015) as having a potential for liquefaction occurrence due to her identification of multiple paleoliquefaction features within the Hinuera Formation, together with Cone Penetration Testing (CPT) data, indicating a high susceptibility in previously liquefied layers. In addition, more recent research by Moon & de Lange (2017) suggests the presence of multiple, potentially active fault traces within the Hamilton Basin, giving local sources of seismic energy to produce liquefaction.

Therefore, future liquefaction might be expected in the Hamilton Basin due to the existence of local seismic sources and existing paleo liquefaction structures. The Hinuera Formation has also been recognised as being potentially liquefiable due to its composition which will be discussed later in Chapter Three.

Based on comparatively simple observations of soil conditions at sites where paleo liquefaction had been identified, Kleyburg (2015) developed a preliminary soil and landscape model. In this model she used published maps of pedological soils overlain on topography to infer from the sites of known liquefaction, where other areas potentially susceptible to liquefaction were likely to be. This inference relied on the assumption that a pedological soil type and its position within the landscape would reflect the underlying material and the underlying water table conditions. With these two factors being essential in determining a soil bodies likely susceptibility to liquefaction. It is noted by Kleyburg however, that the model described was a preliminary one, based on limited observational data with little use of quantitative methods of assessment.

The research within this thesis expands on the soil and landscape model developed by Kleyburg (2015). The addition of quantitative CPT data allows statistical analysis, focusing on the link between mapped pedological soil units and underlying liquefaction susceptibility to be explored. The availability of a comparatively large data set of CPT drill sites (extending 21.8 km) due to the development of the Waikato Expressway, Hamilton Section (Figure 1.2), enabled the establishment of a field area within the Hamilton Basin. Being the basis for which a robust statistical model can be developed, from which a hazard assessment can be inferred to a point between Ngaruawahia and Horotiu and to just south of Tamahere (length wise).

This map provides a means of preliminary assessment with the hope that further research will extend out to eventually cover the entire Hamilton Basin based on methods used within this research.

Figure 1.2 Areal depiction of the Waikato Expressway, with the orange line indicating the field area of this research being the Hamilton Section of the expressway (Opus International Consultants Limited, 2014).

1.3 **Aims and objectives**

This study aims to determine the relative susceptibility of the soils within the Hamilton Basin to liquefaction within a soil/landscape framework, in order to identify areas of high susceptibility to liquefaction. This research project will utilize CPT data obtained along the Waikato Expressway, specifically the Hamilton Section, prior to the highway's construction.

Key objectives include:

1. Collation of pre-existing geotechnical data including raw CPT data for initial pilot study of the Waikato Expressway, Hamilton Section.

2. The use of CLiq™ software to determine whether or not the soils along the Waikato Expressway, Hamilton Section, are susceptible to liquefaction.

3. To utilize ArcMap GIS by importing LIDAR and soil map data in order to visually depict the field area and obtain parameters of slope and elevation for quantitative analysis.

4. To establish a quantitative analysis within STATISTICA™ and attempt to correlate liquefaction potential to other known factors of influence such as soil type, elevation, slope and soil sibling texture.

5. To refine previously developed soil and landscape models based on these data.

6. To use the derived soil/landscape liquefaction model for the Hamilton Basin to produce a hazard map that visually depicts areas that are of higher susceptibility to significant liquefaction events which require additional management to prevent damage if an earthquake were to occur.

Chapter Two

Literature review

2.1 **Introduction**

Liquefaction is the process in which an increase in pore water pressure occurs from seismic stressors, resulting in the loss of shear strength and resultant fluid like behaviour of the affected soil (Obermeier, 2009). The ideal conditions for such an event include relatively recent (Holocene to late Pleistocene) sediments that are cohesionless, coarse silt to medium to fine sand, loosely packed, with a shallow water table (Robertson & Wride, 1998; Owen & Moretti, 2011; Eslami et al., 2014). It is widely accepted that liquefaction occurs most commonly in earthquakes of a magnitude over Mw 5.5. This is an important factor when dealing with a site that has apparent liquefaction, as it is an indication of the relative susceptibility. Associated. features of paleoliquefaction have been established as a good indication of the lower limit of magnitude as well as the potential for another seismic event (Moretti & Sabato, 2007).

This literature review will initially outline the phenomenon of liquefaction defining monotonic and cyclic liquefaction. The conditions for cyclic liquefaction to occur will then be described followed by the main methods to determine that the trigger was of seismic origin. Focus will then turn to paleoliquefaction features, and how they can be identified within the field. A brief description of the Hinuera Formation will then be given as this is where paleoliquefaction features were discovered and what determined the need for further susceptibility assessment. Lastly, the steps in determining a soil's susceptibility to liquefaction will be outlined with the method of Cone Penetration Testing (CPT) being discussed.

2.2 **Soil liquefaction**

Liquefaction and subsequent ground failure of Holocene coarse silt to fine- medium grained sandy soil is a common consequence of earthquake events that are typically over Mw 5.5 (Moretti & Sabato, 2007). During the process of liquefaction, a soil that is saturated and largely cohesionless, when put under sufficient stress, will experience temporary increased pore water pressure and consequential loss of shear resistance (Rauch, 1997). Total loss of shear strength occurs when drainage of the soil is restricted, typically when an overlying impermeable layer (clay cap) is present, leading to significant pore water stresses exerted on the soil body (Obermeier, 1996). As a result of these increased pore water pressures, the overburden stress will move from being grain supported to pore water supported. This increase in pore water pressure is typically attributed to the tendency for granular soils to compact when cyclic stress is applied (Youd et al., 2001). Liquefied soil will then become suspended and typically moves toward an open face such as a river bank (Obermeier, 1996). The phenomenon of liquefaction can be determined as flow liquefaction or cyclic liquefaction (Rauch, 1997; Sağlam, 2015).

2.3 **Flow (strain softening) liquefaction**

Flow liquefaction is a process that occurs when a soil that has an initial void ratio higher than its ultimate line defined as the point at which shear resistance and volume remain constant with continued strain resulting in strain softening. Flow liquefaction often causes large strains before the soil reaches a ‘critical state’ (Robertson & Wride, 1998). Strain softening is a process where soils will experience a decrease in shear stresses upon continuous loading when a specific yield point is exceeded, where soils will typically behave as a viscous fluid (Sağlam, 2015). Flow liquefaction can be a product of both monotonic and cyclic triggers where an undrained soil under saturated conditions will flow as a result of increased static shear stresses that exceed the soil’s resistance strength. Monotonic loading results in tensile or compressional stressors where soil particles will initially condense and then dilate as grains move over one another from continued loading resulting in a complete loss of shear strength. This dilation will then increase if drainage is impeded where pore water pressure will begin to exert a relative force (Rauch, 1997). Holocene, cohesionless sands, silts and very sensitive clays are most

susceptible to flow liquefaction where movement of material occurs by either sliding or flow movement usually being a product of soil type and ground morphology (Youd & Perkins, 1978; Sağlam, 2015). Monotonic stressors typically exhibit linear type progressive stressors such as changes in slope geometry (sediment deposition on slope crests or slope toe removal) as well as drainage causing degradation of soil quality (Rauch, 1997). Flow liquefaction events are generally not common although careful planning is required when considering soils that may be susceptible because, when flow liquefaction does occur, it can be sudden and cause significant damage to infrastructure (Robertson & Wride, 1998).

2.4 **Cyclic liquefaction (loading)**

Cyclic loading is a product of multiple oscillations subjecting the soil to both tensile and cyclic stresses (Sağlam, 2015). Cyclic loading is a common example of shear stress increases due to seismic events where effective stresses reach zero or near to zero due to shear reversal (Rauch, 1997). The density of the susceptible soil and the duration and magnitude of the seismic trigger are important factors in determining the likely degree of deformation during cyclic loading (Robertson & Wride, 1998). The grains will typically reorient as a result of compaction and expulsion following cyclic pressures as before liquefaction occurs there is a relatively strong grain-to-grain contact. The soil structure is disrupted due to cyclic loading where pore water pressure increases and due to rapid and continuous loading means pore water cannot escape efficiently therefore leading to suspension of the liquefied material. If enough pressure is exerted fluidization processes can occur in the form of seismites (discussed in section 2.8). Liquefaction induced by cyclic loading provides the focus of this research.

2.5 Outline of conditions required for cyclic liquefaction associated with seismic events to occur

Owen et al (2011) stated that, in order for soft sediment deformation to occur, there must be three conditions present. A driving force for primary sediment deformation, a deformation mechanism, in this case being the process of liquefaction, and a trigger, most commonly being from a seismic origin in the form of shear stressors. When aiming to identify the trigger agent of these features it is important to determine that the defined soil conditions and relative parameters such as texture have also been met (Table 2.1). In relation to a seismic origin, emphasis must be placed on such features being widespread, with a regional distribution centred around an area of greater observable effects (Obermeier, 1996).

Table 2.1 Soil conditions that are likely to promote liquefaction occurrence (Owen & Moretti, 2011).

Factor	**Ideal conditions**
Grain size	Fine-medium sand
Packing/porosity	Loose/high
Saturation	Saturated/shallow water table
Permeability barriers	Present
Overburden pressure	Low

2.6 Trigger identification

Identification of the correct trigger that results in soft sediment deformation poses a significant challenge, as the features observed within the field typically display similar morphologies (Moretti, & Sabato, 2007). A range of triggers that can result in soft sediment deformation are of non-seismic origin, including ground water intrusion, ocean waves and excessive overload of sediments (Owen & Moretti, 2011). Establishment of the correct trigger is therefore important for the purpose of paleoliquefaction identification as it can indicate previously unknown tectonism within a region and act as a guide for earthquake reoccurrence for probability

purposes (Owen & Moretti, 2011). Cyclic liquefaction is most commonly induced by a seismic trigger, with resultant soft sediment deformation typically occurring from rapid dewatering after initial pore water build up and expulsion. Owen & Moretti (2011) stated that in order to determine the trigger agent, the deformation mechanism must first be identified as liquefaction. As mentioned in section 2.1, liquefaction is a product of increased pore water pressure which can result from either static liquefaction due to groundwater intrusion, cyclic liquefaction, being a series of seismic pulses, or impulsive liquefaction where loosely packed sediments are dislodged and deformed. The process that resulted in these different deformation types is therefore the trigger. There are two common methods of trigger identification, being a criteria and context based approach with the two used in conjunction being common practice (Owen & Moretti, 2011). A criteria-based approach looks at a range of features that most commonly present from an earthquake event, ones that reflect seismic intervention such as decreasing abundance from fault due to decreasing intensity of magnitude at increasing distance from rupture surface (Table 2.2). By summarizing the findings by Owen & Moretti (2011), large areal extent and complexity with distance from fault act as a viable basis for interpretation of trigger as the relative distance can represent the likely magnitude with higher intensities likely resulting in a greater distribution and greater complexity. This interpretation, although not absolute, provides a solid basis as soft sediment deformation structures that have likely developed from other triggers would typically be localised and not repeated over wide areas such as deformation induced by rapid sedimentation (Moretti & Sabato, 2007).

Table 2.2 Criteria based approach for recognition of seismically triggered soft sediment deformation structures (Owen & Moretti, 2011).

Criterion	Comment
Large areal extent	Not exclusive to seismic trigger
Lateral continuity	Not exclusive to seismic trigger
Vertical repetition	Not exclusive to seismic trigger
Morphology comparable with structures described from earthquakes	Not exclusive to seismic trigger
Proximity to active faults	Not exclusive to seismic trigger
Zonation of complexity or frequency with distance from fault	Good criterion

A context-based approach, in contrast, assesses all aspects of the paleo-environment and relative sedimentary successions, often being implemented to rule out non-seismic triggers (Owen, & Moretti, 2011). The primary focus of the context-based method is to determine whether the deformation was a result of depositional processes or the product of seismic stress (Owen & Moretti, 2011). There are several factors that can be looked at when dealing with a context-based approach generally focusing on what characteristics are present that are ideal for having a seismic influence. These factors are outlined in Table 2.3.

Table 2.3 Context based approach for identification of seismically induced features (Owen & Moretti, 2011).

Indicator	Explanation
Appropriate sediment characteristics	Liquefaction is optimal in saturated coarse silt to medium sand, however larger grain sizes could liquefy also
Ductile characteristics	The momentary change to liquid-like behaviour will exhibit ductile characteristics as opposed to brittle deformation, however material above the water table may experience brittle deformation forming lateral cracks
Increased deformation upwards	Liquefied state is prolonged in upper beds
Preserved stratification	Stratification will remain intact as displacement between grains are small during liquefaction
Morphology of deformed layer	Upper surface will be flat after liquefaction due to no shear strength in liquid state

A full facies analysis is the basis of a context-based method, being followed by detailed descriptions of the deformation structures focusing on depositional and erosional features. The stratigraphy prior to the deformation occurring is often reconstructed to determine the probability of a seismic trigger with emphasis on likely time period of emplacement. It is stated by Owen & Moretti (2011) that a more accurate method of interpretation may be required, but that when criteria and context-based analyses are used together a reliable conclusion can be derived.

2.7 **Susceptibility in relation to risk assessment**

The deposits of the Hinuera Formation within the Hamilton Basin have become of interest throughout the geo-engineering community due to recent discoveries of potential Quaternary faulting features as well as evidence of paleoliquefaction. Upon application of CPT methods, the Hinuera Formation which is a alluvially derived deposit consisting of sandy silt materials shows a higher degree of susceptibility than previously proposed by initial screening methods (Clayton & Johnson, 2013). Understanding the susceptibility of the Hinuera Formation is essential in order to determine an accurate risk assessment. The Christchurch Earthquake in 2011 was an important event for future liquefaction research as it gave evidence of the potential for sites that have liquefied in the past to display repeated liquefaction (Lees et al.,2015).

Risk criteria associated with liquefaction susceptibility began with the establishment of the Chinese criteria following data collected after large Chinese earthquake events (Sağlam, 2015). Since these early experiments there has been extensive research undertaken to determine accurate values of indices that are most influential in causing liquefaction events with Liquid Limit (LL), Plasticity Index (PI), and water content (W_C) being the most fundamental factors (Robertson & Wride, 1998; Donahue, 2007; De Magistris et al., 2014; Sağlam, 2015). It was also concluded by Sağlam (2015) that the ratio between excess pore water pressure (pressure caused during cyclic stresses) and the confining stress is an important component of susceptibility. R_u is used as a measure of pore water which can in turn infer how much liquefaction is likely to occur relative to the number of seismic cycles (N) and if the pressure may be significant enough to result in surface deformations, also being a function to distinguish between flow and cyclic liquefaction (Sağlam, 2015). Pore water pressure showed a noteworthy increase when the soils texture was below 5.5 PI, suggesting that this may be the upper threshold of plasticity for liquefaction to be a plausible event within the soil having these properties (both flow and cyclic liquefaction). In relation to strain of a higher degree, soil with a relatively high W_C/LL (>0.95) may be susceptible to cyclic mobility even with PI values <15 although they will not exceed 0.95 R_u so will not display a complete loss of shear strength (Sağlam, 2015). Age can also act as an indication of susceptibility with more recent soils of Holocene age (typically <11,700 years old) being most susceptible with late Pleistocene deposits having low

to moderate susceptibility (Heidari & Andrus, 2010; De Magistris et al., 2014). Finally, the report by Eurocode 8 (2004) stated that if the following equation was met and also one of the following conditions were met then that particular soil body will not liquefy.

$$\frac{a_g}{g} \cdot S < 0.15 \quad (1)$$

- Clay content >20 % and a PI >10;
- Silt content >35 % and an SPT blow count normalized for overburden stress and an energy ratio of $N_{1(60)}$ >20.
- Clean sand and an SPT blow count normalized for overburden stress and an energy ratio of $N_{1(60)}$ >30.

The equation can be explained as a_g being the ground acceleration, g being the acceleration of gravity and S being the soil factor. The equation thus gives a limit for ground acceleration at a particular area ≥ 0.15 g.

It was concluded by Eurocode 8 (2004) that a threshold of >0.1 g for surface ground acceleration is an appropriate limit for when liquefaction may occur if susceptible conditions are present.

2.8 **Paleoliquefaction features (seismites)**

The term ‘seismite’ has been used within the literature when referring to soft sediment deformation features that have been formed through strong seismic activity that exceeds Mw 5.5 (Bizhu & Xiufu, 2015). Seismites can occur in a range of tectonic and sedimentary environments and, according to Bizhu & Xiufu (2015), classification of such structures has not been well defined and agreed upon, with many terms referring to a single feature.

A commonly referred to seismite associated with earthquake-induced liquefaction is that of sand injections through areas of weakness in the strata in the form of clastic dikes and sills (Ettensohn et al., 2002). Dikes are most abundant, being vertical intrusions from upward injection of sediment rich pore water; sills, being horizontal intrusions are often observed alongside dikes in vertical outcrop. A semi-permeable cap, usually clay rich, overlying liquefied sediments is a common requirement for the formation of dikes and sills, with dikes often pinching at the tip in response to cap thickness or reduced flows. Sill development underneath the cap is common or when present beneath root mats where soil strength inhibits dike intrusion (Figure 2.1).

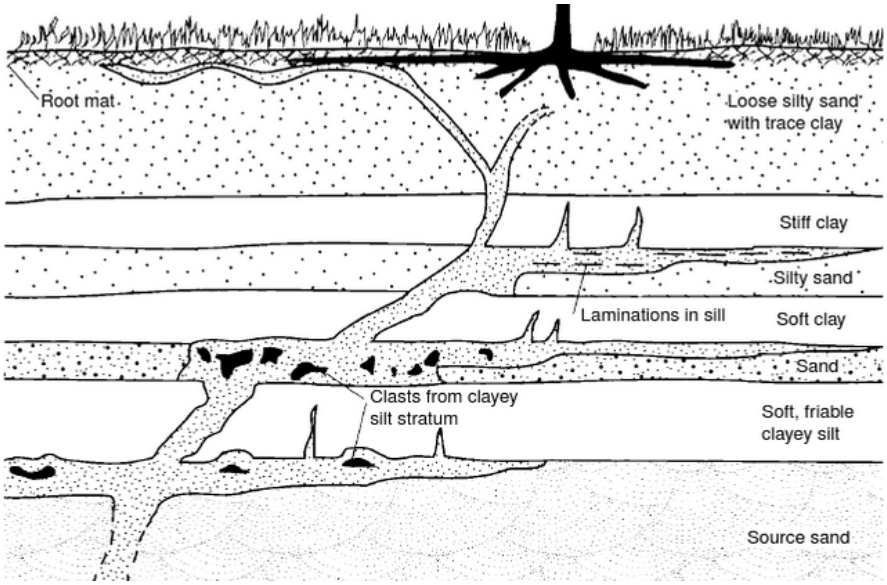

Figure 2.1 Schematic diagram of sill development and dike pinching (Obermeier, 2009).

Ettensohn et al (2002) states that ~1 m of liquefied sediment, typically consisting of clean sand, is sufficient to induce dike formation. Holocene alluvial-derived dikes readily intrude into overlying cap horizon (~1-5 m), where distance of intrusion is relative to strength of seismic events. Commonly described as tabular in shape, dikes can form in parallel or irregular arrangements, which are relatively narrow when formed through hydraulic fracturing (Obermeier, 2009). Dike formation can be explained as the combination of both grain reorientation during water expulsion and the influence of shearing or normal stresses acting upon the liquefied fluid (Jolly & Lonergan, 2002). The presence of angular clay aggregates is a clear indication of rapid short lived (~1 day) injection allowing inference that

such features may be seismically induced, alongside observations of intrusion within weathered or younger horizons. Coastal South Carolina is a good example of a location where dike formation within fluvial and back-barrier environments has occurred, with few sills observed. In contrast, an abundance of dikes and sills have been identified in drainage holes (3-4 m) in the New Madrid Seismic Zone (NMSZ).

The ejection of pore water to the surface, if sustained, often leads to the development of conical features most commonly referred to as sand blows/boils or volcanoes (Obermeier, 2009). Sand blows can vary in size, with the typical dome being ~8-15 feet in width and 3-6 inches high as described by Fuller (1912) in relation to the NMSZ. Earthquakes of high magnitude often result in their formation, with multiple large sand blow craters being observed within the Banni Plain as a result of the 2001, Mw 7.7 Bhuj Earthquake in western India (Maurya et al., 2006). Pore water was continuously ejected over three weeks following the quake, with sediment-rich water infilling the blow crater for ~1 year. Figure 2.2 shows typical dome morphology overlying a main feeder dike. Coarse silt to fine/medium sand forms the base of the dome, with angular clay aggregations (1-5 cm) only being observed in these lower limits and concentrated around the vent. Deposits grade into much thicker layers in upper limits with coarser to medium clean sand, lacking structure or with weak to moderate lamination. Caps containing clay and organic matter may also be present in depressions above the vent or at distance from the dome itself (Obermeier, 2009).

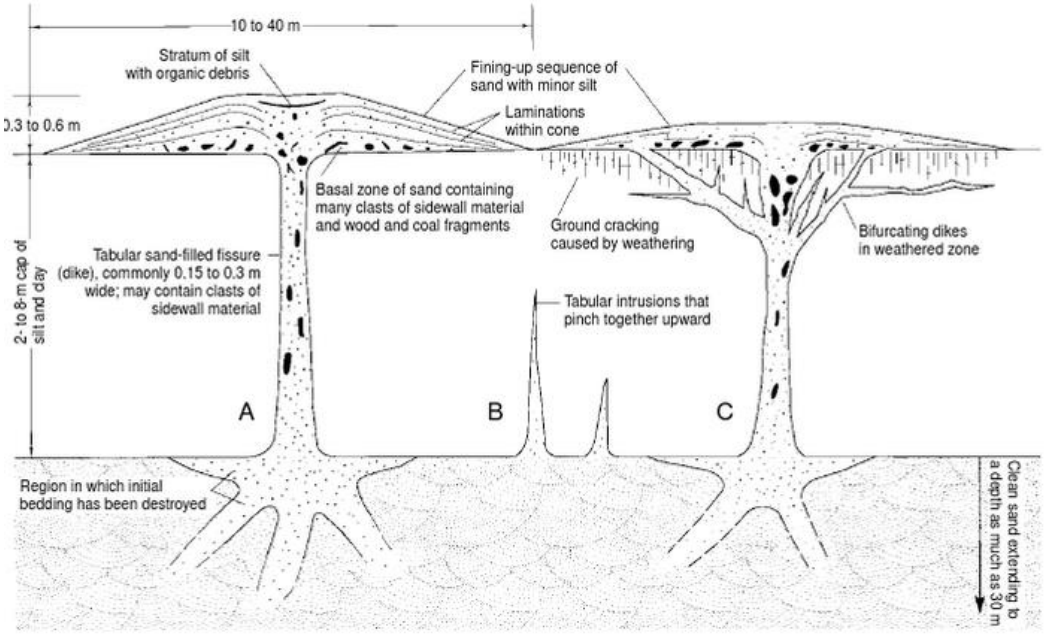

Figure 2.2 Typical sand blow morphology, resultant features from the 1886 Charleston quake, South Carolina (Obermeier, 2009).

Soil type is an important factor for paleo-liquefaction research, with many sand blows being eroded to crater type morphologies, where sediments have had a lower resistance. Such craters can be observed in South Carolina where the soil is thin, contains humus and has weak cementation. In contrast to this many domes can be observed in the NMSZ where soil contains clay with thicknesses from 2-10 m (Obermeier et al., 1990). Obermeier (2009) states that craters form from rapid expulsion of pore water, removing the overlying material. A resultant crater develops with graded infill of sediment with coarser sediments at the base (Figure 2.3).

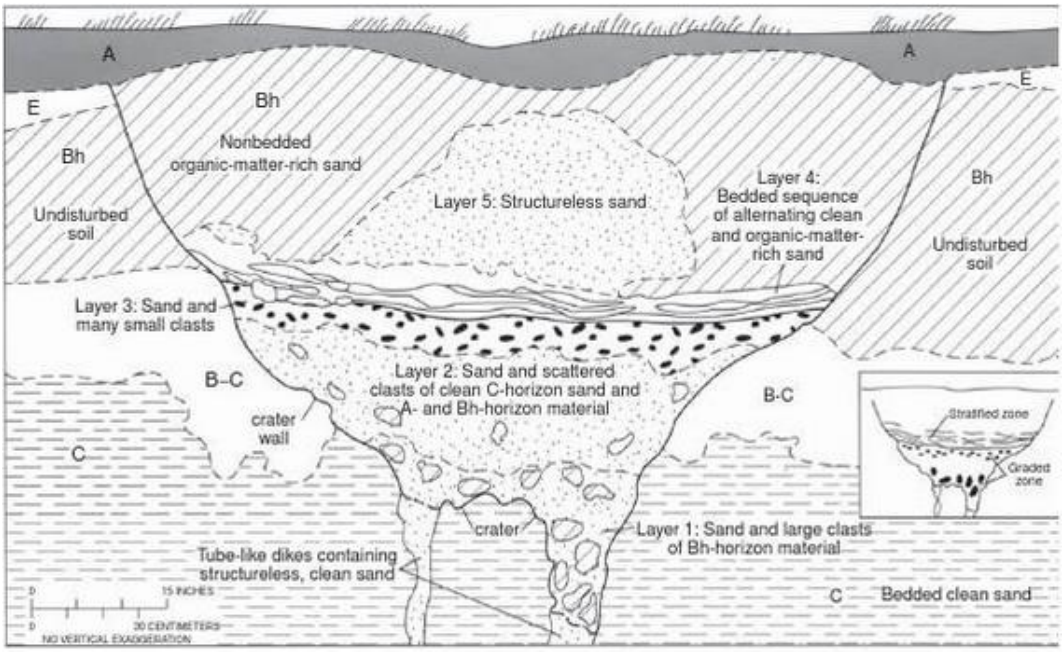

Figure 2.3 Schematic representation of a sediment filled crater in vertical section (Obermeier, 2009).

There are contrasting views within the literature on the formation of liquefaction-induced craters, ranging from erosion of sand blows (Obermeier et al., 1990) or from violent expulsions of land due to rapid ejection of sediment rich pore water (Obermeier, 2009). In contrast, Rydelek & Tuttle (2004) infer development of dry craters during the 2001 Bhuj earthquake to be through rapid ground subsidence during the late stages of liquefaction (Figure 2.4).

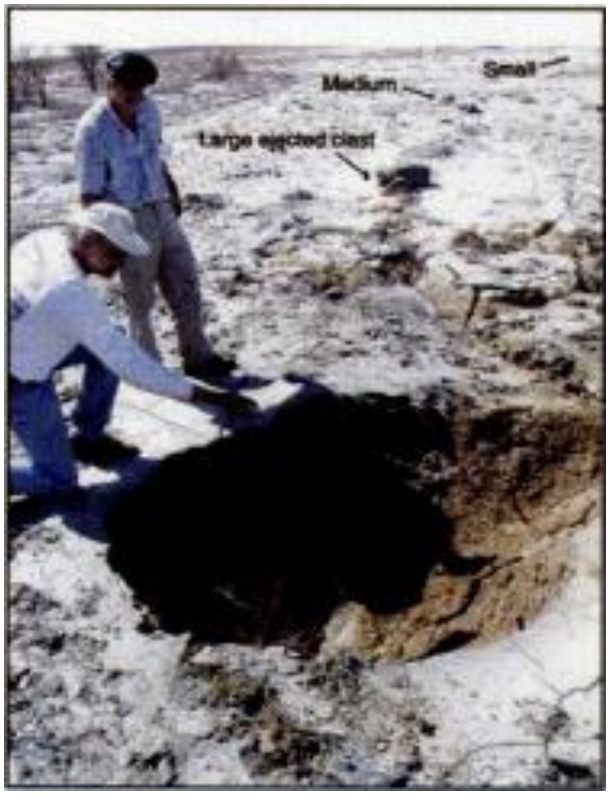

Figure 2.4 Image showing dry craters from the 2001 Bhuj quake, with ejected clasts in the background (Rydelek & Tuttle, 2004).

Seismites have been referred to as ‘chaotic’ in the literature, due to high diversity among features resulting from seismically induced liquefaction (Montenat, 2007). This range of features (Figure 2.5) includes ball and pillow structures, being defined as rounded masses overlying one another in outcrop; pseudo-nodules, being a single row of such features often having intruding flame structures that pinch at the top; and dish (horizontal and flat) and pillar features (vertical) (Berra & Felletti, 2011).

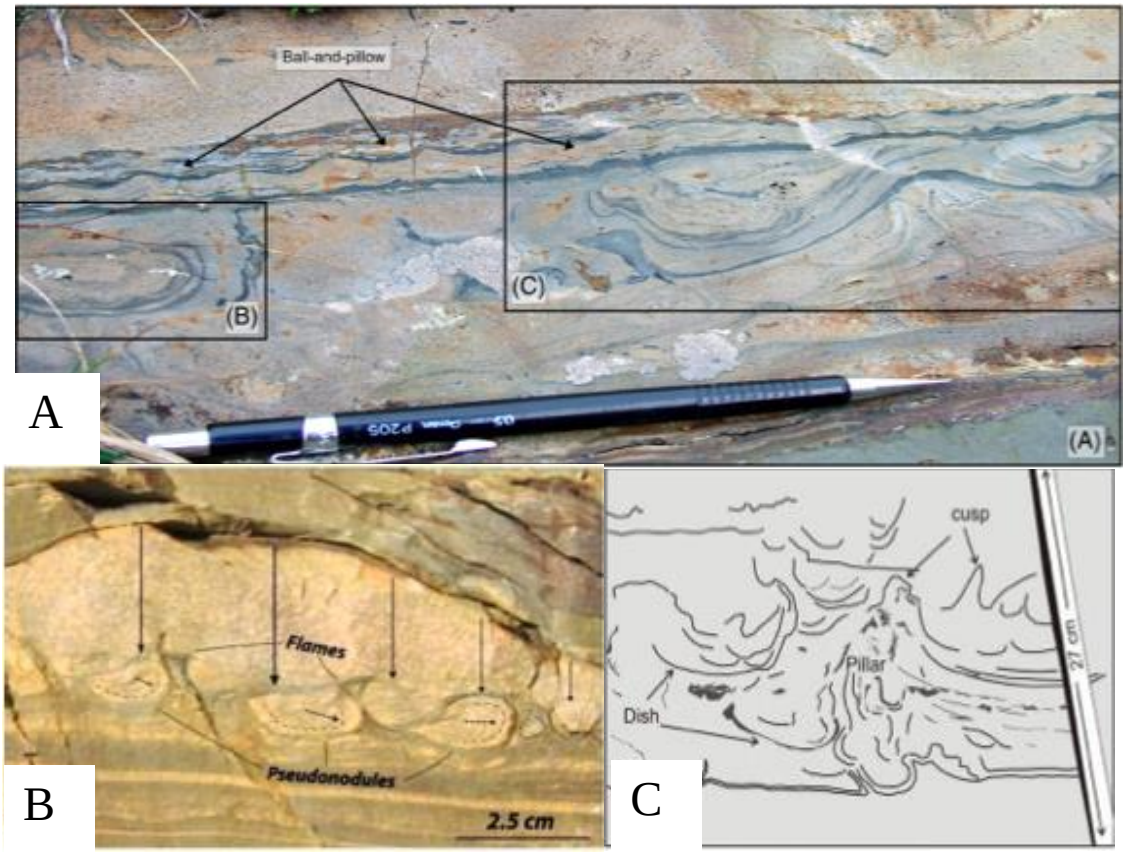

Figure 2.5 Seismite diversity within outcrop. A) Ball and pillow B) Flame structures and pseudo nodules and C) Dish and pillar structures (Berra & Felletti, 2011).

2.9 **Ground surface displacement**

Lateral spread develops from seismic liquefaction, where permanent displacement can occur at ground level (Figure 2.6), defined as the horizontal displacement of liquefied soil, most commonly toward an open face such as a riverbank or alluvium scarps (Obermeier, 2009). The increase in pore water pressure results in expansion of sandy sediment usually underlying a semi permeable cap, which impedes drainage (Seid-Karbasi & Byrne, 2007). Lateral spread can be seen in paleo-deposits by determining the degree of displacement or the width of feeder dikes (Obermeier, 2009). An example of displacement can be observed in Christchurch following the 2011 earthquake (Mw 6.2), being around 1-1.5 m along the river banks and 100-170 m inland (Haskell et al., 2013). Typical liquefaction-induced dikes are thin, being ~0.1-10 cm thick, whereas dikes resulting from lateral spreading are much wider (~0.5-0.7 m), due to horizontal cracking during failure giving a good indication that such a process may have occurred (Obermeier et al., 2005).

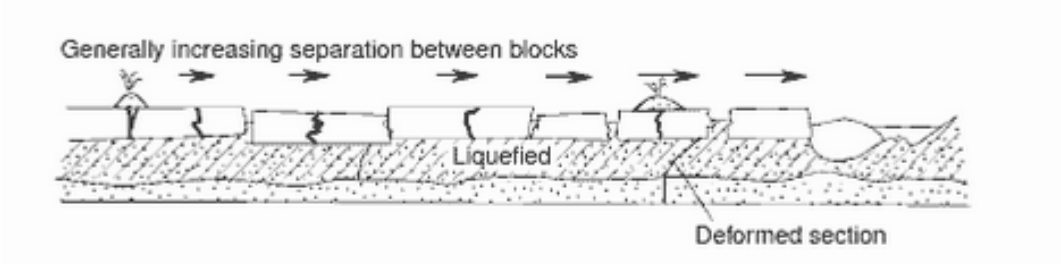

Figure 2.6 Vertical profile of showing resultant deformation due to lateral spread, where ground surface has been separated, bounded by dike intrusions (Obermeier, 2009).

2.10 **Liquefaction susceptibility evaluation**

The ability to accurately determine the susceptibility of soils to liquefy is an important step in establishing the risk factor associated with an area in relation to geotechnical practices (Lee et al., 2004). Shen et al (2016) propose that the most accurate and widely used methods for liquefaction evaluation are simplified in situ tests including the Standard Penetration Test (SPT), the Cone Penetration Test (CPT) and the shear wave velocity test (Vs) (Andrus & Stokoe II, 2000). These methods were developed from the initial establishment of 'simplified' method by Seed & Idriss (1971), using field observations as empirical evidence for susceptibility, which reduced the limitations that arose from laboratory methods. These particular tests are most common for geotechnical purposes as they are inexpensive and more simplified relative to dynamic testing. There are two primary variables that must be calculated or inferred when looking at liquefaction susceptibility of soils: (1) Cyclic Stress Ratio (CSR) being the degree of seismic energy influencing the soil body; and (2) the capability of that soil body to resist liquefaction deemed Cyclic Resistance Ratio (CRR) (Youd et al., 2001). Once CSR and CRR have been determined they are then expressed as a factor of safety (Fs), being CSR/CRR, with the soil being considered as liquefiable when $Fs \leq 1$ and non-liquefiable when > 1 (Youd et al., 2001). Robertson and Wride (1998) used the sleeve friction ratio (Rf) and soil behaviour type index (Ic) in order to calculate CRR directly from a CPT profile, but this method had a limited statistical component being largely dependent on empirical analysis (Shen et al., 2016).

A liquefaction probability (PL) has since been proposed, based on a logistic or linear regression model (Youd et al., 2001; Lee et al., 2004; Lai et al., 2006; Shen et al., 2016). The probability of liquefaction to occur is expressed by Lai et al (2006) as being based on factors that will influence and ultimately result in a liquefaction event when present. The logistic model is based on a binary regression analysis that compared data set from seismic events that resulted in liquefaction and those that did not with PL being expressed as

$$\mathbf{P_L(X)} = \frac{1}{1+\exp[-(\beta_o+\beta_1 x_1+\ \ldots \beta_n x_n)]} = \frac{1}{1+\exp\left[-\left(\beta_0+\sum_{i=1}^{n}\beta_i x_i\right)\right]} \quad (2)$$

PL (X) being the probability of liquefaction with all explanatory factor being assumed as independent of one another and linearly independent from estimated outcome as well as being normally distributed when applied to CPT data.

2.11 **Cone penetration test (CPT)**

The Cone Penetration Test (CPT) will be the focus of this research work as it is a widely used method for determining the susceptibility of soil to liquefaction as well as having the advantage of providing a more continuous soil profile. CPT methods are more reliable in outcome when compared to standard penetration testing methods (SPT), with more frequent detection of even the thinnest layers that may liquefy (Rauch, 1997; Juang et al., 2002; Shen et al., 2016). The CPT method involves the penetration of a cylindrical steel cone into the soil at 22 mm/s while determining the soils resistivity to the constant rate of penetration (Mayne et al., 2001). A typical penetrometer has a tip of 60º and a diameter of 35.7 mm being ideal for soft sediment analysis (Figure 2.7). A piezometer may also provide a valuable addition to basic CPT data such as CPTu which acts to measure the change in pore water pressure (Δu) during penetration as well as the duration of peak pressure and drainage period (Mayne et al., 2001). Among the methods that employ CPT for liquefaction susceptibility, Olsen (1997), Robertson and Wride (1998) and Juang et al (2000) are typically used, with Juang et al (2002) proposing that CPT

should be used in conjunction with SPT in order to obtain soil types and comparable resistance measurements. It was found, however, by Shen et al (2016) that both the Robertson & Wride (1998) & Olsen (1997) methods when applied to soils that had a known high cone tip resistance (qc), underestimated the degree of liquefaction. All three methods output different factors of safety so therefore not being a standardized method of evaluation.

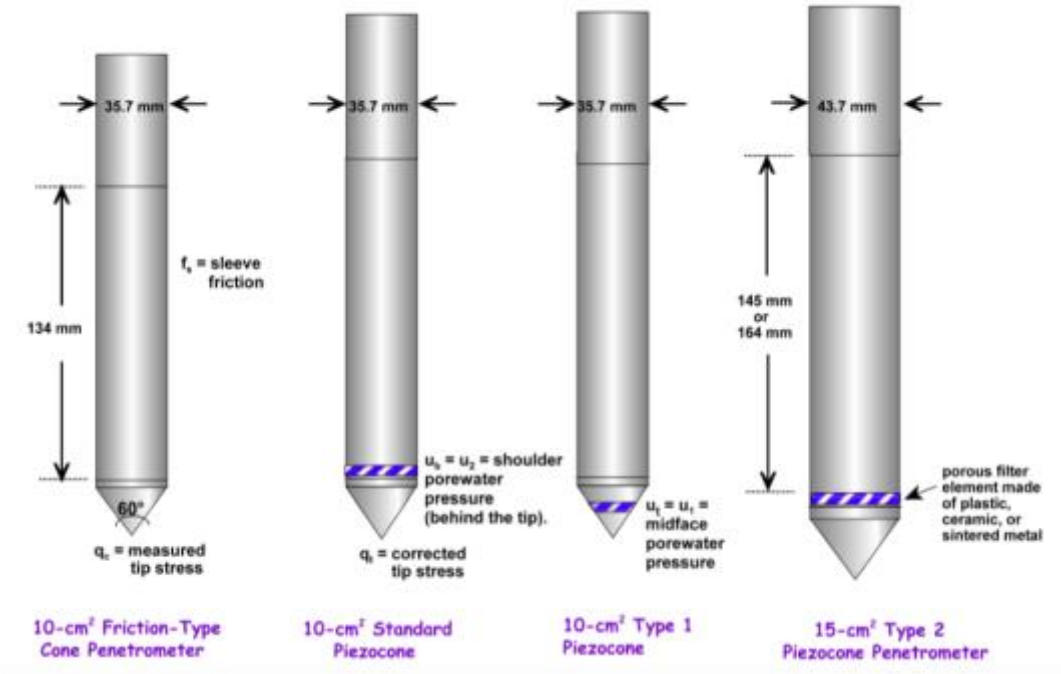

Figure 2.7 **S**chematic drawing of a typical cone penetrometer used for CPT testing (Mayne et al., 2001).

2.12 **Cyclic shear ratio (CSR)**

For a CPT method, CSR can be expressed as:

$$CSR = \left(\frac{\tau_{av}}{\sigma'_{vo}}\right) = 0.65\left(\frac{a_{max}}{g}\right)\left(\frac{\sigma_v}{\sigma'_v}\right)r_d \quad (3)$$

τ_{av} = average cyclic shear stress
σ_v = total vertical stress
σ'_v = effective vertical stress
a_{max} = peak horizontal acceleration
g = acceleration due to gravity (9.81 ms^{-1})
r_d = stress reduction coefficient (dependent on depth)

In order to determine the CSR, the peak ground acceleration must be evaluated (Shen et al., 2016) as CSR is first and foremost a product of seismic energy, being expressed as (amax/g). Overburden normal stress (σv/σ'v) is another integral component of the CSR equation, assuming that the soil body acts as a single rigid entity, therefore to accommodate the variation that occurs within a single soil profile the stress reduction coefficient (rd) is used (Shen et al., 2016).

2.13 **Cyclic resistance ratio (CRR)**

CRR is generally determined using 15 cycles of continued loading to represent a magnitude earthquake of Mw 7.5 determined from the cone tip resistance (qc) (Shen et al., 2016), with PI being of high influence to whether a soil will display a high or low CRR dependent on the amount of cohesive material (clay) within the fines of the predominantly sandy soil profile (Robertson & Wride, 1998). CRR can be expressed as:

$$(q_{c1N})_{cs} < 50 \quad \mathrm{CRR}_{7.5} = 0.833[(q_{c1N})_{cs}/1{,}000] + 0.05 \tag{4}$$

(OR)

$$50 \leq (q_{c1N})_{cs} < 160 \quad \mathrm{CRR}_{7.5} = 93[(q_{c1N})_{cs}/1{,}000]^3 + 0.08 \tag{5}$$

to indicate whether or not the soil has the potential to liquefy (< 50 qc1N)cs or whether it is unlikely to liquefy (> 50 qc1N)cs in clean sand conditions (Youd et al., 2001). A simple method to determine the CRR value in a computable form was defined by Lai et al (2006) as

$$\mathrm{CRR}_{7.5} = \left(\frac{\tau}{\sigma'_v}\right)_{7.5} = \exp(A\sqrt{q_{c1N}} - B) \tag{6}$$

where the standard earthquake magnitude is 7.5 and the correlation coefficient (R2) is 0.99. Equations 3 and 6 can then be divided to give the factor of safety (fs)

$$F_S = \mathrm{CRR}_{7.5}/\mathrm{CSR}_{7.5} \tag{7}$$

2.14 **Conclusion**

It is evident due to the discovery of paleoliquefaction features that the Hamilton Basin is an area that has likely experienced localized faulting and subsequent liquefaction. The Christchurch Earthquake in 2011 gave new evidence for the phenomenon of re-liquefaction which has meant that upon the discovery of these paleoliquefaction features, it is now necessary to determine the relative susceptibility of the soils within the Hamilton Basin. In particular the Hinuera Formation, to determine the potential for liquefaction during a future seismic event. The methods to determine this susceptibility have been reviewed with the CPT method being deemed an accurate one able to measure pore water increase as well as deduce soil behaviour *in situ*. The potential risk to liquefaction that may be present within the Hamilton Basin motivates this study with the need for development of a more comprehensive soil/landscape model and susceptibility map to identify the general risk of the region as well as the areas that display a higher susceptibility relative to areas of lower susceptibility which will require less geotechnical intervention.

Chapter Three

Hamilton Basin- Geological setting

3.1 Introduction

This chapter aims to provide in depth information about the specific field area as well as the greater Waikato region. Tectonic history will be outlined with focus on the Kerepehi Fault as well as more recently discovered fault traces within the Hamilton Basin. The depositional history is also an important historical influence on the Hamilton Basin's present day pedology, with the Hinuera Formation being extremely variable and consisting of many differing lithofacies. The main lithofacies within the basin will therefore be described derived from Hume et al (1975) research as well as from more recent research carried out by Kleyburg (2015) who both undertook detailed ground–truth work in order to determine the lithofacies that make up the diverse Hinuera Formation. This chapter will describe the nature of the Hamilton Basin in terms of physiography, tectonic setting, and depositional history.

3.2 Tectonic setting

The Waikato Region (Figure 3.1). can be divided into areas of uplifted ranges being the Western Uplands, Central Hills (north) and the Eastern Ranges and down faulted depressions with the most prominent being the Hamilton Basin and the Hauraki Basin (Lowe, 2010).

3.2.1 The Hamilton Basin

The Hamilton Basin is an oval shaped depression of ~ 2000 km^2, being ~80 km in length (north/south) and ~40 km wide (east to west) with the city of Hamilton being near to its centre (Kamp & Lowe, 1981). The Hamilton Basin can be defined as a depression (down faulted by ~200-300 m to the west) comprising of late Tertiary and Pleistocene aged strata, being bounded by uplifted (~300 m) low permeability Mesozoic sediments of the Manaia Hill Group and the Waitemata and Te Kuiti Groups (Selby & Lowe, 1992; Petch & Marshall, 1988; Edbrook, 2001; Lowe, 2010). The Mesozoic basement comprises much of the higher relief within the Hamilton Basin, however it is not consistently continuous within the south and the east and is less prominent within the south west due the presence of Mount Pirongia.

The Hamilton Basin formed more or less its present day position during the Kaikoura Orogeny (~4-5 Ma) where the largely subsurface Waipa Fault formed the western flank of the Hamilton Basin. The Waipa Fault is a NNE trending fault through the western side of Pirongia and running to the north-north east toward the Hakarimata Range (Kamp & Lowe, 1981).

Figure 3.1 General structure of the Waikato region showing the location of the Hamilton Basin (Lowe, 2010)

3.2.2 **The Hauraki Basin**

The Hauraki Basin, which is to the east of the Waikato Region and contains the Hauraki Rift, is more elongated relative to the Hamilton Basin, with its bounds reaching the Taupo Rift and extending NNW to the Hauraki Gulf (Persaud et al., 2016). The Hauraki Basin can be divided into three topographical features, with the Hauraki Gulf in the north, through to the Firth of Thames and the Onshore Hauraki Depression toward the south (Figure 3.2). The Hauraki depression lies within the back-arc of the Hikurangi subduction zone and is parallel to the once active volcanic arc within the Coromandel Region.

3.2.3 **The Kerepehi Fault**

The Kerepehi Fault (Figure 3.2) is the prominent active fault within the Hauraki depression and one of the potential sources of liquefaction within the Hamilton Basin (Persaud et al., 2016). The Kerepehi Fault, once being perceived as a relatively simple system (e.g. Selby and Lowe, 1992), has recently been analysed using LIDAR imagery and is now interpreted as a much more complex system of two main fault lines with many secondary displacements and splay formations extending from them (Persaud et al., 2016). The predicted recurrence interval of the Kerepehi Fault is <5 ka with a potential for a Mw 5.5-7 earthquake (Persaud et al., 2016; Wallace et al., 2016).

3.2.4 **Fault traces within the Hamilton Basin**

Since 2015, multiple fault traces have become evident within the Hamilton Basin itself, posing another possible source of seismic energy alongside the Kerepehi Fault (Moon and de Lange, 2017). Upon the first discovery of possible faulting along an exposed road cutting (north east Hamilton) further investigation has been undertaken. Multiple faults have since been identified with the majority being recognised in the west of the Hamilton Basin. With the methods used by Persaud et al (2016) suggesting that the calculated maximum credible earthquake (MCE) within the Hamilton Basin for a ~25 km fault rupture is likely to be Mw <6.6. As the faults within the Hamilton Basin are more local than the Kerepehi Fault, they would likely pose a greater threat to liquefaction potential in relation to the Hamilton Section of the Waikato Expressway.

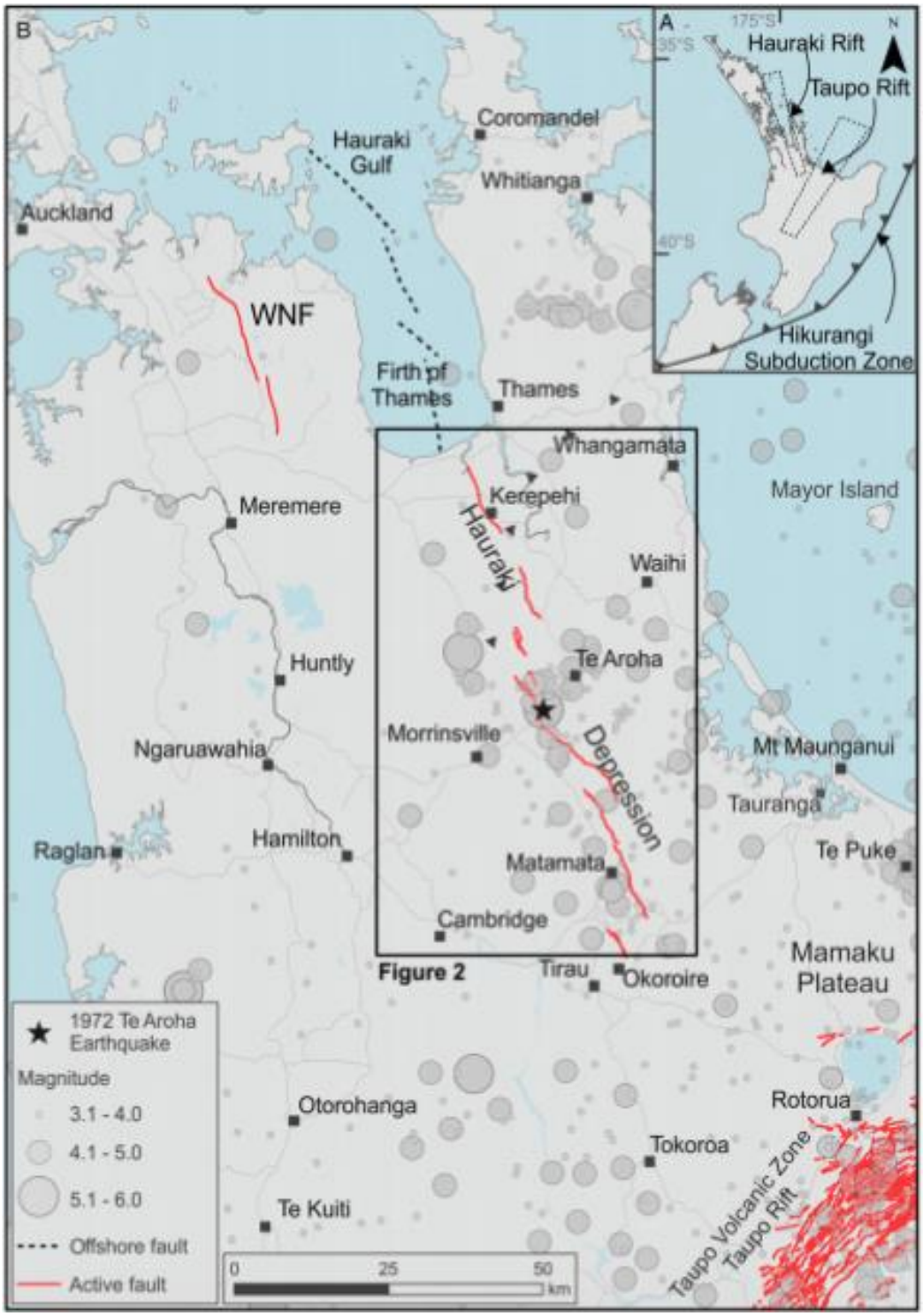

Figure 3.2 Depiction of the Hauraki Depression within the upper North Island with the location of the Hauraki Rift indicated by the dash rectangular shape in the left hand corner, associated with the Taupo rift also indicated by a dashed rectangle. Red lines are associated with the Kerepehi Fault and the historic earthquakes in the area indicated by different sized circles (see key, bottom left) (Williams, 1991). Note that the Kerepehi Fault has been remapped by Persaud et al (2016) since this figure was published.

3.3 **Depositional history**

The Hamilton Basin is one of the only closed basins within New Zealand where the main form of outlet is via surface overflow from alluvial systems, predominantly the Waikato River (Petch & Marshall, 1988; Lowe, 2010). The nature of the sediments within the basin itself has been the result of a complex depositional history due to the low lying position of the basin, its proximity to abundant loose deposits of the Taupo Volcanic Zone, and climatic influences. The Waikato River extends a total distance of 425 km, with its head water being sourced from Lake Taupo, entering the Hamilton Basin at the Maungatautari Gap and travelling through the centre of the Hamilton Basin, shallowing as it travels north to exit the basin via the Taupiri Gap (Selby & Lowe, 1992; Manville, 2002). The ancestral Waikato River flowed into the Hauraki Basin from at least 100 ka before switching to the Hamilton Basin c. 22,000 years ago (Manville, 2002; Manville and Wilson, 2004), where it deposited volcanogenic sediments (Hinuera Formation) in a series of low-angle fans from c. 22,000 to about 17,000 years ago when it entrenched into its current course. The Hinuera Formation now forms the extensive low lying plains – technically a series of low-angled fans (Hume e al., 1975) – within the Hamilton Basin (older Hinuera Formation sediments occur in the Hauraki Basin and elsewhere (Edbrook, 2005). The surface of the alluvium is referred to as the Hinuera Surface, and has distinct features of peat bogs, multiple lakes, and shallow paleochannels (Sherwood, 1972; Manville, 2002; McCraw, 2011). The braided channels and bars of the ancestral river, despite being capped by an incremental accumulation of thin distal tephra deposits up to ~0.6 m in places, remain evident on the land surface and were mapped by Bruce (1978). The Taupo break-out flood that occurred around 20 to 30 years after the Taupo eruption of AD 232 ± 10 resulted in the formation of the low terrace alongside the modern Waikato River, comprising the Taupo Pumice Alluvium (Manville et al., 1999; Edbrooke, 2005).

The Hamilton Basin can be categorised into four geomorphic features (Figure 3.3): the rolling hills, the alluvial plain, low terraces and gullies (Bruce, 1978; Lowe, 2010). The low rolling hills are underlain by weathered ignimbrites c. 1 Ma in age, volcanogenic alluvium (Walton Subgroup), and mantling tephra beds named Kauroa and Hamilton Ash formations. The hills are capped with thin post-50 ka tephras. The Hamilton hills protrude through the extensive alluvial plain within the Hamilton Basin consisting of the Hinuera Formation, which is up to ~ 60 m thick

and formally within the Piako Subgroup of the Tauranga Group (Schofield, 1965; Petch & Marshall, 1988; Selby & Lowe, 1992; Lowe, 2010).

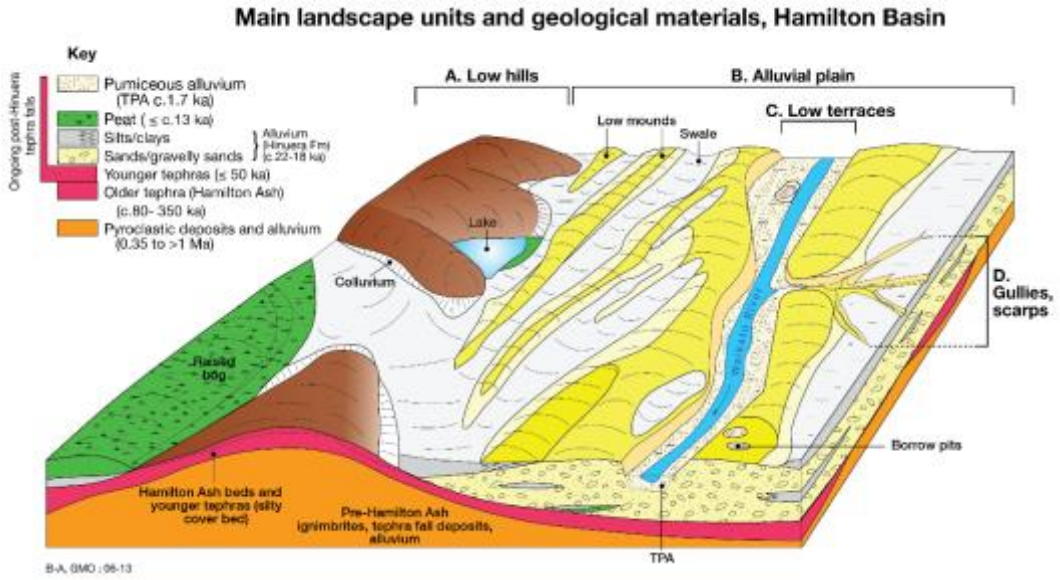

Figure 3.3 Schematic of the main topographic features and associated geological materials within the Hamilton Basin (Lowe, 2010).

3.4 **The Hinuera Formation**

The Hinuera Formation can be described on a regional scale as unconsolidated, coarse and typically cross bedded (~90 m thick) comprising of predominantly sandy gravels and gravelly sands that are mainly rhyolitic or pumiceous in composition. Silts are also prominent within the formation, consisting of siliceous volcanic quartz, plagioclase, pumiceous fragments and glass shards and mafic (heavy) minerals of hypersthene, magnetite, hornblende, augite, epidote and biotite (Hume et al., 1975). This composition of sands and silts make the Hinuera Formation particularly susceptible to liquefaction based on the criteria described in Chapter Two, in particular when associated with a high water table. When observed in detail the Hinuera Formation is highly variable consisting of multiple lithofacies comprising of varying textures and sedimentary structures even those a few metres apart (Schofield, 1965; Hume et al., 1975). These variations both laterally and vertically relate to the pre-entrenchment depositional mechanisms of the high-energy, sediment-laden ancestral Waikato River system that moved from one location to another laterally within the basin whilst building upwards (McCraw,

2011). Five major lithologies were recognised by Hume et al (1975) and are summarized in Table 3.1.

Table 3.1. Summary table of the five major lithologies recognised by Hume et al (1975) including brief descriptions of structure, composition and texture.

Lithofacies	Structure	Composition and texture
1	Cross stratification, moderately to poorly sorted	Rhyolitic and pumiceous gravels and quartzofeldspathic sands
2	Massive, poorly sorted	Rhyolitic sands to gravelly sands
3	Cross stratification, moderately to well sorted	Quartzofeldspathic sands
4	No structure described (massive)	Pumiceous silts
5		Peat

In relation to more recent research undertaken by Kleyburg (2015), evidence of paleoliquefaction within the Hinuera Formation has been identified at two locations which can be seen in Figure 3.4 indicated by the red circles (sites 15 and 16). At both locations injection structures were recognised as paleoliquefaction features with a source bed of sandy material being evident. A correlation was also observed between the presence of silt materials and organic materials at the sites that had observable paleoliquefaction structures suggesting these soil textures may be linked to a higher liquefaction susceptibility. From this empirical evidence it can be concluded that liquefaction has occurred within the Hamilton Basin since c. 20,000 years ago (the age of the sediments in which the features were described) and, based on recent evidence of the re-liquefaction phenomenon that occurred within the 2011 Christchurch Earthquake, liquefaction will likely occur again in the event of an earthquake proximal to or within the Hamilton Basin. More detailed lithofacies analysis by Kleyberg (2015) identified 14 different lithofacies within the Hamilton Basin highlighting the complexity of determining just what soil textures and

stratigraphy pattern correlated to a higher liquefaction potential due to the shear amount of possibilities within the highly diverse Hinuera Formation.

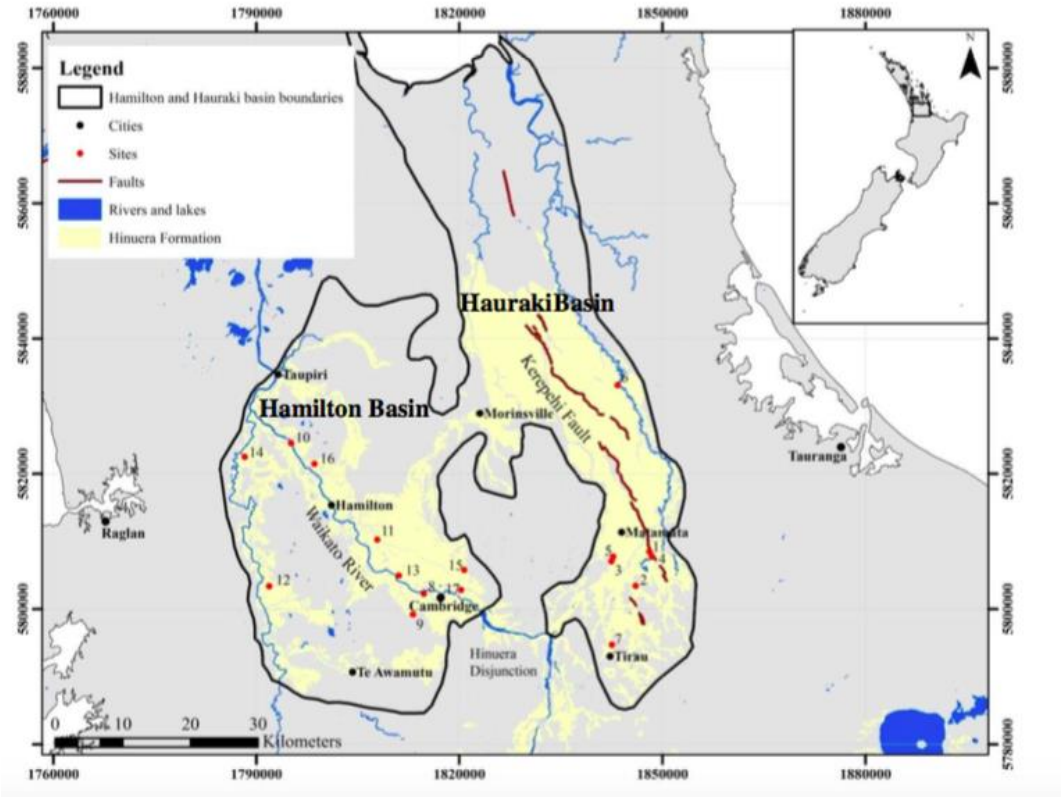

Figure 3.4 Site localities where paleo liquefaction features were found by Kleyburg (2015) within the Hinuera Formation.

Chapter Four

Methods

4.1 Introduction

Data analysis initially involved input of CPT data into CLiq™ to undertake quantitative assessment of the CPT data, with particular emphasis on the liquefaction potential index. Statistical analysis was employed to determine the most influential factors on liquefaction potential, with ArcMap GIS then being used to visually present these results in a way that areas of higher susceptibility to liquefaction are represented clearly and explicitly. This chapter outlines the methods used at each stage of the analysis.

4.2 Site selection/data acquisition

The Hamilton Basin was chosen as the area of study because of the hazard a liquefaction event would pose to its many residents (population ~ 141,612, Statistics New Zealand 2013). A total of 216 CPT data points were derived from the New Zealand Geotechnical Database (NZGD) over a distance of ~18.5 km from Horsham Downs (north of Hamilton) to Tamahere (south of Hamilton) which makes up the Hamilton section of the developing Waikato Expressway were utilized for analysis (Figure 4.1). This access to CPT data allowed the development of a localised field area for detailed investigation (Figure 4.2). Supplementary data such as LIDAR data for the chosen field area were then sourced from Waikato Regional Council and base map imagery from the GIS online resource. The pedological soil map (S-map: a new soil spatial information system for New Zealand, 2016) was provided by Waikato Regional Council with the permission of Landcare Research.

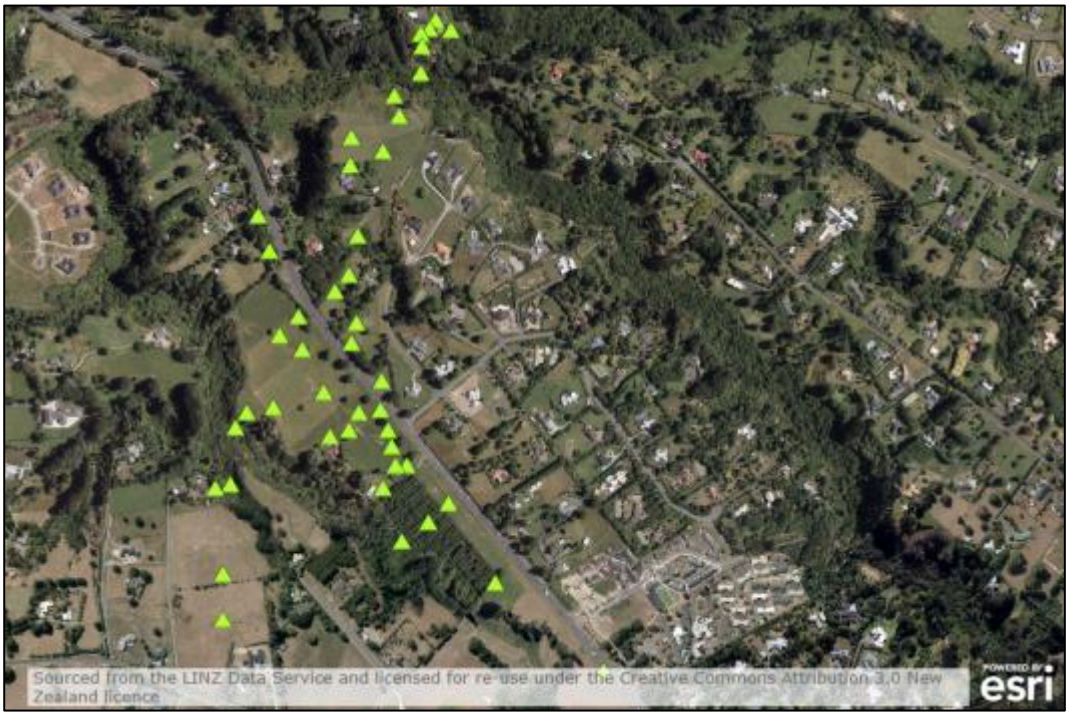

Figure 4.1 Aerial imagery showing a section of the future Waikato Expressway, Hamilton section, with individual CPT drill sites shown as green triangles (New Zealand Geotechnical Database, NZGD).

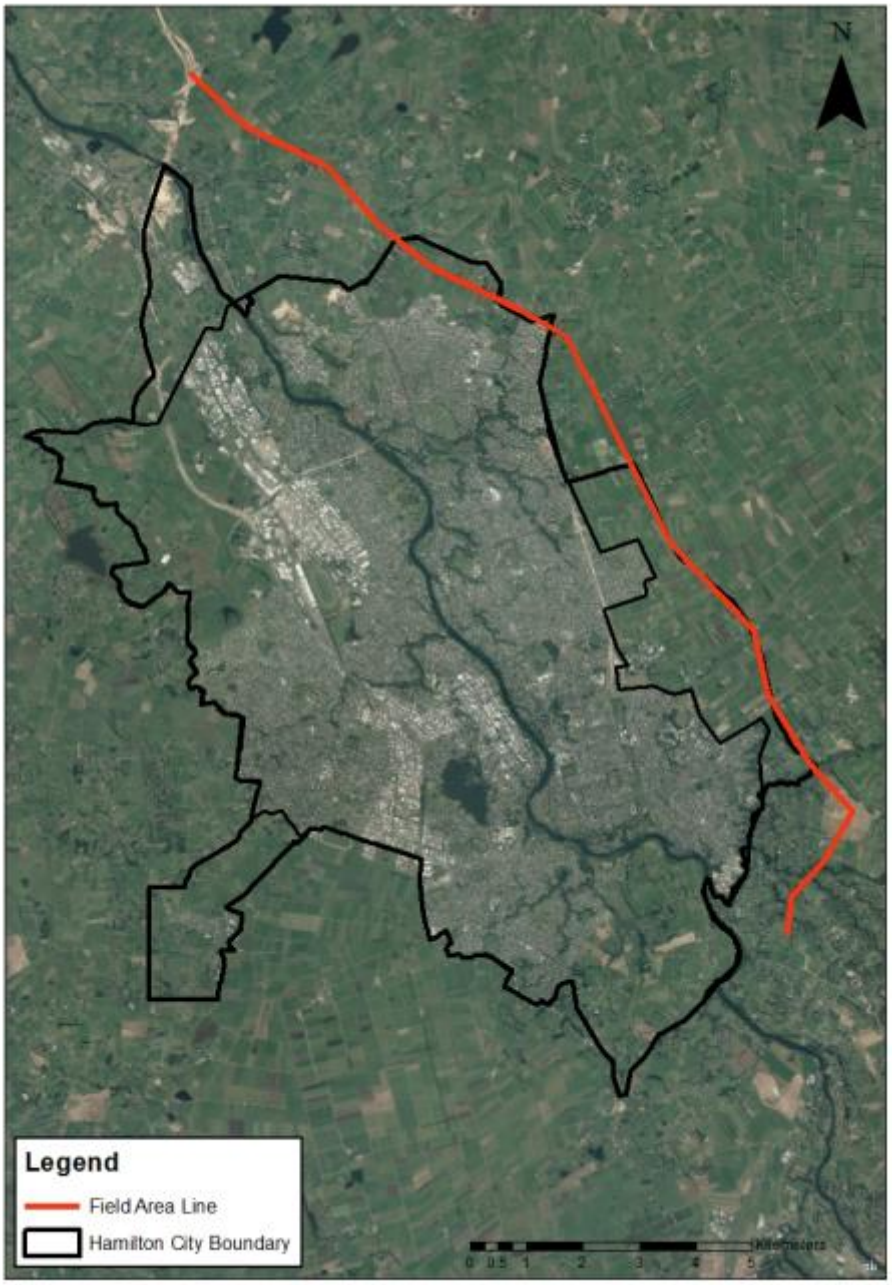

Figure 4.2 Aerial imagery showing proposed field area of the Waikato Expressway, with the Hamilton section depicted as the red line. Black line marks outline of Hamilton City.

4.3 **CLiq™ analysis**

Raw CPT data were entered into CLiq™ (Appendix A) software to obtain the predicted liquefaction potential index (LPI). The LPI was developed by Iwasaki et al (1978) for assessing liquefaction potential based on the depth of the liquefiable layer in relation to ground surface as well as its thickness and its computed factor of safety (FS) (Toprak and Holzer, 2003). The LPI value, initially computed from raw data obtained from CPT drills sites (NZGS) was then displayed within LPI output graphs as an increasing cumulative value. This cumulative LPI value was then classified within CLiq™ as either low (<5), moderate (5-15), or high (>15) potential based on the Robertson and Wride calculation method (Robertson and Wride, 1998; Robertson., 2009). CLiq™ input parameters (Appendix A) included: horizontal peak ground acceleration (pga); earthquake moment magnitude (Mw); water table depth; and fines content. Horizontal pga was computed as 0.38 (g) using ah = ZRC where Z (Hazard factor) = 0.16, R (Return period factor) = 1.8, and C (Site response factor) = 1.33 according to New Zealand Standard (2004); NZ Transport Agency (2014); New Zealand Geotechnical Society INC (2016) A magnitude Mw = 7 event was assumed as worse-case selected from ranges of Mw 5.5-7 suggested for the Kerepehi Fault (Persaud et al., 2016; Wallace et al., 2016). There is a relatively wide range within the literature regarding ground water table depth within the Hamilton Basin, with values as low as 0.6 m and as high as 4 m recorded in the field area. To give a conservative result a water table depth of 1 m was used following the examples of Opus (2014) and Ministry of Business Innovation and Employment (2017). CLiq™ also had an option to detect areas of soil behaviour transition into more fines dominated material and remove them according to a specified Ic cut off range. This function was not included in analysis as the LPI results should illustrate *in situ* conditions therefore reflecting how differing soil behaviours including those that are more fines dominated influence one another and not just the LPI on an individual soil level (Figure 4.3).

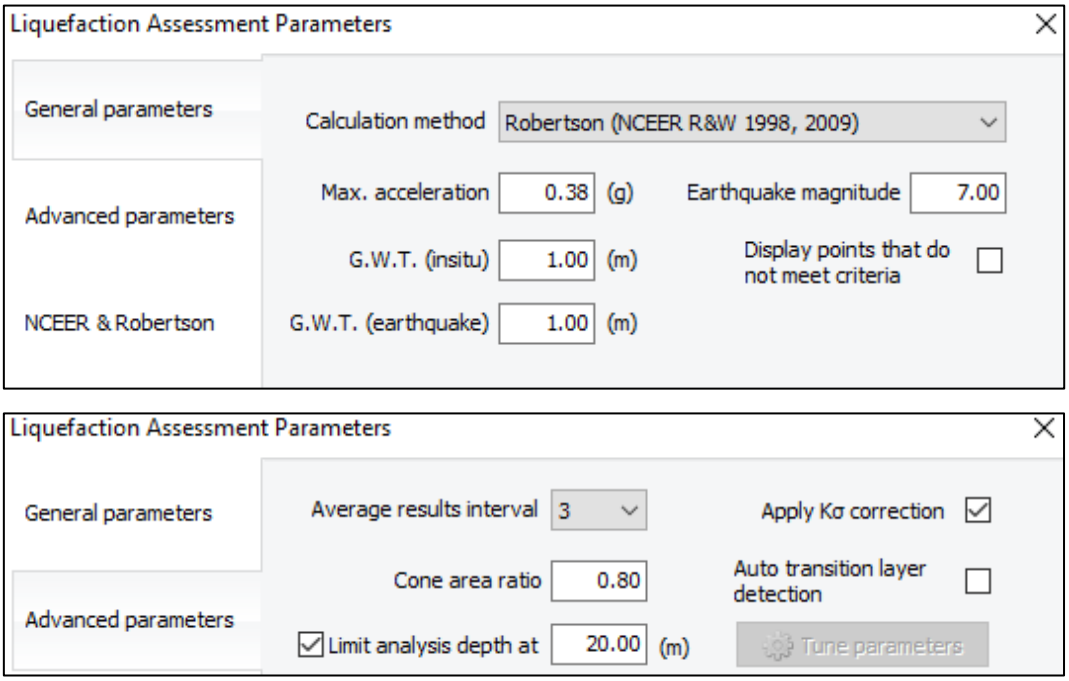

Figure 4.3 Screenshot of CLiq™ advanced parameters tailored to this particular research; including calculation method, max. acceleration, ground water table (GWT), earthquake magnitude and auto transition layer detection.

4.4 Statistical analysis

Data were compiled in Excel into a uniform format that could be easily imported into the software that would carry out the statistical analysis (Figure 4.4). The Excel spreadsheet (Appendix D) consisted of each CPT having an appropriate label, alongside GPS coordinates, and the specific cumulative LPI values for 3, 5, and 10 m depths derived from the raw results of CLiq™. Factors of slope, elevation (derived from LIDAR DEM data) and 'soil family' and associated soil texture from S-map (Lilburne et al., 2011; Landcare Research, 2016) were included in the spreadsheet that was then imported into STATISTICA™. A 'soil family' is a class (4th category) within the New Zealand Soil Classification system (Hewitt, 2010), identified by a geographical name with a suffix *f*. The suffix is used to distinguish families from soil series with which they have similarities and both have geographic names (Webb & Lilburne, 2011). Soil families are classified on the basis of their physical attributes which includes the nature of the soil profile material to 100 cm depth, parent rock, dominant texture class to 60 cm depth, and permeability of the slowest horizon within 100 cm depth. Soil families and in particular those identified within this research are constrained to the upper 1 m of land surface making the identification of soil families essential in land use classification. The classification of soils into families is more focused around similarities in physical attributes rather than genesis with soil families primarily being identified based on their most dominant lithology with organic soils being recognised as having different

lithological criteria, being split away at order level (Webb and Lilburne, 2011). Liquefaction potential was considered at a depth of 3 m as shallow liquefaction will be the most damaging in general according to Tonkin and Taylor, (2013), yet shallower materials are unlikely to liquefy due to lack of normal stress (Luo et al., 2013). A maximum depth of 10 m was considered because liquefaction deeper than this is not likely to extend to the ground surface, only for very large proximal earthquakes (Huang and Yu, 2013).

Id	Elevation	Slope	Soil family	Soil sibling num	Liquefaction potential 3m	Liquefaction potential 5m	Liquefaction potential 10m
73224	23.39	0.48	Otorohanga	9	3.94030238	9.67373448	15.56017423
73225	24.22	1.05	Otorohanga	9	1.82438498	2.04672994	13.81440057
73227	23.91	1.42	Otorohanga	41	6.73534896	8.48435935	14.71786395
73228	24.79	0.99	Otorohanga	41	5.40821208	11.60188713	15.20749218
73229	25.45	3.88	Otorohanga	41	3.55070568	5.76263503	8.10340222
73230	23.29	1.1	Pukehina	8	1.67429572	1.75455853	12.98170905
73231	21.98	2.62	Moeatoa	2	7.9171522	8.97232856	16.00568844
73232	21.26	1.38	Pukehina	8	1.65227062	2.64301151	13.329425
73233	19.51	1.14	Moeatoa	2	3.45106018	7.37067866	7.37067866
73234	24.74	4.43	Kainui	3	1.41764097	6.43887215	24.05859025
73235	29.55	0.29	Pukehina	8	2.62374681	4.50540167	30.4974624
73236	53.69	11.1	Kainui	2	2.34418791	4.39378913	10.53607394
73237	49.48	11.27	Kainui	2	6.93882668	14.54908313	16.16272508
73238	44.48	9.5	Kainui	2	2.29962158	2.41762732	6.58802788
73239	33.2	1.48	Matakana	2	4.82608141	4.82608141	9.36961489
73240	32.62	1.22	Kainui	2	5.24513089	14.5159179	19.09091735
73241	46.58	7.77	Kainui	2	4.78897433	6.79387501	15.32710411
73242	33.32	3.42	Rotokauri	2	1.92081707	5.29203724	6.478404
73243	53.25	3.62	Kainui	2	2.35539484	2.35539484	7.31641089
73244	48.62	7.73	Kainui	2	4.58214033	12.15814911	13.81639123
73245	36.36	6.4	Kainui	2	1.31578129	5.50013843	14.76583954
73246	36.43	3.91	Kainui	2	4.01768044	6.60741465	9.04287747
73247	35.9	0.54	Te Puninga	4	6.9904671	16.41248703	32.80968242

Figure 4.4 Screenshot of Excel spreadsheet for input into STATISTICA™ including; CPT ID, elevation, slope, soil family, soil sibling number and liquefaction potential at 3, 5 and 10 m. Boxes highlighted yellow indicate CPT data that did not reach 10 m depths.

4.4.1 **STATISTICA™ analysis**

Parameters of LPI, slope, elevation, soil family, and soil texture were put into STATISTICA™ software to determine the most influential factors to liquefaction at 3 m, 5 m and 10 m depth. Multiple methods including the simpler Scatterplot graphs as well as more complex regressive I-Tree analysis were utilized within the STATISTICA™. Scatterplot graphs where converted into bubble graphs for each recorded depth of 3 m, 5 m and 10 m against soil families with liquefaction potential being used as a weighting in order to show the range of data points associated with each soil family as well as the degree of liquefaction potential.

Neural Network analyses were run as well as regressive I-Tree analyses being explored to identify and categorize parameters that influence LPI (Appendix D). Regressive exhaustive CHAID (CHi-square Automatic Interaction Detection) was the method used to represent the relationship between the parameters (Section 4.4) and liquefaction potential. Liquefaction potential was input as the predictive value (dependent variable), with slope, elevation and soil texture then input as continuous variables and soil family as a categorical variable (independent variables). Each tree graph was then 'pruned' to remove less influential factors in order to show more clearly those factors that are most influential to LPI (Figure 4.5). The resultant tree graph then displays each independent variable as separate classes (low, moderate and high liquefaction potential) based on their associated LPI. Due to limited data availability some soil families only had one CPT test undertaken within them and therefore only one recorded LPI value. These soil families were not included within the I-Tree analysis as only one LPI value could not represent the liquefaction potential for that particular soil family. Once soil families that only had one associated data point were removed from the analysis there were 10 soil families identified; Pukehina*f*, Moeatoa*f*, Kohuratahi*f*, Kainui*f*, Rotokauri*f*, Otorohanga*f*, Matakana*f*, Te Puninga*f*, Utuhina*f* and Kaipaki*f*. ArcMap GIS was then used to depict the results from the statistical analysis in terms of liquefaction susceptibility.

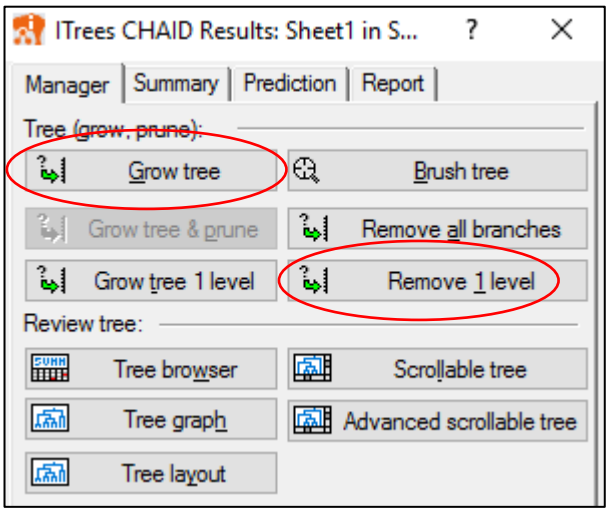

Figure 4.5 Screenshot of ITrees CHAID results (manager tab) showing how tree can be 'grown' and levels of analysis can be removed (pruned) for simplification of analysis (shown in red circles).

4.5 Geographical Information Systems (GIS) analysis

GIS was used to visually represent the data and the field area. All imagery used the NZ Transverse Mercator coordinate system. LIDAR data was loaded and laid over aerial imagery of the North Island of New Zealand (derived from the online ArcMap GIS database), and also converted to slope and elevation within GIS for multiple means of topographical interpretation. A geomorphic map was then developed in order to assess the overall topographic pattern of the field area (Appendix C). General data points (CPT points) based on LPI were then categorised within an excel spreadsheet as 1 for low, 2 for moderate and 3 for high liquefaction susceptibility (Figure 4.6) (Appendix C). CPT data were then put into ArcMap GIS and given a traffic light colour pattern (green: low, orange: moderate, and red: high) to visually represent the field area and the distribution of data points within each soil family (Figure 4.7). Soil family map was then overlain to indicate which soil families had data actually within them and which appeared to have higher LPI relative to others.

Id	Easting	Northing	LPI_3m	LPI_5m	LPI_10m	Gen_Sus3	Gen_Sus5	Gen_Sus10
CPT_73224	1795453	5826524	3.94030238	9.67373448	15.56017423	1	2	3
CPT_73225	1795614	5826532	1.82438498	2.04672994	13.81440057	1	1	2
CPT_73226	1795758	5826441	6.52215417	9.9157439	17.99405671	2	2	3
CPT_73227	1795415	5826184	6.73534896	8.48435935	14.71786395	2	2	2
CPT_73228	1795524	5826261	5.40821208	11.60188713	15.20749218	2	2	3
CPT_73229	1795525	5826090	3.55070568	5.76263503	8.10340222	1	2	2
CPT_73230	1795631	5826180	1.67429572	1.75455853	12.98170905	1	1	2
CPT_73231	1795770	5826267	7.9171522	8.97232856	16.00568844	2	2	3
CPT_73232	1795840	5826377	1.65227062	2.64301151	13.329425	1	1	2
CPT_73233	1796010	5826112	3.45106018	7.37067866	7.37067866	1	2	2
CPT_73234	1797147	5825662	1.41764097	6.43887215	24.05859025	1	2	3
CPT_73235	1798250	5824776	2.62374681	4.50540167	30.4974624	1	1	3
CPT_73236	1798933	5823914	2.34418791	4.39378913	10.53607394	1	1	2
CPT_73237	1799011	5823856	6.93882668	14.54908313	16.16272508	2	2	3
CPT_73238	1799047	5823817	2.29962158	2.41762732	6.58802788	1	1	2
CPT_73239	1799380	5823613	4.82608141	4.82608141	9.36961489	1	1	2
CPT_73240	1799720	5823408	5.24513089	14.5159179	19.09091735	2	2	3
CPT_73241	1800037	5823218	4.78897433	6.79387501	15.32710411	1	2	3
CPT_73242	1801010	5822795	1.92081707	5.29203724	6.478404	1	2	2
CPT_73243	1801720	5822384	2.35539484	2.35539484	7.31641089	1	1	2

Figure 4.6 Screenshot of Excel spreadsheet for input into ArcGIS with easting and northing coordinates, LPI at 3, 5 and 10 m depths with and additional categorisation of LPI (Gen_Sus) traffic light colour scheme where if LPI (< 5) its allocated a 1 for low susceptibility (indicated also by green colour), 2 is >5<15 for moderate susceptibility (orange) and 3 is >15 for high susceptibility (red). Again, yellow highlighted boxes indicate CPT data that did not reach 10 m depths.

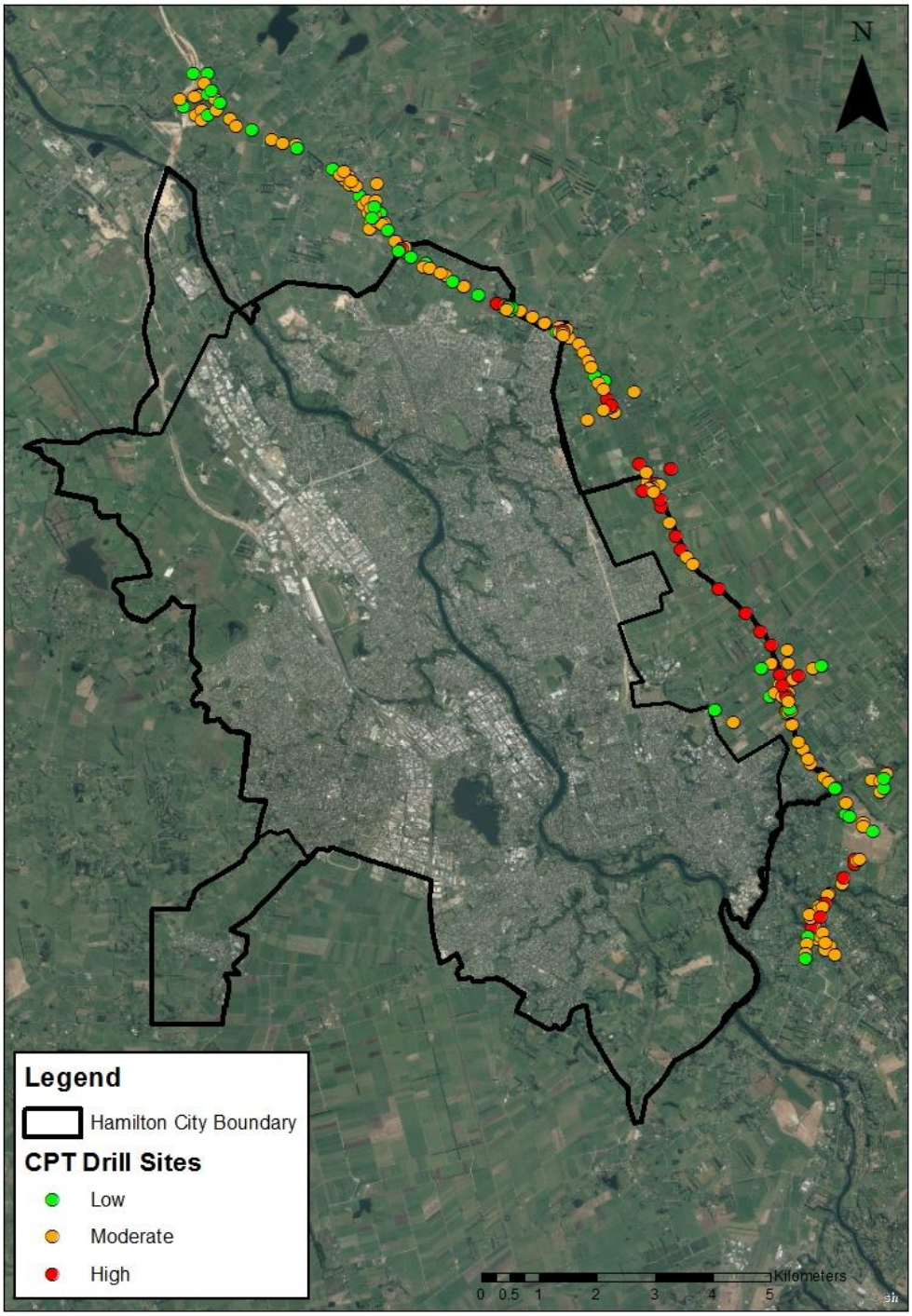

Figure 4.7 Aerial imagery showing visual depiction of raw data from Figure 3.6 where the same 'traffic light' colour scheme can be seen with green representing low, orange moderate, and red high susceptibility. This particular image shows LPI at 5 m with each circle representing each individual CPT drill site.

Chapter Five

Results

5.1 Introduction

Three primary methods were used to determine the relative susceptibility to liquefaction of soils within the field area (Hamilton Section of the developing Waikato Expressway), focusing in particular on areas that show higher susceptibility than others. CLiq™ software was used to analyse the non pedalogical soil materials in order to identify any patterns within a much more specific context. With STATISTICA™ then being used to determine whether or not there was a correlation between the CPT data and the soil types (families) within the field. ArcMap GIS was then used to visually interpret the findings within both STATISTICA™ and CLiq™.

5.2 CLiq™ analysis

Liquefaction susceptibility, displayed as data points to the east of Hamilton City, shows an increasing cumulative susceptibility with an increase in depth (Figure 5.1). At 3 m depth susceptibility is low (119 sites) to moderate (97 sites) with the majority of sites being considered as having a low susceptibility to liquefaction (LPI <5). At greater depths, susceptibility can be seen to range from low to high with 10 m depths being dominated by high liquefaction susceptibility. When referring to Figure 5.1A, areas of moderate susceptibility at 3 m depths appear more concentrated toward the southern end of the field area; within Figure 5.1B at 5 m depths, high susceptibility appears within the middle/lower (southern) region of the field area also. In contrast to these shallower depths of 3 and 5 m, at 10 m depth the high susceptibilities appear to dominate the field area with moderate susceptibilities being sporadic throughout the field area and the low susceptibilities more concentrated at the northern and southern ends of the field area (Figure 5.1C).

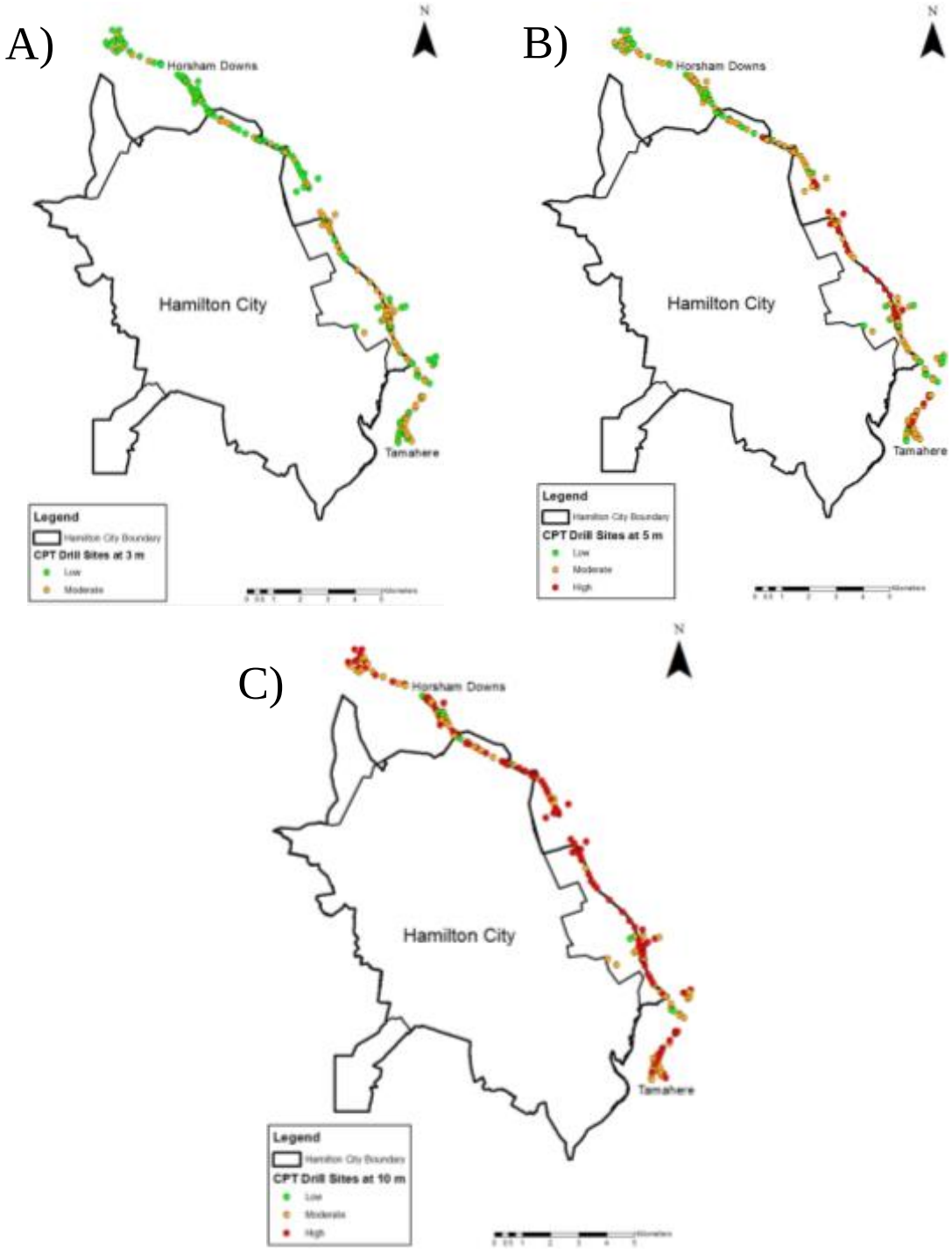

Figure 5.1 Field area (Hamilton city with Waikato Expressway Hamilton section under construction to the east). Data points represent CPT sites and subsequent LPI based on Robertson & Wride (NCEER 1998, 2009) calculation method. (A) 3 m depth, (B) 5m depth, (C) 10 m depth.

Figure 5.2 illustrates eight individual CLiq^{TM} output traces up to 10 m depths with colours (see key) representing normalized Soil Behaviour Type (SBTn) and the yellow line indicating the recorded soil behaviour at each particular depth. These eight profiles were chosen because they illustrate how variation in soil behaviour can affect the resultant liquefaction potential, with each profile illustrating a different degree of LPI (from no liquefaction to moderate-high potential liquefaction occurrence from ground surface to 10 m depths). Profiles were derived from upper (northern), middle, and lower (southern) sections of the field area to give an accurate representation of entire data set.

As soil contents increases in silt to sand textures, susceptibility is seen to increase. This is illustrated well within Figure 5.2D when compared to Figure 5.3D. The SBTn indicates a soil with a sandy silt rather than either granular (coarse sand) or clay-like texture has a higher liquefaction potential (Figure 5.3D). In Figure 5.2C compared to 5.3C, the idea that this sandy silt texture correlates with higher liquefaction potential is also shown. A slight increase in fines from 6.5 m occurs alongside a large increase in liquefaction potential, suggesting that ~1.8-2.4 SBTn is likely to produce the highest liquefaction potential as can be seen in all profiles (Figure 5.2). In each graph it can be seen that in portions of the profile liquefaction potential is essentially 0 (illustrated by a vertical line) and that the SBTn corresponds to one of two ends of the spectrum, one being that the soil is too granular (coarse sand) or the texture is too rich in fines with a suspected clay-like behaviour (relative plasticity). It should also be noted that although there are many differences between each of the interpreted CPT profiles, most show a similar pattern of a sand-rich texture at the base of the profile then leading into finer grained material within the upper profile. In contrast to this, however, the soil properties in some profiles then change into a finer texture within the lower portion (Figure 5.2A, B, D and F).

When CRR plots within Figure 5.4 are related back to soil behaviour a particular pattern can again be identified where CSR will increase and at times surpass CRR at depths at which the soil behaviour moves toward a more silty sand/sandy silt texture (e.g. at ~5.5 m in Figures 5.2A and 5.4A). In contrast to this, if soil behaviour moves into clay behaviours, then CSR will decrease much below the CRR threshold such as at 1.2 m (Figures 5.2G and 5.4G). When looking at the overall pattern within each CRR graph, it can be seen that within graphs that are associated with a higher LPI reading, the points at which CSR exceeds CRR becomes much more consistent with large portions of CSR exceeded. In contrast, those of lower susceptibility (Figures 5.4A and D) show a more intermittent pattern of CSR exceedance.

In Figures 5.5 and 5.6, the patterns displayed relating to low LPI for vertical settlement and lateral displacement are not as clear. Lower LPI figures do show a lesser portion of the profile exhibiting potential settlement and displacement, but that does not seem to correlate with a lower overall settlement and displacement depth. The same pattern observed for SBTn is apparent where when soil behaviour is at or near the sandy silt interface (of a sandy/silt, silty/sand texture) displacement and settlement is at its greatest.

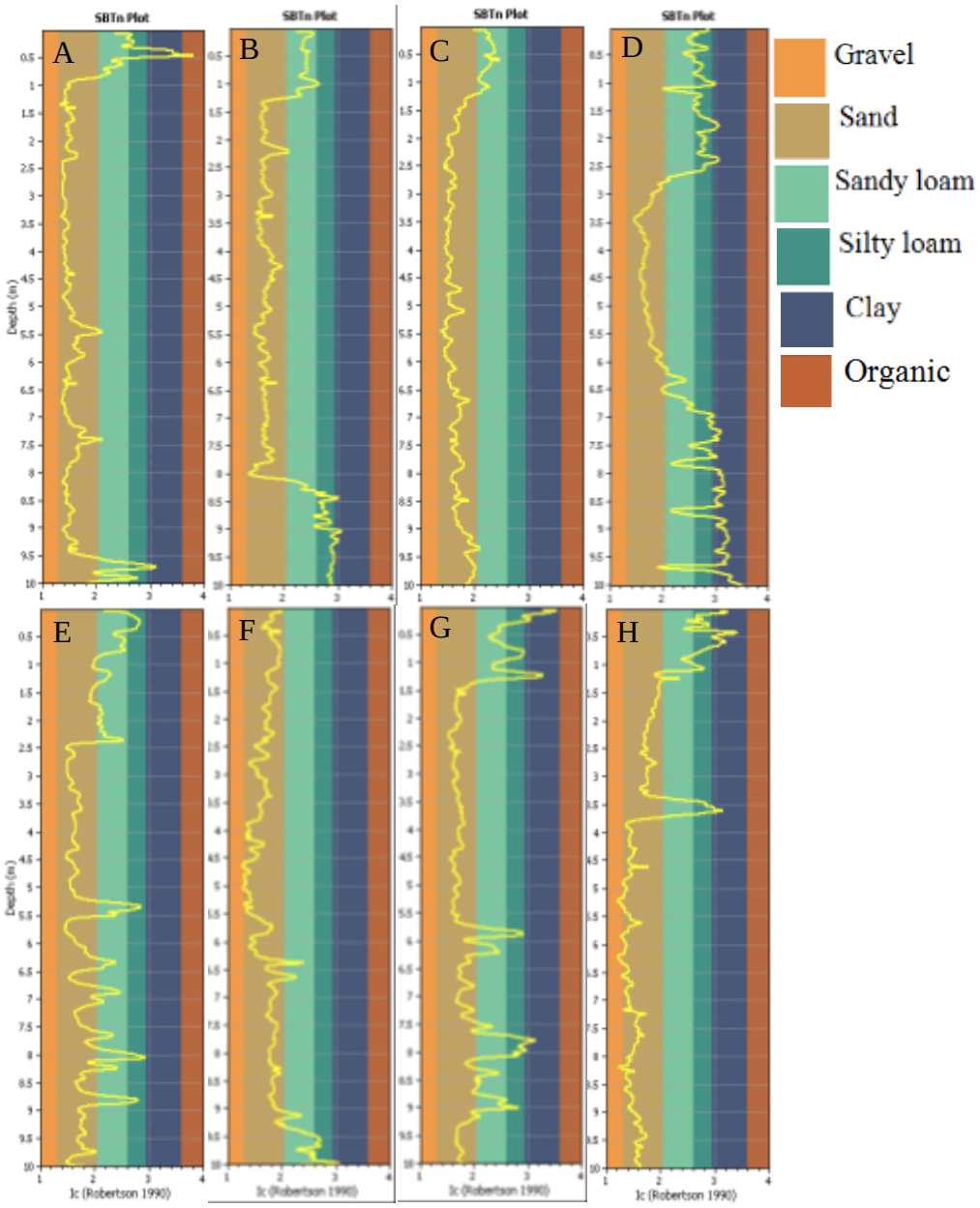

Figure 5.2 SBTn plots showing changes in proposed soil behaviour from 0.1 to 10 m with each profile illustrating a different LPI value from low to high where the yellow line indicates the soil behaviour at that particular depth.

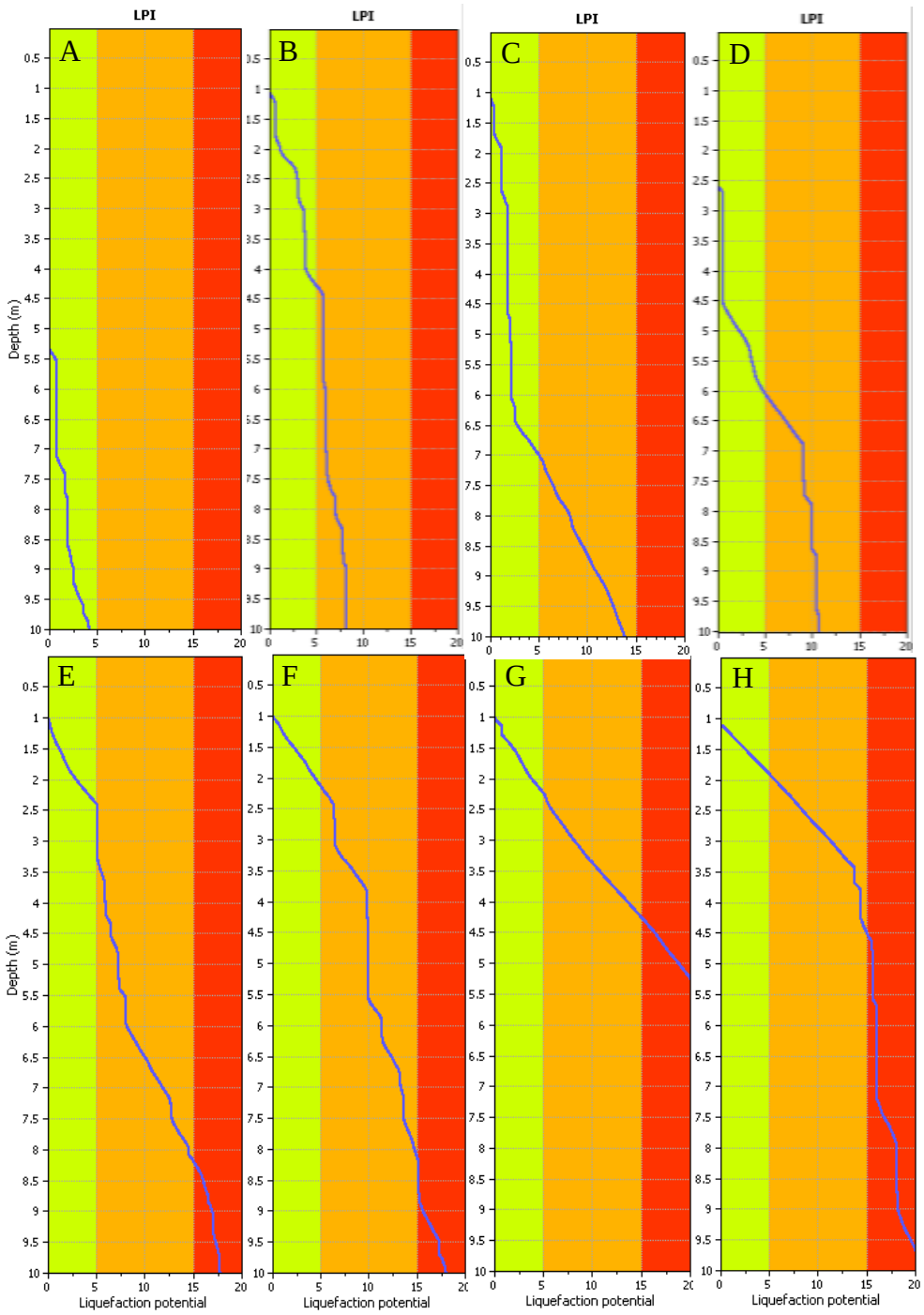

Figure 5.3 LPI plots showing changes in calculated liquefaction potential from 0.1 to 10 m with each profile illustrating a different LPI value from low to high. Where the blue line is vertical, there is no calculated LPI, and where it has a slope liquefaction potential has been calculated. Green is low, orange is moderate and red is high LPI.

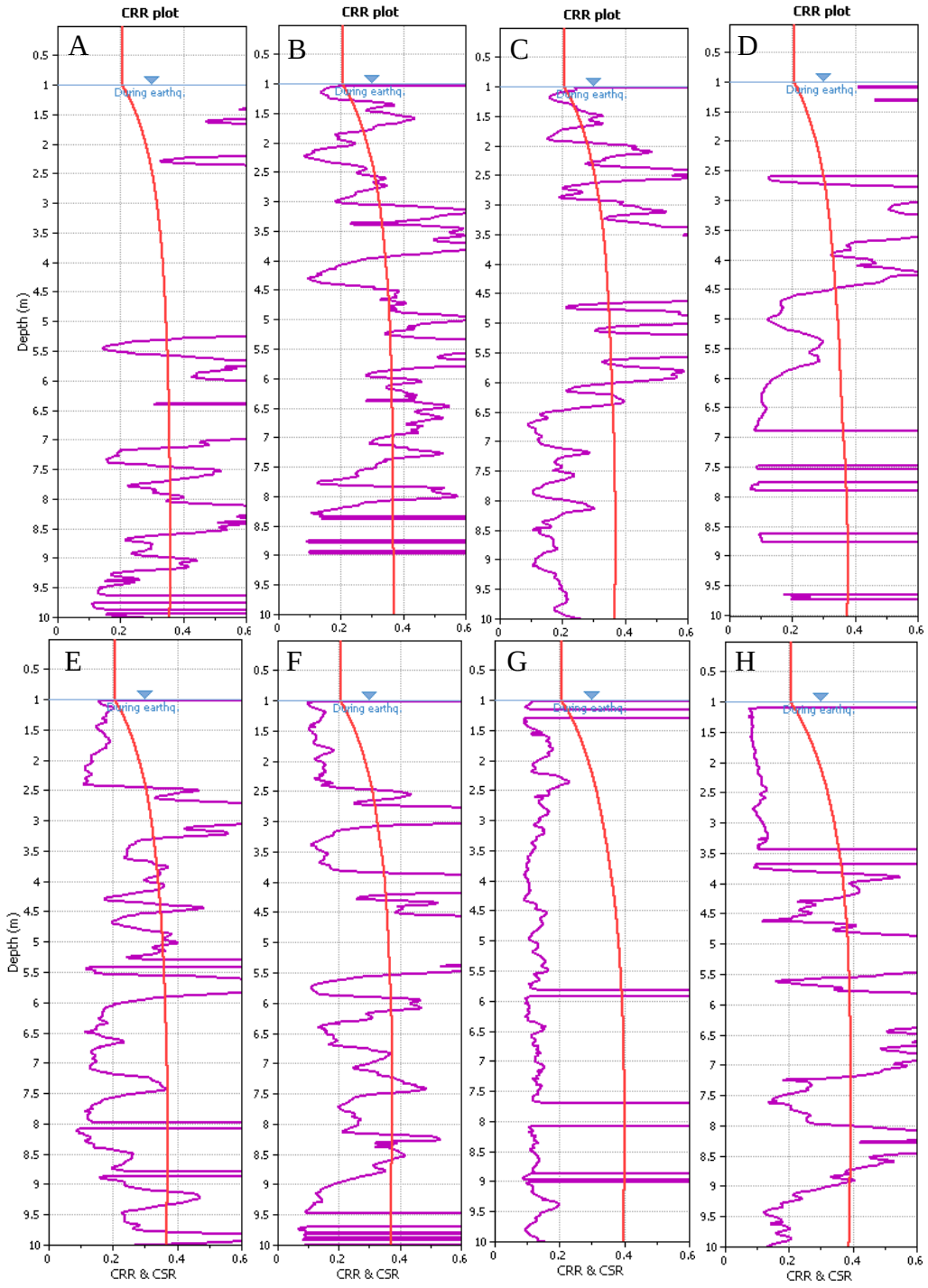

Figure 5.4 CRR plots showing changes in calculated CSR relative to CRR from 0.1 to 10 m with each profile illustrating a different LPI value from low to high. The pink line indicates CSR while the red line indicates CRR.

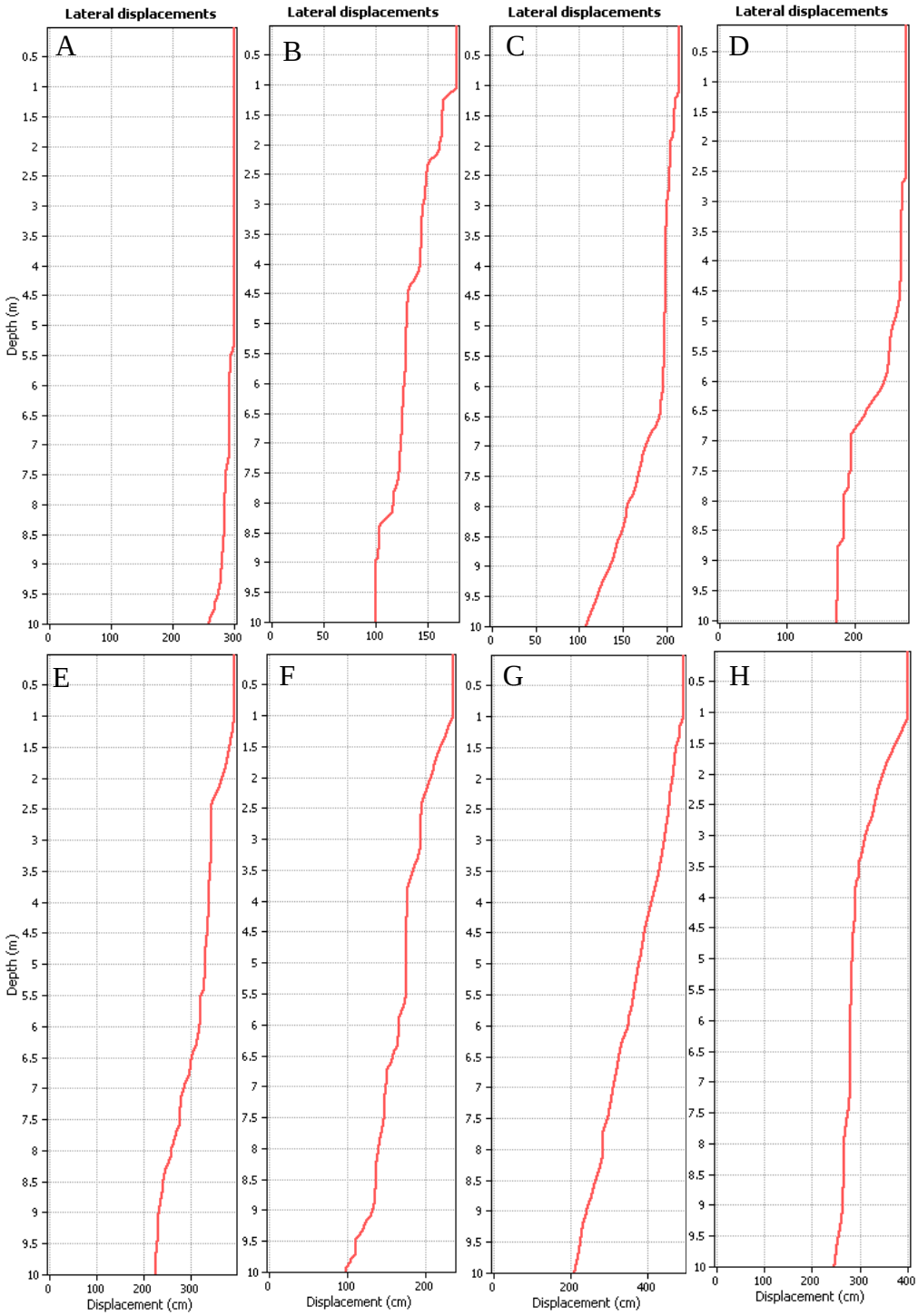

Figure 5.5 Lateral displacements plots showing changes in calculated lateral displacement from 0.1 to 10 m with each profile illustrating a different LPI value from low to high. Where the red line is vertical, no displacement has occurred and where it is sloped there has been calculated lateral displacement.

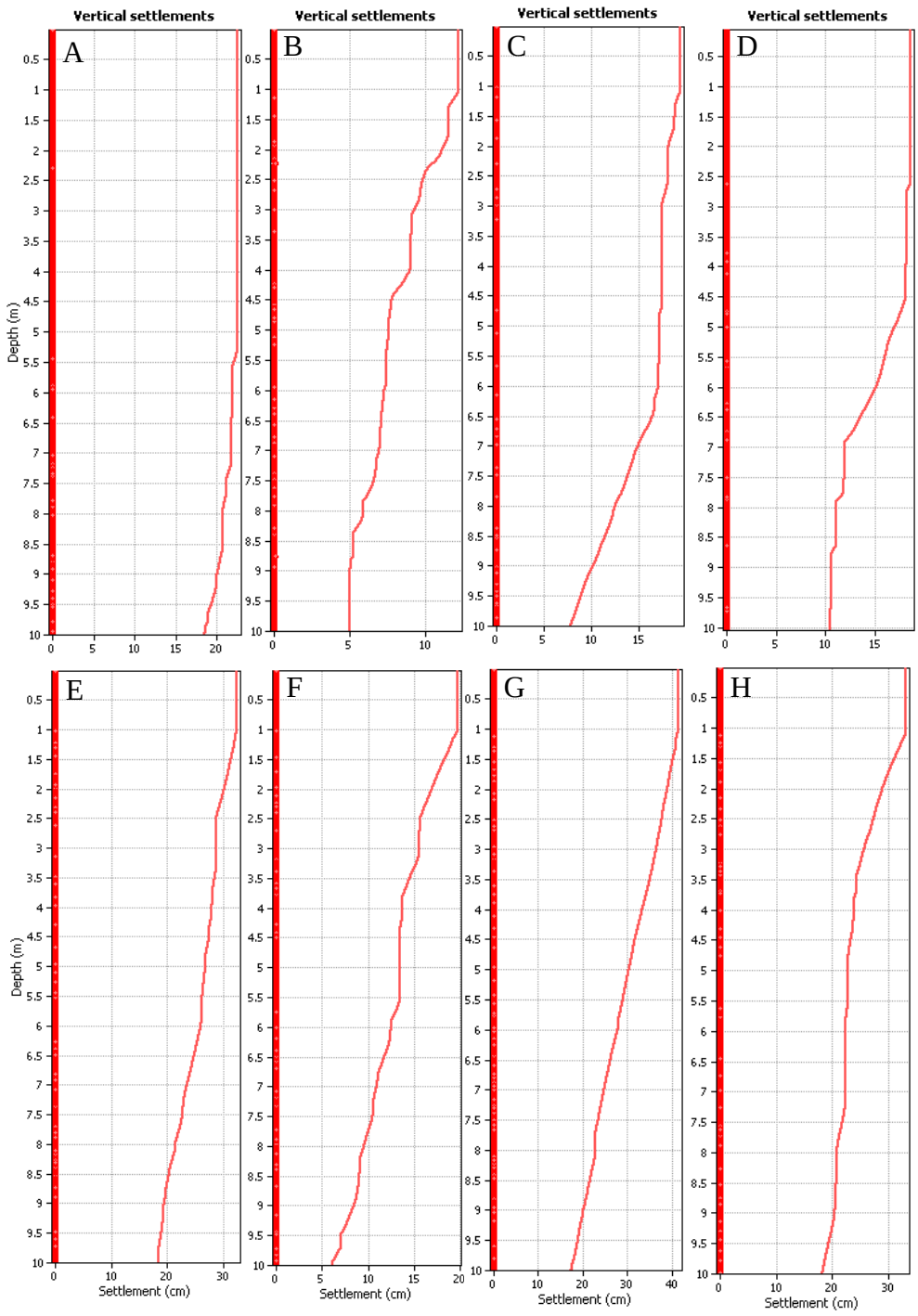

Figure 5.6 Vertical settlements plots showing changes in calculated vertical settlement from 0.1 to 10 m with each profile illustrating a different LPI value from low to high. Where the red line is vertical no settlement has occurred, and where it is sloped there has been calculated vertical settlement.

5.3 **STATISTICA™ analysis**

5.3.1 **Bubble plots**

It is clear when looking at each plot (Figures 5.7, 5.8 and 5.9) that Otorohanga*f*, Kainui*f*, Matakana*f* and Utuhina*f* have more available data compared with the other soil families. The soil families that consistently have the highest values for liquefaction susceptibility at 3, 5 and 10 m are Otorohangaf, Kainuif, Matakana and Utuhinaf. In addition, Kaipakif soils have only two available data points, however both of these points are within the higher susceptibility ranges.

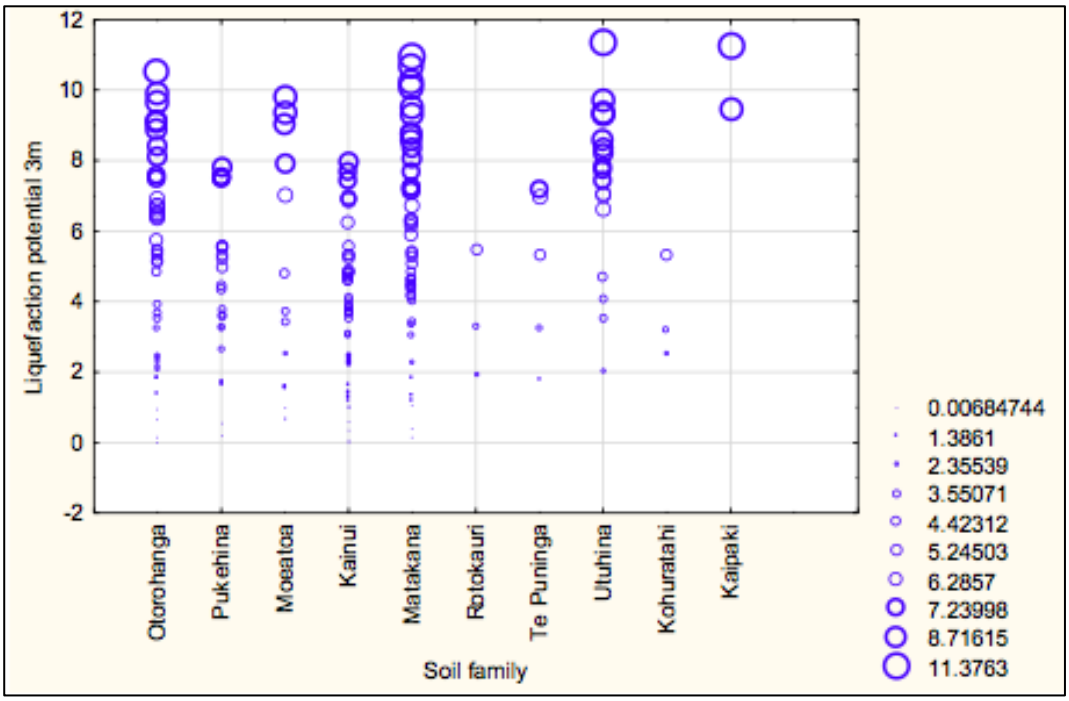

Figure 5.7 Bubble plot of liquefaction potential at 3 m depths against soil family; weighted by liquefaction potential at 3 m. Circles represent individual CPTs and their calculated LPI within that specific soil family.

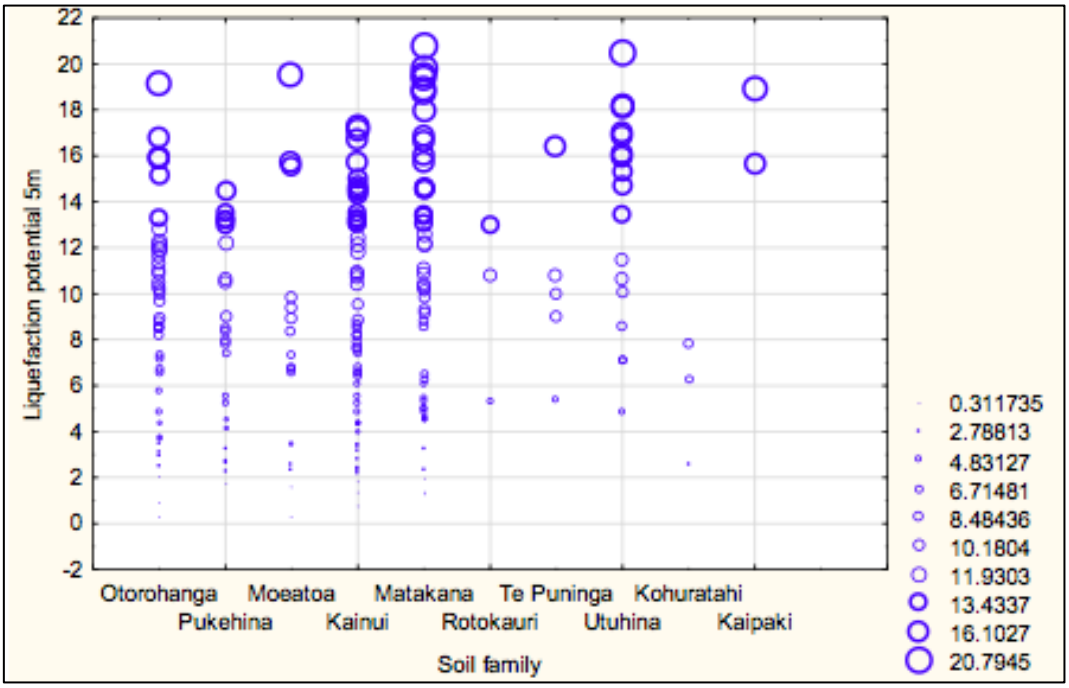

Figure 5.8 Bubble plot of liquefaction potential at 5 m depths against soil family; weighted by liquefaction potential at 5 m. Circles represent individual CPTs and their calculated LPI within that specific soil family.

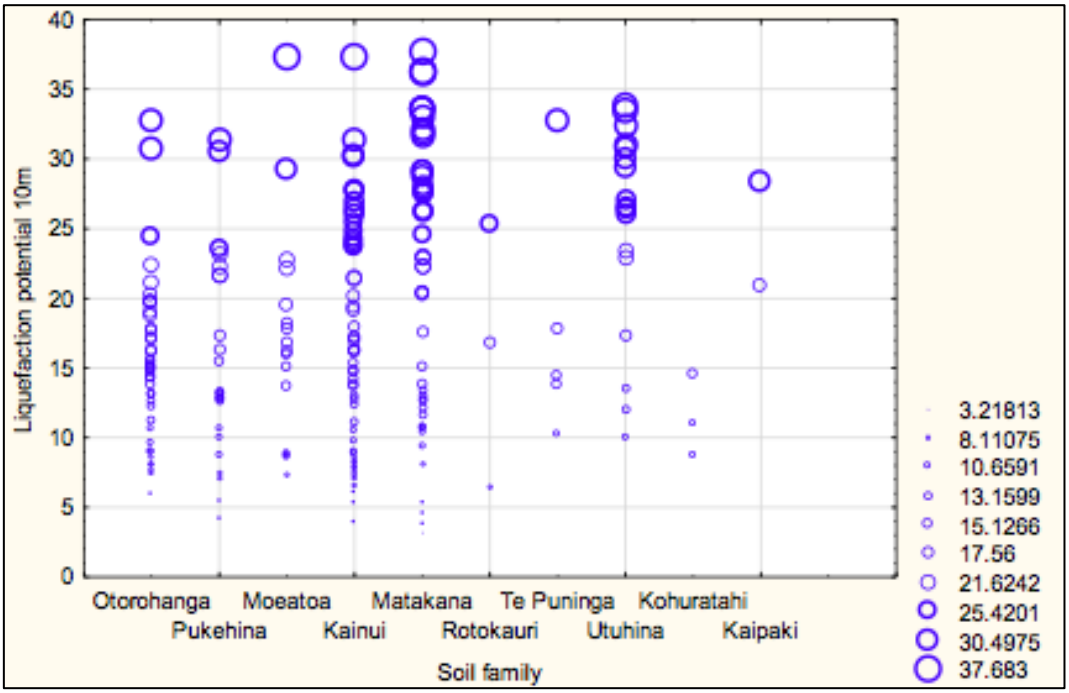

Figure 5.9 Bubble plot of liquefaction potential at 10 m depths against soil family; weighted by liquefaction potential at 10 m. Circles represent individual CPTs and their calculated LPI within that specific soil family.

5.3.2 **I-Tree analysis**

Figures 5.10, 5.11 and 5.12 present the result of Exhaustive CHAID I-Tree analysis, in which LPI at each depth (3, 5 and 10 m) is categorized on the basis of input data of soil family, slope, and elevation. From these figures (Figures 5.10, 5.11 and 5.12) it can be seen that soil family is consistently identified as the most influential factor to liquefaction potential where Utuhina*f* and Kaipaki*f* families are consistently regarded as having the highest susceptibility to liquefaction. The remaining soil families of Pukehina*f*, Moeatoa*f*, Kohuratahi*f*, Kainui*f*, and Rotokauri*f*, appear variable being output as either low or moderate susceptibility relative to Utuhina*f* and Kaipaki*f* families. Note, however, that there is relatively high variance within each class reflecting the variability within the soil families.

When another level is added to the tree graph, elevation becomes important for soil families classified as having low to moderate susceptibilities, while in contrast the high susceptibility node terminates at soil family. When looking at the range of LPI relative to the range in elevation it can be noted that soils have the highest susceptibility to liquefaction when elevation is between 38−39 m. In contrast to this, however, at greater depths (5−10 m) in those soils categorised as lower LPI, the pattern relative to elevation becomes less apparent where those that are correlated to higher elevation >39 m to 44.5 m are output as having higher LPI.

When the tree graph is grown to its full extent only sibling number appears at the lowest level and, when other methods such as C&RT were developed, slope and sibling number appeared interchangeable and therefore not of high influence to LPI relative to soil family and elevation. Siblings (the 5th category of NZSC) are defined within soil families on the basis of various physical attributes and functional horizons; they are identified by numbers and provide the primary entity depicted in S-map (Webb & Lilburne, 2011).

The susceptibility map (Figure 5.13) visually depicts the categorization from Figures 5.10, 5.11 and 5.12. The diverse nature of the field area is illustrated here with all three levels of susceptibility being apparent over short distances. However, it can be seen that on average the susceptibility class predominantly ranges from low (green) to moderate (orange) with high values being confined to the north/east of Hamilton City. The three main topographical features that can be identified on

the surface of the Hinuera Formation along the Hamilton Section of the Waikato Expressway, are small ridges up to a few metres in height, channels (paleo and current), and the interfluve and flood plain zones (flat areas with little topographical relief). When comparing Figure 5.13 with Figure 5.14 it is apparent that when the topography becomes more complex, the susceptibility is seen to decrease. Examples are low to low/moderate susceptibility in the drainage channels as well as along the ridges. The areas that are displaying moderate to high susceptibilities are mainly within the interfluve and floodplain zones where ground is near to level.

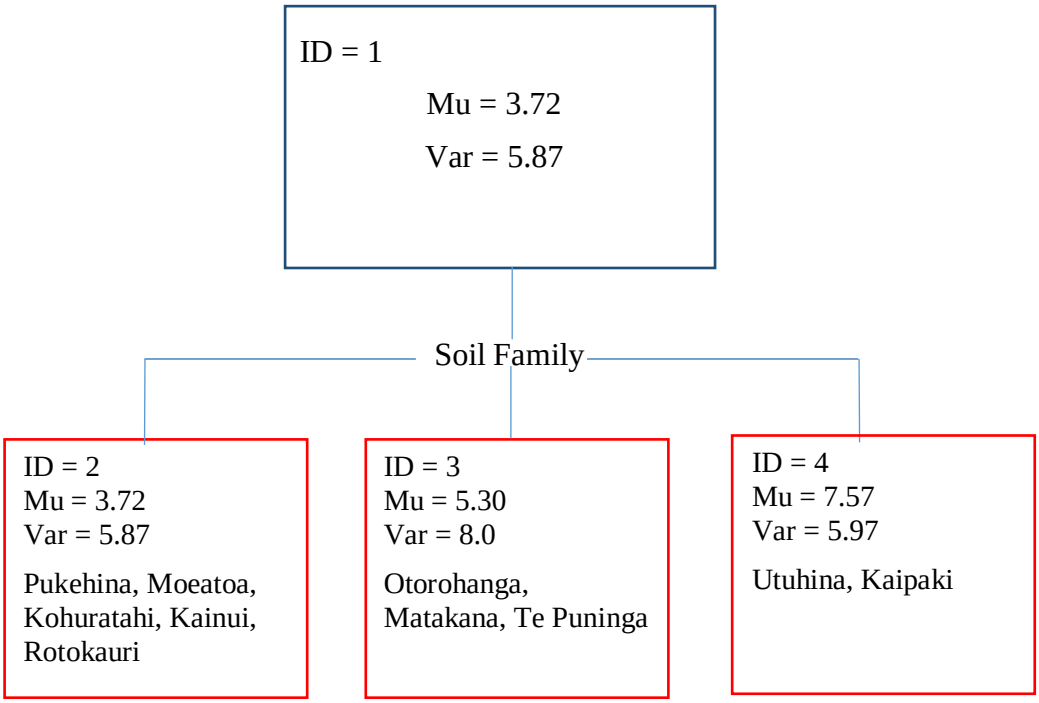

Figure 5.10 I-Tree regression analysis using Exhaustive CHAID method at 3 m depths with ID 2 including Otorohanga, Te Puninga, Matakana families; ID 3, Pukehina, Moeatoa, Kohuratahi, Kainui, Rotokauri families; and ID 4, Utuhina, Kaipaki families. In the boxes, the mean LPI (Mn) and variance (Va) are shown.

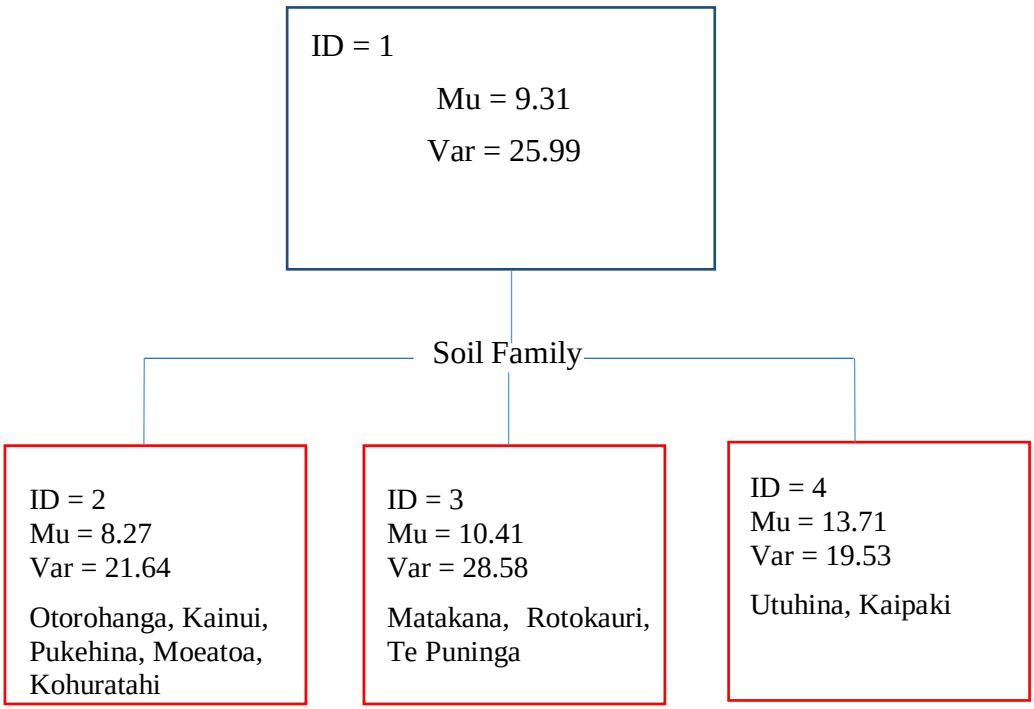

Figure 5.11 I-Tree regression analysis using Exhaustive CHAID method at 5 m depths with ID 2 including Otorohanga, Kainui, Pukehina, Moeatoa and Kohuratahi families; ID 3, Matakana, Rotokauri, Te Puninga families; and ID 4, Utuhina, Kaipaki families. In the boxes, the mean LPI (Mn) and variance (Va) are shown.

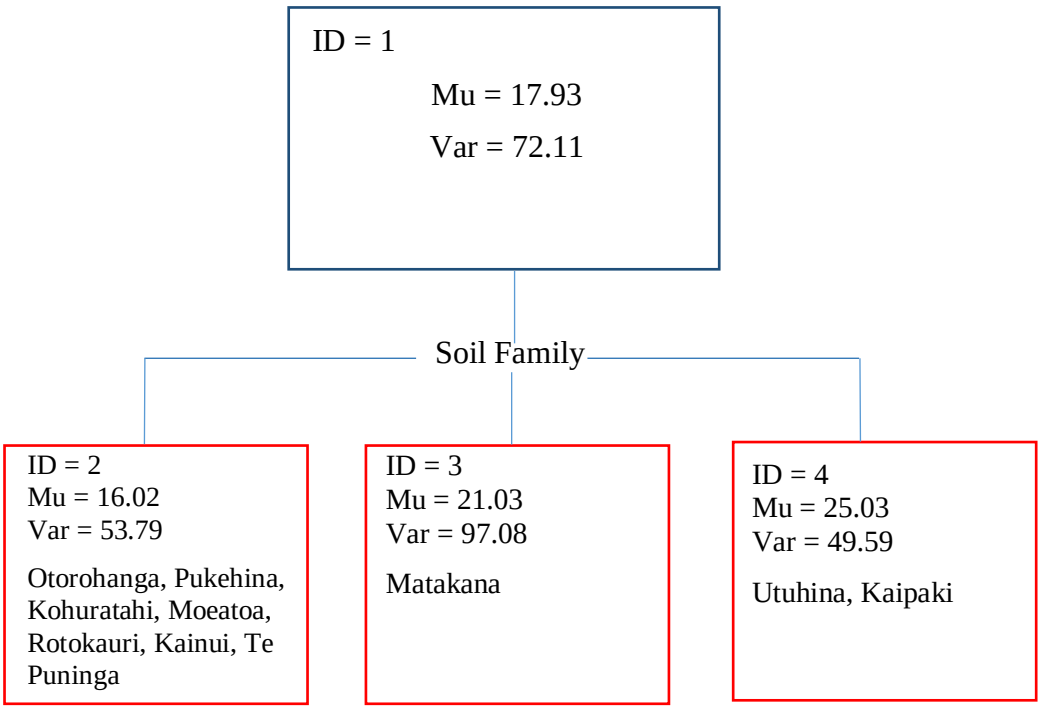

Figure 5.12 I-Tree regression analysis using Exhaustive CHAID method at 10 m depths with ID 2 including Otorohanga, Pukehina, Kohuratahi, Moeatoa, Rotokauri, Kainui, Te Puninga families; ID 3, Matakana family; and ID 4, Utuhina, Kaipaki families. In the boxes, the mean LPI (Mn) and variance (Va) are shown.

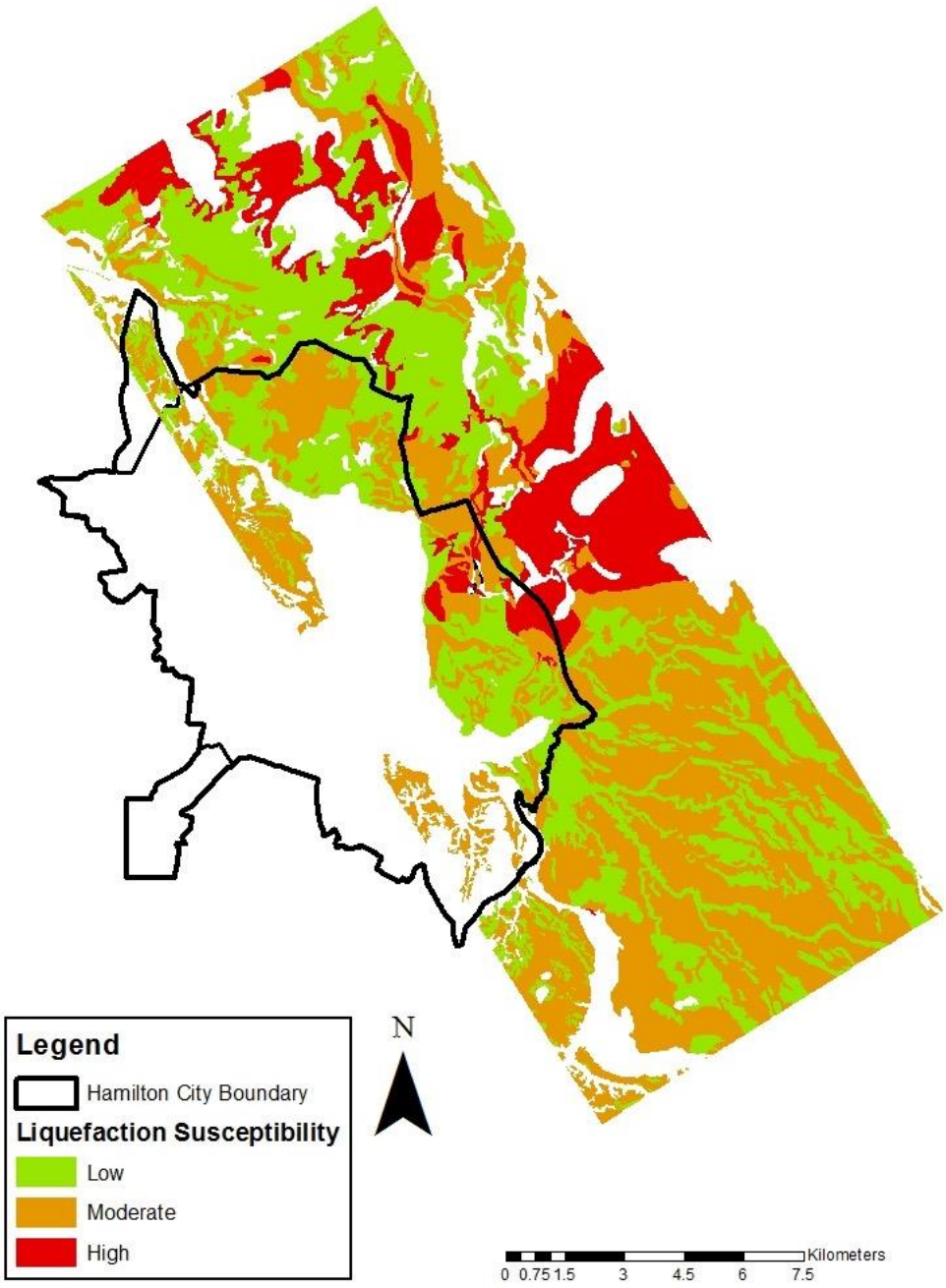

Figure 5.13 Generalised liquefaction susceptibility map of the field area based on STATISTICA™ analysis. Green= low susceptibility, Orange= moderate susceptibility and Red= high susceptibility.

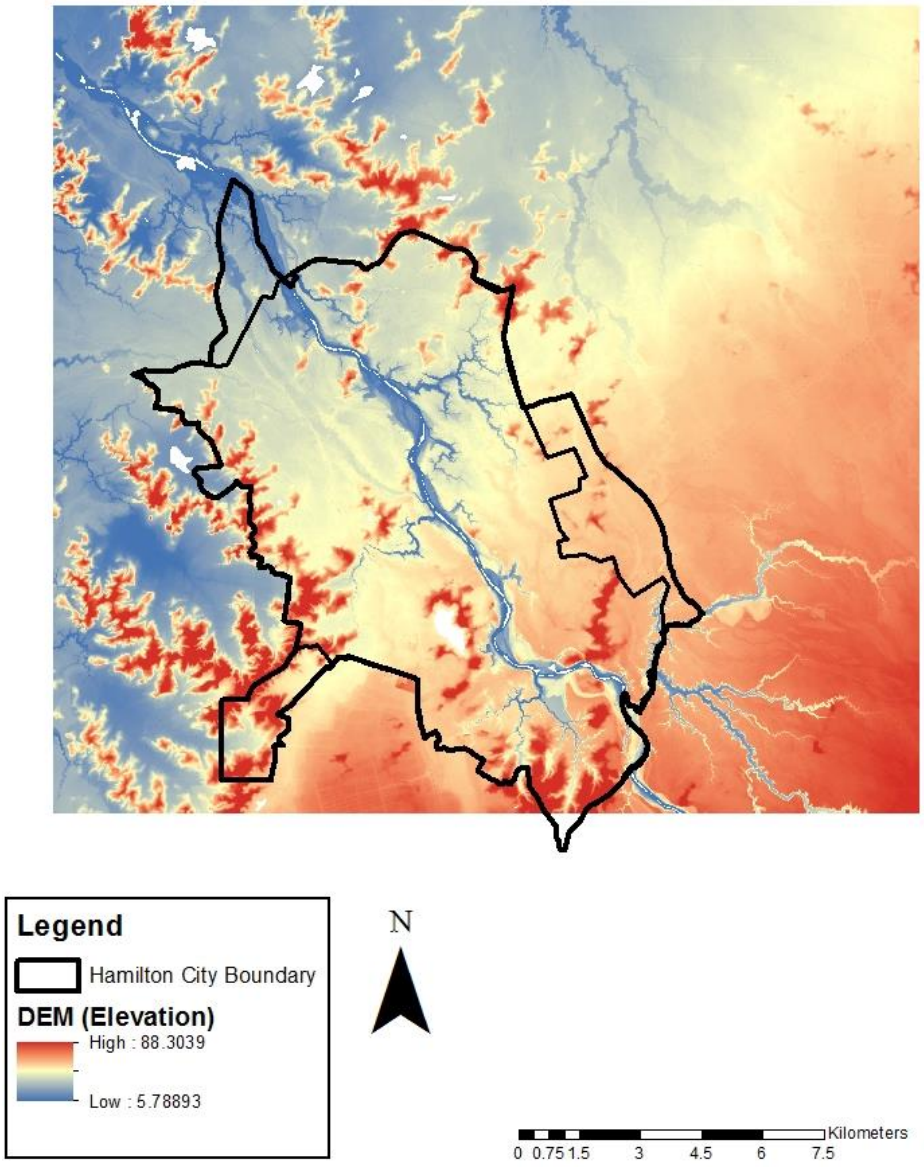

Figure 5.14 DEM of field area and greater Hamilton Basin used as comparison with Figure 4.13 to show what elevation (topographical features) are associated with depicted LPI. Black line is Hamilton City outline.

5.4 **Soil profile on Matangi Road**

The stratigraphy within Figure 5.15 was exposed during the ongoing development of the Waikato Expressway (Hamilton Section) which enabled new investigation into possible paleoliquefaction sites which would in turn further support the need for liquefaction susceptibility mapping within the Hamilton Basin. A field sketch was then drawn up illustrating the differing soil textures and the areas of distribution or irregularities and therefore areas of potential historic liquefaction.

Upon analysis of the Matangi Road soil cutting it was clear that the profile consisted of the Hinuera Formation with soil textures being predominantly silty sand to sandy silt. It can be seen in Figure 5.15 that there is clear evidence for disruption within the upper horizons to the right showing minor disruption relative to the left of the profile. At the left of the profile, there is clear evidence for vertical infiltration of water in the form of orange-brown injection like structures but with no clear source region. The left of the profile also has vertical layering of soil that upon analysis was coarser than the surrounding soil textures and greyish light brown in colour compared with the surrounding predominantly light brown to orangey brown soils. Manganese oxide mottles (redox segregations) are also present in areas of disruption with multiple pockets of greyish-light brown soils bounded by thin orange-brown horizons.

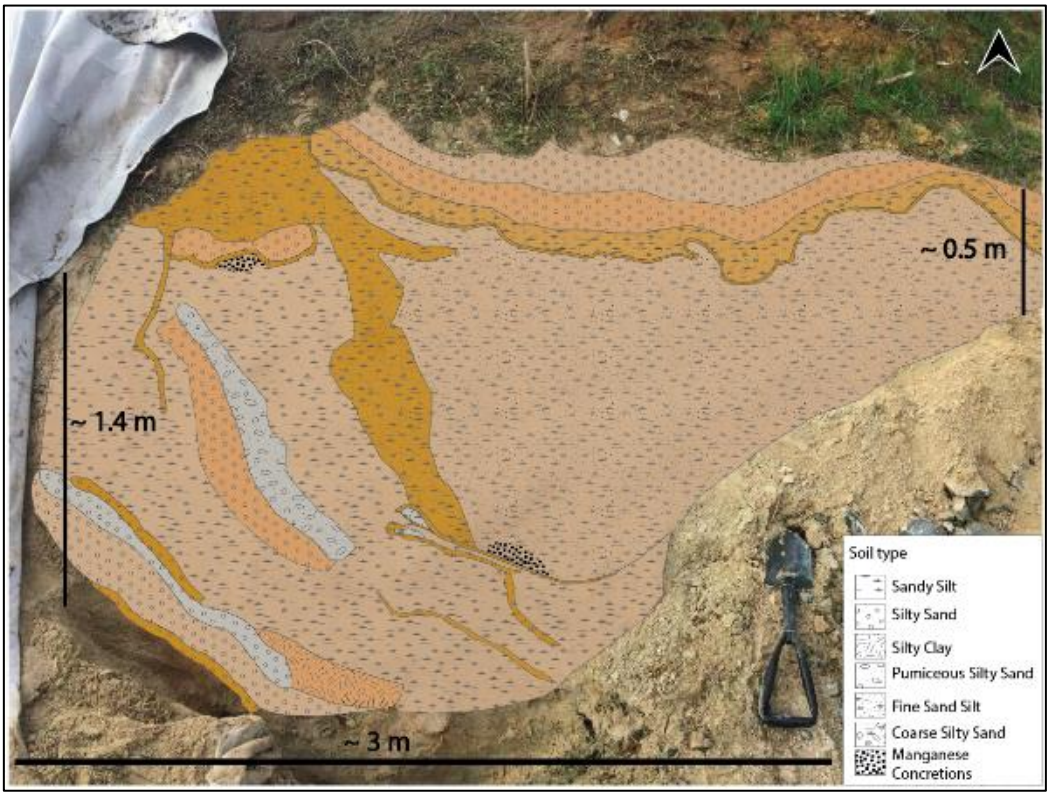

Figure 5.15 Soil cutting on Matangi Road showing disrupted stratigraphy in particular to the left of the image.

Chapter Six

Discussion

6.1 Introduction

This discussion will focus on the information that has been obtained through Cliq™ analysis. The general pattern that each CPT profile shows in relation to depositional environment will be described as well as the textures observed and how they are either aiding or inhibiting liquefaction potential based on graphs that show predicted normalized soil behaviour (SBTn). SBTn profiles then compared to Cyclic Resistance Ratio graphs (CRR), Liquefaction Potential Index graphs (LPI) and both lateral displacement and vertical settlement graphs to determine how each correlates to one another and if any commonalities can be identified. The results derived from STATISTICA™ are then discussed with focus on the correlation between soil type and topography and how the two factors may act as a preliminary assessment tool for liquefaction susceptibility of a given area.

6.2 CLiq™ interpretation

6.2.1 Soil behaviour index (SBTn)

Because of its alluvial origin the Hinuera Formation is extremely diverse spatially in texture and sedimentary structure, and hence shows considerable lateral and vertical variability in liquefaction susceptibility. Typical stratigraphies show sand-dominated materials at the base, with an increase in fines content towards the upper profile. This decrease in grain size is expected when deposition is of alluvial origin, in particular a river channel that has changed course many times, as the grain size and pattern is indicative of flow dynamics with larger, more granular (clean sand) material being deposited where energy is at its highest (upstream or at depth), while finer grains are typically deposited closer to channel termination where shallowing occurs as a result of decreasing energy by decreasing gradient downstream. (Nichols, 2009). This pattern of increasing fines within the upper profile is evident within the CPT data with the majority of profiles having a sand–dominated lower section with an increase in fines in the upper profile. However, the proportion of fines and the degree of plasticity does vary, with some profiles having some fines

content yet are still sand dominated, while others exhibit more clay-dominated behaviours (Figures 6.1) which will become important for surface manifestation which will be discussed later within this chapter.

When applying a more detailed perspective such as at the level of soil behaviour and individual horizonation, variability in LPI is likely due to differences in sand/silt/clay ratios. Higher LPI values are therefore more evident within mixed, low plasticity textures (silty sand/sandy silt) relative to profiles with predominantly coarse sand (granular) or fines (clayey silt/silty clay) textures, which predict lower LPI values. Silty sand/sandy silt textures are therefore likely to exhibit a higher liquefaction potential relative to sand (granular) or fines (clayey silt/silty clay) textures. Another interesting observation is the sharp change in texture from sand-dominated soil behaviour through to clay-like behaviour at depth (>7 m) within Figures 6.1A, B and C. The occurrence of finer grained materials at depth may suggest multiple depositional periods at that particular site.

Finer grained material may not only indicate a waning of energy but also the presence paleo floodplains. When incorporating floodplains into the paleo environment a more complex stratigraphy is presented as floodplains span a greater distance than a singular drainage channel. Floodplains have therefore likely influenced the variability of present-day soil textures notably where a new river channel cuts through an old floodplain soil texture would move from fine to coarse. This observation supports the idea that the Hamilton Basin in relation to liquefaction susceptibility is a complex one, with the often sharp changes in soil textures making site specific analyses imperative.

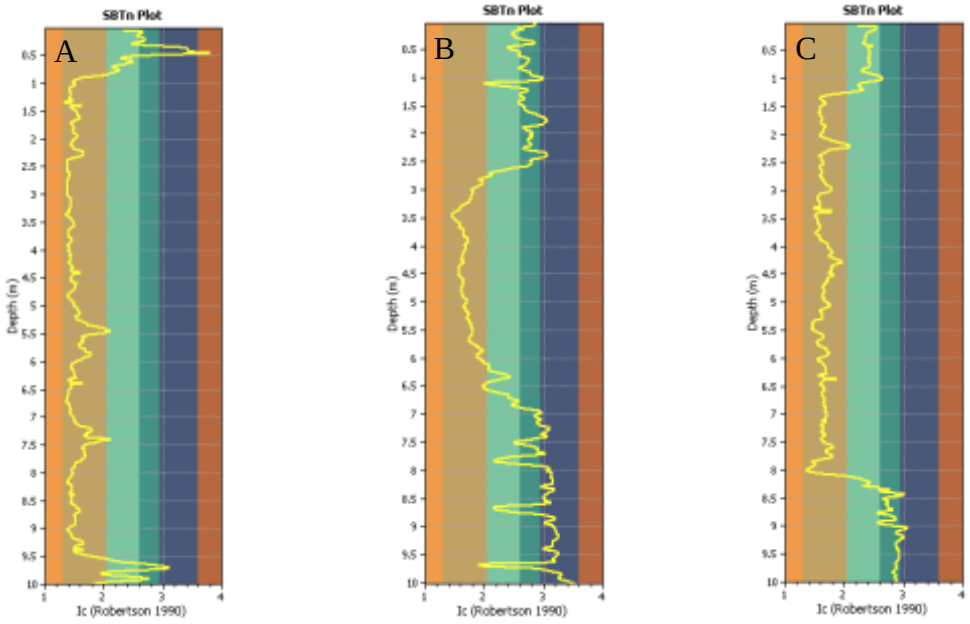

Figure 6.1 SBTn plots showing the general stratigraphic pattern within each CPT profile of the field area, with A, B and C being examples of the common pattern observed. Yellow line indicates what the soil behaviour index of the soil is at that particular depth.

It is important to take the soil behaviour derived from CLiq™ as simply a guide and not a definitive conclusion, as it merely reflects the way the soil behaves in response to penetration with no empirical evidence of the texture itself. It should also be noted that CLiq™ may underestimate the degree of plasticity within soil (Robertson & Wride, 1998). As well, the crushability of pumiceous material may overestimate LPI due to lower computed soil resistance which is particularly important to the field area as the Hinuera Formation has a prevalent pumiceous component in many horizons (Opus, 2013; Orense & Pender, 2013). In Figure 6.2A, an example of computed low susceptibility (LPI <5) can be seen, which is likely due to the soil behaviour on average being near to granular in nature, therefore increasing cyclic resistance as well as a larger grain size preventing sufficient pore water pressures due to increased drainage. In contrast, the textures in Figures 6.2B appear closer to the sandy silt (Ic>2.6) boundary in majority of the profile where there is likely a higher proportion of fines while remaining sand-dominant with an assumed low plasticity (Guo & Prakash, 1999). It was observed that soils that have a silty sand to sandy silt texture with an Ic of ~1.84-2.6 (value derived from an average of each CPT at the depth at which liquefaction potential began) may be those that are most susceptible to liquefaction (keeping in mind that this observation

is specific to the Hamilton Section of the Waikato Expressway where the CPT drill site data were obtained). This increased susceptibility to liquefaction may be due to increased settlement and subsequent pore water pressure increases under seismic stress due to the more poorly sorted nature of a mixed soil, where the finer silty material act to infill remaining pore space that medium to fine sand grains would otherwise not occupy once post seismic settlement occurs (Thevanayagam, 2000; Ibrahim, 2014).

It can be seen from Figure 6.3 that there is a narrow range in Ic where a soil behaviour will likely exhibit liquefaction potential and where it will not. Profiles with an Ic value of 1.4 showed no potential for liquefaction whereas those with 1.6 Ic had liquefaction potential indicating that even a slight change in soil texture (behaviour) can have a significant effect on LPI. A fines content of ~30–40% has been proposed as the threshold that will increase liquefaction potential while still maintaining pore space assuming low plasticity. Therefore, a soil body must still be considered as sand-dominated with a clay content less than 20% to be susceptible to liquefaction based in this criterion (Ibrahim, 2014). Plasticity is a significant factor that can act to inhibit liquefaction potential because it increases soil resistance and therefore decreases liquefaction potential. Soil textures that are clay-like in behaviour and therefore deemed as having relative plasticity act as an impermeable layer during seismic events which inhibit the expulsion of water and subsequent settlement (Sonmez and Ulusay, 2008). In contrast to this, plasticity of overlying finer grained material would likely aid liquefaction potential as it has been observed to act as a barrier to increase pore water pressure within the underlying liquefiable layer (van Ballegooy et al., 2015), therefore potentially creating preferential flow within the overlying material causing liquefaction structures that manifest at ground surface if 1- 3 m thick as suggested by Sonmez and Ulusay (2008) and . It is important, however, to consider the ratio between the overlying impermeable layer (clay cap) and underlying liquefiable layer, as in some cases if the overlying clay cap is relatively thick, it may help to inhibit surface penetration due to lack of penetrative energy from the liquefiable layer beneath, particularly if the liquefaction has happened at considerable depth.

6.2.2 **Cyclic resistance**

From the CRR plots shown in Figure 6.4, a more detailed representation of the exact depths at which liquefaction is likely to occur can be seen. This is a useful tool for looking into the factors that may influence the degree of liquefaction occurrence at the scale of individual soil horizons. Figure 6.3, for example, shows that CSR exceeds CRR at ~2.5 m and at 4.6–6.8 m where the soil behaviour exhibits a more fines-dominated texture. In contrast, when CRR is seen to exceed CSR, such as at ~3.5 m or ~9–9.5 m depth, the soils behaviour has moved into a more granular or clayey texture. This change in soil behaviour represents, in turn, a decrease in fines or an increase in plasticity therefore supporting the idea that an SBTn <1.8 or >2.8 Ic will likely not liquefy. The abundance of pumiceous material within the Hinuera formation however needs to be considered when interpreting the calculated CRR plot as it has been suggested that pumice due to its readily crushable nature does show a much lower CRR reading that would actually occur *in situ* and in the event of an earthquake.

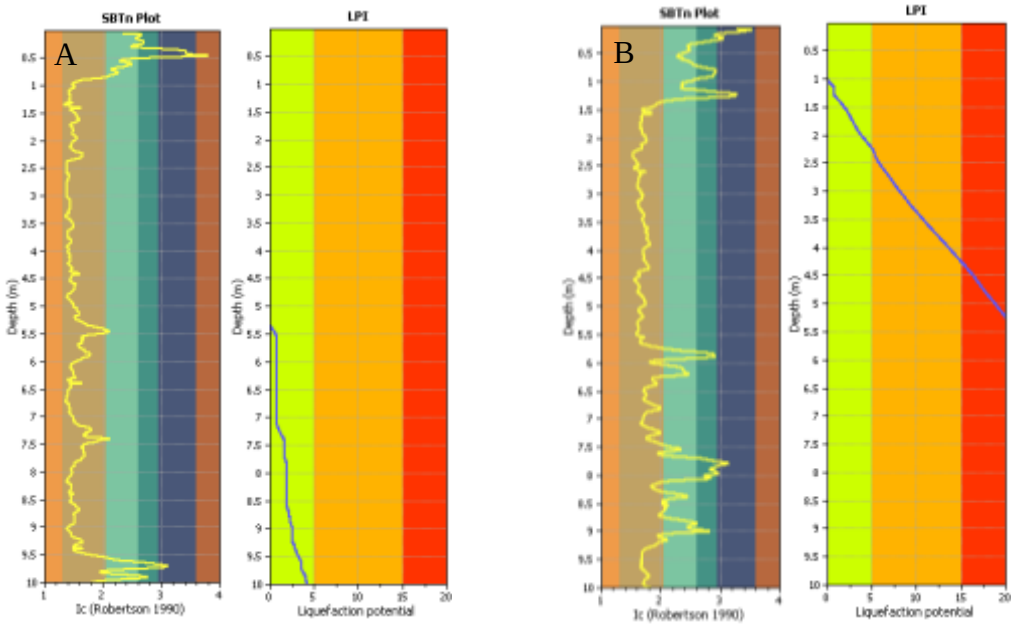

Figure 6.2 SBTn plots and their corresponding LPI plots are depicted where A represents a profile that has an overall low susceptibility to liquefaction, and B represents a profile that has an overall high susceptibility to liquefaction.

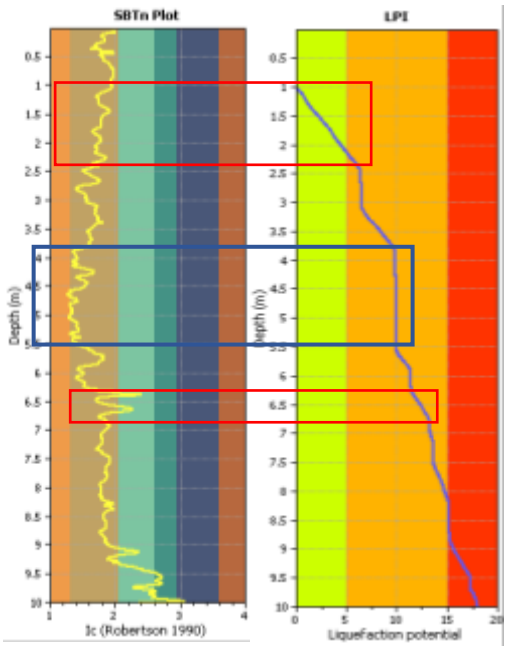

Figure 6.3 SBTn plot and their corresponding LPI plot is depicted with the red box showing that soil at that particular depth has liquefaction potential where the blue line is sloped, and the blue box indicating a soil at that particular depth that has no liquefaction potential where the blue line is vertical.

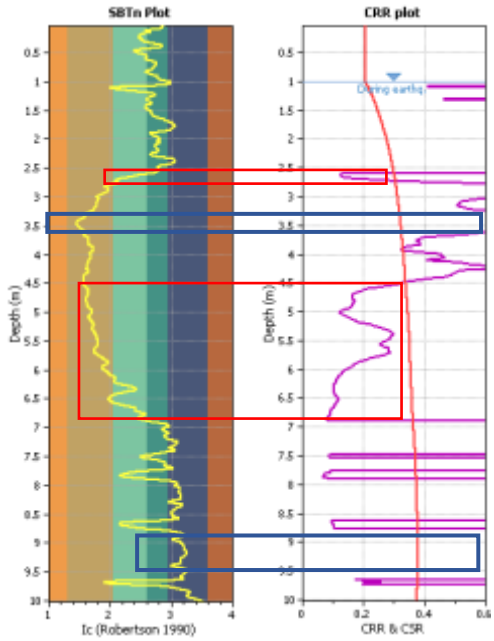

Figure 6.4 SBTn plot and their corresponding CRR plot is depicted with the red box showing particular depths where CSR exceeds CRR and what the soil behaviour at that depth is, and the blue box depicts where CSR does not exceed CRR.

6.2.3 **Vertical settlement**

Figure 6.5 in relation to settlement supports the idea that the sand/silt interface is of most concern for liquefaction susceptibility. In particular, at the depth that settlement occurs the soil behaviour is a sand/silt mixture. This observation remained true when each CPT profile was analysed. Settlement occurs in two steps, the first being the product of compaction due to seismic energy causing the soil grains to reorient and pore water pressure to subsequently increase, and the second being subsequent expulsion of pore water either laterally or to the Earth's surface in the form of injection structures (dikes or sills). This process often removes coarse sediment, therefore increasing the degree of settlement (Obermeier, 2009). For settlement occurrence and predicted influence on infrastructure, the depth at which the settlement is likely to occur will become important. If a predicted liquefiable layer is close to the surface, it is likely that in the event of an earthquake, surface manifestation will occur, either producing ejection structures or sand boils and lateral spread, each of which can be very damaging to overlying infrastructure.

6.2.4 **Lateral spread**

It is well documented that lateral spread is most likely to occur when the soil body in question is near to a free face or steep gradient such as a river channel (Obermeier, 1996). Within the Hamilton Basin, this environment is limited to the main river channel and some paleo-channel banks or gully walls that may have enough of a gradient to promote lateral spread. In the field area, the main river channel's influence will be restricted to the southern end, suggesting that the potential for lateral spread may be of most concern within this area (Figure 6.6). However, within this particular research, slope data associated with the specific CPT drill sites used were not available and therefore any interpretation pertaining to lateral spread potential is merely speculative based on observation of the field areas DEM and computed LPI. Therefore, empirical evidence with consideration on the effect that site specific factors such as the presence of a free face (paleo channel walls, gully sides) may have on liquefaction induced lateral spread needs to be considered.

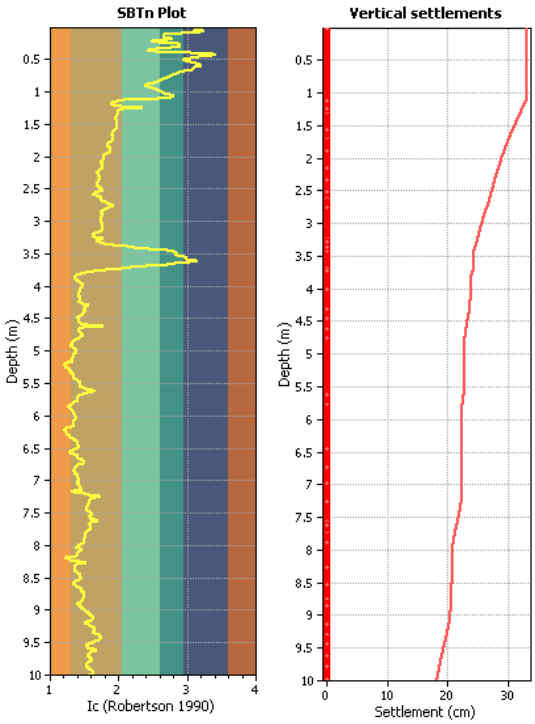

Figure 6.5 SBTn plots and corresponding vertical settlement plot is depicted with the red box showing particular depths where vertical settlement occurs.

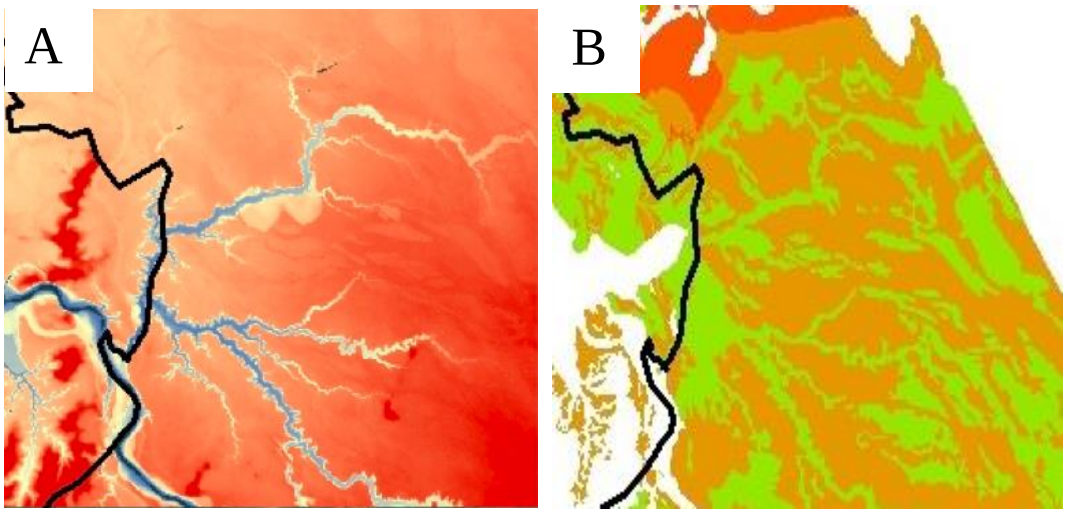

Figure 6.6 Snap shot of the southern end of the field area with focus on the abundance of drainage channels (gullies) within this section with the black line indicating the Hamilton City outline. A, is derived from DEM imagery and B is from liquefaction susceptibility map which will be discussed later in this chapter.

6.2.5 **Liquefaction potential index (LPI)**

In relation to a more generalized interpretation of liquefaction potential within a soil body, the cumulative value of Liquefaction Potential index (Figures 5.3 A–H in Chapter 5) allows classification into low, moderate or high susceptibility. These LPI graphs, although simple are useful as they not only show whether or not a specific drill site has liquefaction potential but also will show at which point the profile begins to exhibit that potential. The average depth of liquefaction occurrence observed in this study is ~1.2 m. Depth of liquefaction occurrence is dependent on water table depth which is set at 1 m for this research and therefore explains why liquefaction does not occur above 1 m. Liquefaction potential is also reliant on overburden, where if a liquefiable soil layer is at too greater depth (>20 m), the overburden is likely to be too great, where the soil would have insufficient pore space to begin with due to increased packing under normal stress as well as there being too greater distance for injection structures to exhibit surface manifestation if liquefaction did occur. If a soil body that would otherwise have the potential to liquefy is too shallow, however, then it is likely that there would not be sufficient normal stress to generate pore water pressure to a point where liquefaction would occur. In contrast to this, however, is if an overlying and impermeable layer were present it may generate sufficient pore water pressure to a soil horizon that would otherwise be considered as too shallow. An impermeable layer can be in the form of a rooting mat from vegetation, soil with a relative plasticity (>20%), and in an urban setting overlying infrastructure such as concrete could act as a barrier to pore water dispersal in the underlying soil.

There are many variables, however, that influence the occurrence of liquefaction which can vary drastically just a few metres apart, which is why site-specific investigation is crucial. CLiq^{TM} does not account for the influence of an overlying impermeable layer nor does it account for the presence of overburden. Therefore, other *in situ* conditions must be considered at the specific site of interest when making developmental decisions regarding CPT analysis (van Ballegooy et al., 2015).

Based on the information that has been presented within this section, a profile that shows stratigraphy consistent with high LPI output is proposed (Figure 6.7). The key features within this profile are the presence of an impermeable 'barrier' (>3 Ic) overlying the liquefiable layer (~1.8-2.6 Ic). The ratio of these two layers in relation to their relative thickness should also be noted as the impermeable barrier is smaller but not insignificant. This impermeable 'cap' aids in pore pressure increase but is thin enough for the underlying soil material to penetrate through. Subsequent liquefaction injection structures and in turn surface manifestation would then result (liquefiable layer is around 3 m). This profile has been derived not only from information gained from the CPT data within this research (mainly the SBTn value for the higher liquefaction potential) but also from review of the literature in relation to the impermeable layer effects as this is not accounted for within CLiq™ as explained earlier.

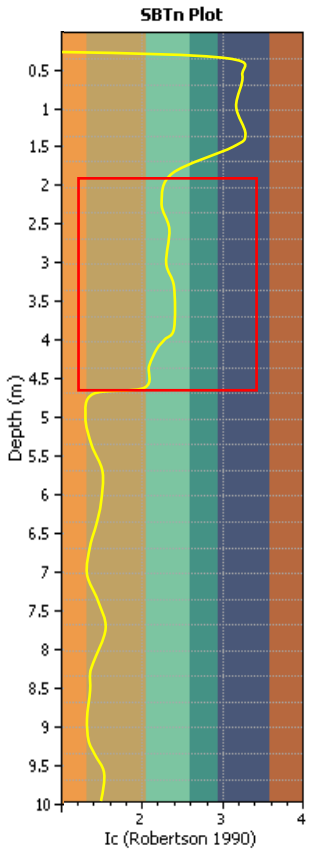

Figure 6.7 Profile depicted is a simple representation of a stratigraphic pattern that based on this research would be consistent with a high LPI with the red box showing the proposed 'liquefiable' layer.

6.3 **STATISTICA™ interpretation**

Statistical analysis showed that there may be a relationship between soil family and the underlying soil (Hinuera Formation) that is subject to liquefaction. It is therefore suggested that factors that influence pedological soil formation, such as water table level, soil texture (relative to genesis), and topographic position, are similar factors to those that influence liquefaction susceptibility. With this idea in mind, commonalities that each soil family within each category of low, moderate and high liquefaction susceptibility were determined (Appendix B). Commonalities that were of most focus included soil texture, genesis and drainage properties to see whether a pattern could be established as to why such soils were placed within the same category of liquefaction potential.

Both Utuhina*f* and Kaipaki*f* are peaty (Appendix B) which indicates a sustained, high water table with underlying textures associated with alluvium (sand and silt). Within this research, the Utuhina and Kaipaki soil families consistently have LPI values within the high-moderate range at all depths. Another significant factor of these soil families is that peat formation is indicative of less complex topography (flat to undulating) due to the process of peat formation needing level or slightly concave topography in order to sustain a saturated and therefore anoxic condition for partial organic matter decay (Davoren, 1978; Green and Lowe, 1985; Buol et al., 2011; Dargie et al., 2017). A high water table is a prerequisite for liquefaction, and organic surface soils reflect this water table level as well as sand/silt mixtures being most likely to liquefy as shown by Cliq™ analysis with the diverse nature of an alluvial system typically having these soil textures. While the organic soils or peats themselves are unlikely to liquefy, the underlying materials (Hinuera Formation) are potentially highly susceptible. Soil families that were classified as having lower susceptibilities on average were more of a mixed texture and lacked that dominant organic component, suggesting lower water tables due to better drainage conditions, or a more complex topography.

6.3.1 **Topography and liquefaction potential**

Complex topography can be defined as a change in relief where if elevation is seen to increase or decrease past a specific point, and in the case of this particular research if ground level is above or below ~38 m, then it can be assumed that the topography has changed into higher ground, i.e. a ridge structure, or lower ground likely a paleo channel and therefore this topography is deemed in this particular case to be 'complex'. As outlined within Section 4 (results), three distinguishing topographical features were recognized (Table 6.1). It can be predicted that flat to undulating topography within the Hamilton Basin corresponds to the interfluve and floodplain zones that would have existed alongside its corresponding river channels system. The soils within the interfluve and floodplain zones during the time of deposition would have been deposited in a low energy environment (relative to the centre of an active river channel) and therefore a relative proportion of fine grained material has been deposited within these areas developing a mixed (sand/silt/clay) soil type. As explained earlier this is likely to have a higher susceptibility to liquefaction if the clayey (plastic) soil is limited to the upper profile.

In specific relation to topographical influence within the interfluve and floodplain zones, water table levels are likely to be high and poor draining due to the lack of slope gradient which would be otherwise generated by changes in relief. In contrast to the interfluvial and floodplain zones, which is suggested as an environment that will likely increase liquefaction susceptibility, elevated land (ridges and low mounds) and paleo-channels or swales, will both likely decrease liquefaction susceptibility according to the data gathered within this research. For ridges, slope and overburden become the important factors for liquefaction potential as the gradient that elevated land creates will increase water flow and subsequent drainage and therefore result in a lowered water table and reduced pore water pressure increase in the event of an earthquake. Over burden, as discussed earlier within this section, if too great will compress the soil beneath and therefore reduce the available pore space to enable pore water increase. Within drainage channels this decreased susceptibility is likely due to the fact that within high energy portions of river systems coarser materials are deposited and therefore have increased drainage. One other reason that elevated land would inhibit liquefaction potential is the distance it

creates from a liquefiable soil and the ground surface. Surface manifestation is therefore inhibited, where injection structures may not be penetrative enough to reach the surface and cause significant displacement. It can therefore be suggested that areas of flat to undulating land of ~38 m elevation above sea level within the Hamilton Basin are likely to have the most potential to liquefaction in a seismic event.

Table 6.1 Three main topographical features within the field area, their associated elevation and the predicted liquefaction potential.

Topographical feature	Associated elevation	Predicted liquefaction potential
Interfluvial and floodplain	38-39 m	Moderate to high
Ridge or low mound	>39	Low to moderate
Paleo-channel or slight depression (swale)	<38	Low to moderate

As an extension of the idea that topography can act as a predicting factor for liquefaction potential, the origin and texture of overlying pedological soil can also provide a simple first-pass predictor of liquefaction susceptibility at a site as they indicate the physical conditions of the soil below as well as being a product of topographical influence. It is important to remember, however, that soil family attributes simply act as a guide that aids in decision making on whether the site should be investigated further. Pedological soil is unlikely to liquefy itself due to it being near surface and therefore lacking sufficient overburden for pore pressure build up under seismic stress.

With these observations it is likely that areas of potentially significant liquefaction occurrence can be identified in advance. Low relief topography is a requirement for liquefaction occurrence and, within the Hamilton Basin, the Hinuera Formation is the dominant soil parent material of the alluvial plains with more recent alluvial sediments only being found in close proximity to the Waikato River and therefore not within the field area (Manville, 2002; Edbrooke, 2005). Organic soils, such as Kaipaki*f*, and Utuhina*f* assuming they are underlain by Hinuera Formation, could very well warrant the need for further liquefaction testing based on the conclusions derived from statistical analysis. This idea is then further supported in Figure 6.8

with the higher liquefaction potential (A) occurring on areas of lower relief and less complex topography (B). It can also be seen, however, that when looking at Figure 6.8 that areas of moderate susceptibly (orange) can also occur on areas of higher elevation as due to the undulating nature of the Hamilton Basin, there are many features that although not considered as ridges are elevated above the defined interfluvial and floodplain zones. These areas may be of importance as the slight gradient they pose may aid in lateral spread occurrence much as an open face would. Low liquefaction appears to be corresponding most commonly with low lying land and in particular drainage channels. Upon analysis from STATISTCA™ and the development of Figure 6.8, some inference could be made. Using the knowledge obtained within the study related to the apparent relationship between liquefaction, soil texture and topography. Areas that have localized peat formation within the Waikato region could therefore be determined as having a likely high susceptibility as seen in Figure 6.9 and therefore a preliminary assessment map for areas of high liquefaction potential could be developed.

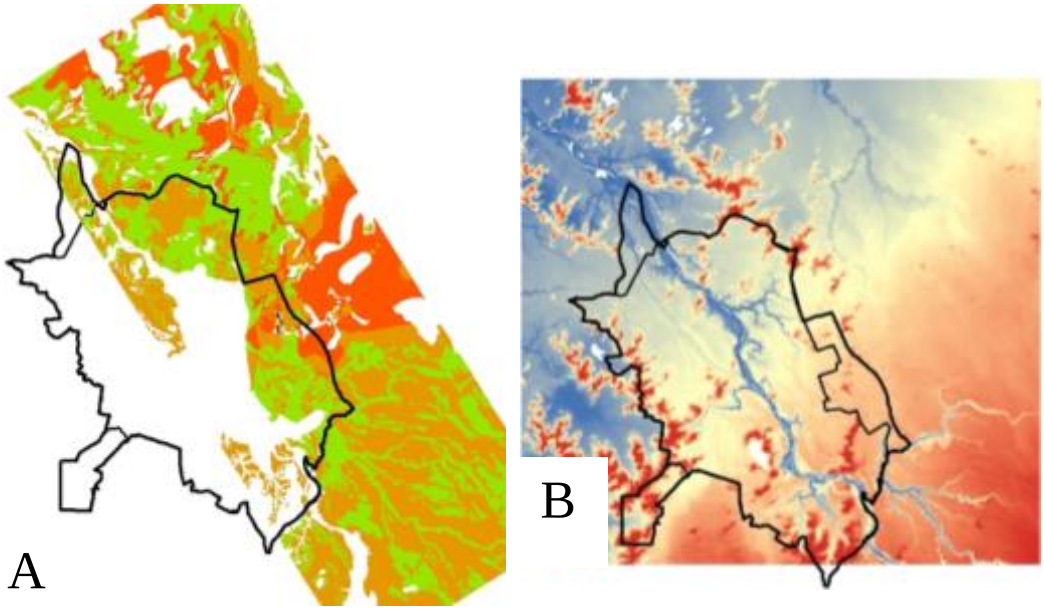

Figure 6.8 Susceptibility map (A) developed from results of this research with corresponding DEM map (B) to illustrate what topographical feature corresponds to which LPI output.

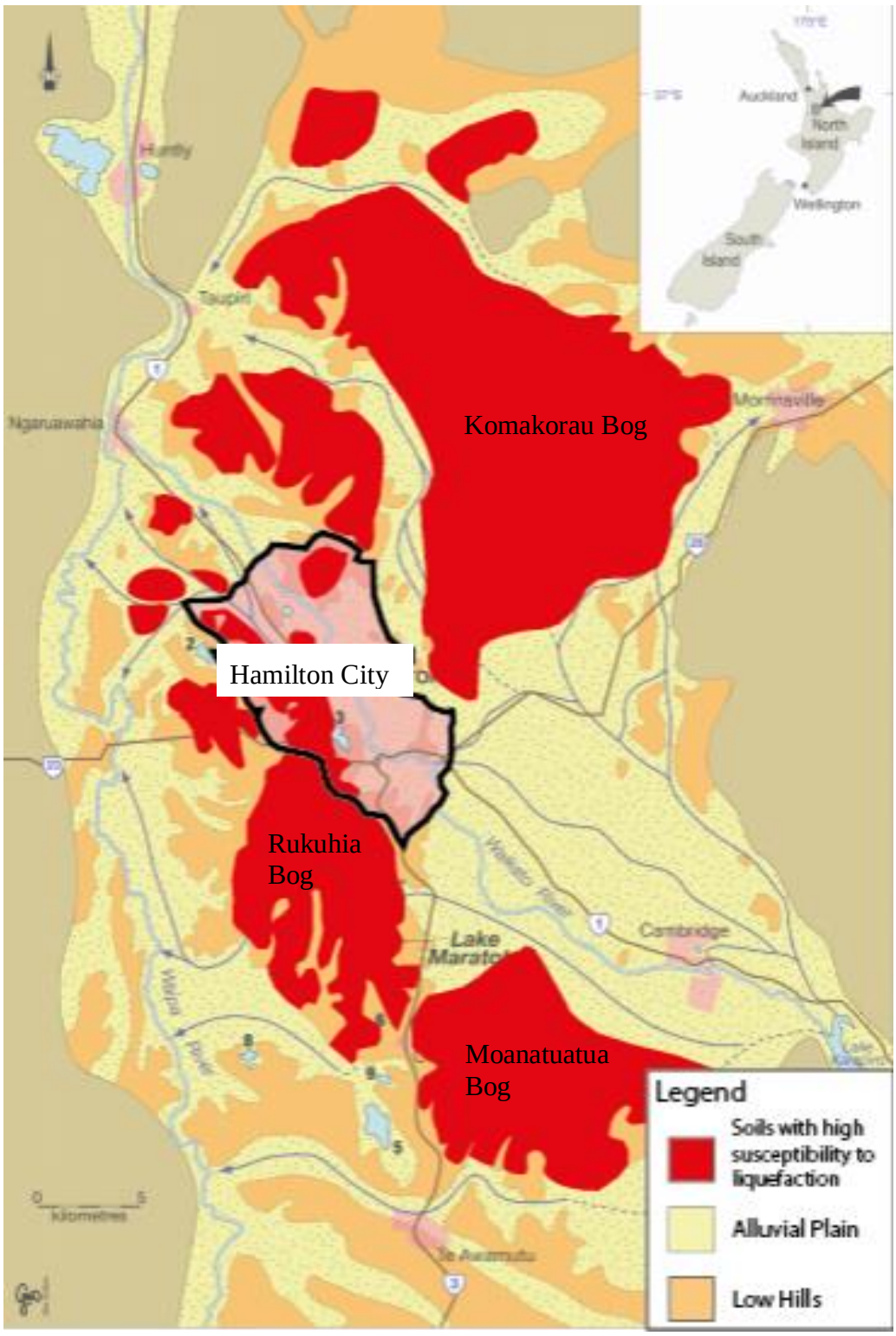

Figure 6.9 Hamilton Basin landscape features, present day from Lowe (2010) with red shapes drawn overtop of localized peat formation/bogs to indicate where soil will be of highest susceptibility to liquefaction. Other important features to note from the map included the sediment depicted in yellow being the alluvial plain (Hinuera Formation) and the orange features being the low hills.

6.4 **Limitations of the research**

6.4.1 **Data availability**

The availability of the data was a significant limitation within this research due to it being very site specific where CPT drill sites are only created when they are directly related to a particular development site such as in the case of the Waikato Expressway, Hamilton Section. As geotechnical work is a recent phenomenon with its need being realized after the Christchurch Earthquake, CPT sites and their available raw data within the Hamilton Basin have limited accessibility. Such location-specific data meant that spatial variability was a significant restriction with the data presented within this research having a linear pattern with little lateral variation. The nature of the data used in this research limited the amount of analysis that could be carried out such as predictive contouring that would be based on established data points as well as limiting the extent as to which a susceptibility map could be developed.

6.4.2 **Statistical analysis**

In relation to soil families, the spatial variation of the data set was again a significant limitation as there was not a standardized amount of CPT drill sites that passed through each soil family. When looking at the statistical component of this research, in particular within the bubble plots, the inconsistency is clear with soil families such as Otorohanga*f* and Matakana*f* having many CPT drill sites relative to Kaipaki*f* and Kohuratahi*f* with only 2 or 3 drill sites. Soil families that had only one data point were removed from the analysis as such lack of data could not serve an accurate representation of the relationship between liquefaction potential and soil type for that particular soil family. The range that is seen within these bubble plots then leads into limitations within the I-Tree analysis. A soil family with a larger range (more data points of differing values) will have a lower average and would likely be categorized into lower susceptibility classes even though they may have many that fall within the upper reaches of LPI. In contrast, those that have few data points that fall within the upper reaches of LPI will have a lower range and therefore a higher average and will be computed as high susceptibility whereas if more data were available the range may have been larger and therefore have computed a different outcome. This is a limitation when looking at the overall susceptibilities of specific Hamilton soils, as those soil families that have many data points that

read as a higher LPI, regardless of the range, should still be considered as having a potential susceptibility to significant liquefaction.

6.4.3 **Quantitative analysis**

The lack of quantitative parameters (continuous and not categorical) also poses a limitation which leads onto future field work obtaining parameters such as texture (sand, silt and clay) percentages as well as grain size and density measurements which would enable more extensive statistical analyses to be carried out to show the proposed complex relationship between soil texture and liquefaction potential. A practical experiment may also aid in showing this relationship such as a shaking table test with soils derived from in field that have differing textures to obtain more exact soil behaviour values that pertain to a high liquefaction susceptibility as well as concluding on the degree of plasticity in which a soil may exhibit before liquefaction will not occur. SPT or bore hole test pits would also aid in accurate soil behaviour results as it is well known that CLiq^{TM} soil behaviour outputs can misinterpret soil type such as a very plastic soil being output as a dense sand due to its high resistance to penetration. Therefore a physical *in-situ* assessment of that specific soil would enable more confident conclusions to be drawn. Other site-specific investigations must also be carried out, as factors such as an impermeable barrier (clay cap) which would aid increases in pore water pressure and therefore likely increase the degree of liquefaction are not considered within CLiq^{TM} calculations. However, in contrast to this need for empirical evidence, new methods developed by Maurer et al (2015), inspired by Ishihara deemed LPI$_{ISH}$, do incorporate the effect that the relative thicknesses of the liquefiable layer and overlying impermeable layer have on LPI. This inclusion of seemingly influential surface features will likely led to a more confident prediction of liquefaction potential and its surface manifestation as well as supporting in a quantitative method their influence on the degree of liquefaction occurrence.

6.5 **Summary**

Soils that have a behaviour (texture) of sandy silt to silty sand are most likely to exhibit moderate to high liquefaction potential. Soils that are of a granular (coars sand) or clay-like (plastic) texture will likely exhibit a low liquefaction potential. Consideration of the relative thickness of the liquefiable layer and an overlying impermeable ‘cap’ (if present) must be given to determine probable surface manifestation. Topographical influence has been deemed as important in relation to liquefaction potential in a given soil body, where ‘complex’ topography will likely exhibit lower liquefaction potential relative to areas of flat to undulating land, i.e within the interfluve or along floodplains.

Chapter Seven

Summary and conclusions

7.1 CLiq™ analysis

CLiq™ analysis using CPT raw data showed that soils associated with the proposed Waikato Expressway, Hamilton Section, do have on average a liquefaction potential (factor of safety <1). When the profiles were separated into 3 m, 5 m and 10 m depths, liquefaction potential ranged from low to high where at 10 m depths susceptibility on average was high. At 3 m depth, which is most likely to show surface manifestation, liquefaction potential was low to moderate with the majority considered as having a low LPI.

Soil textures (behaviour types) ranged from coarse sand to silt to clay with few organics. Those that showed a 'mixed' sand texture, such as those that displayed a silty sand to sandy silt texture (~1.8-2.4 Ic), were the most likely to be susceptible to liquefaction upon seismic stress, whereas those soil textures that were calculated as being too granular or clay-like in behaviour are likely to inhibit liquefaction occurrence. Clay–like soils, however, were shown to aid liquefaction occurrence and in particular surface manifestation when overlying the liquefiable layer and near to ground surface.

7.2 STATISTICA™ analysis

7.2.1 Bubble plots

Bubble plots showed that the data collected were limited with respect to consistency of how many data points passed through each soil family. However, bubble plots did show clearly which soil families had the higher LPI values, those being Otorohanga*f*; Kainui*f*; Matakana*f*; Utuhina*f* and Kaipaki*f*.

7.2.2 **I-Tree analysis**

I-Tree analysis calculated soil family as the most influential factor to liquefaction when compared against slope, elevation and soil sibling number. Soil families that were consistently classified as being associated with the highest liquefaction potential were Utuhina*f* and Kaipaki*f*. Both of these are peaty in texture and associated with organic soils. It was found that where peat resided, the land had little relief (flat to slight depression) and was associated with a high water table. The presence of a high water table and a near to level ground surface are both factors that are likely to promote liquefaction under seismic stressors. Elevation was calculated as second most influential factor for liquefaction potential. Where soils are at ~38-39 m in elevation, they are likely to have a higher susceptibility to liquefaction. Therefore, flat to undulating land corresponding to interfluve and floodplain zones were computed as most likely to liquefy. The low ridges and paleo-channels of the basin were computed as having a lower susceptibility to liquefaction.

7.3 **ArcMap GIS analysis**

When the results of the I-Tree analysis were displayed within ArcMap GIS and compared to landscape feature maps, it appeared that those soils that were computed as having a higher susceptibility to liquefaction corresponded to localized peat formation. The results of the I-Tree analysis enabled the development of a two preliminary liquefaction assessment maps. One showing all levels of liquefaction susceptibility (low–high) relative to topography (Figure 5.13) and the other showing just those soils that were calculated as high LPI and correlated to localised peat bog formation (Figure 6.9). These two maps may aid in identifying areas that are most likely to liquefy and will therefore require further investigate to determine an accurate risk.

7.4 **Conclusions**

This study has resulted in four key conclusions

- Soils of a silty sand to sandy silt texture (mixed sand soil) have the highest susceptibility to liquefaction (~1.8-2.4 Ic).

- Soil family is the most influential factor to liquefaction with elevation being the second most influential factor.

- Pedological organic soils (Peat formation) have shown a correlation to high liquefaction potential with the Hamilton Basin.

- A correlation between soil liquefaction and topographical features show that interfluve and floodplain zones have the highest liquefaction susceptibility relative to the low ridges and the paleo channels of the Hamilton Basin.

7.5 **Future work**

Suggestions for future work following on from this study are outlined below

It is suggested that further research includes the addition of empirical evidence to expand the quantitative database that this research has provided. Empirical evidence collected should include numerical representations of texture (percentages pertaining to sand/silt/clay quantities) to determine a more accurate range where soils will likely liquefy and where they will not. Particular interest should be paid to soils that are pumice rich to determine just how much influence pumice has on LPI. Further investigation into the ratio between the thickness of the liquefiable layer and the overlying clay cap if present should also be carried out to determine when soil layer is too narrow or too thick to display liquefaction.

Incorporation of empirical evidence into research by gathering *in situ* samples of soils that have been concluded in this study as having a high susceptibility to liquefaction is also suggested. Soils underlying peat bogs should be tested to see if these soils do display significant liquefaction occurrence i.e. shaking table test.

A wider range (particularly spatially) of CPT data should then be collected to enable expansion of the susceptibility map established within this study. SPT data should also be collected to ensure accuracy of results as discussed within this study, CPT data can misinterpret soil behaviour (texture). Finally, the gained spatial variability in CPT data should then be utilised within ArcMap GIS in order to create contours which will provide another method of determining the field areas pattern of liquefaction susceptibility.

References

Andrus, R. D., & Stokoe II, K. H. (2000). Liquefaction resistance of soils from shear- wave velocity. Journal of geotechnical and geoenvironmental engineering, 126(11), 1015-1025.

Berra, F., & Felletti, F. (2011). Syndepositional tectonics recorded by soft-sediment deformation and liquefaction structures (continental Lower Permian sediments, Southern Alps, Northern Italy): stratigraphic significance. Sedimentary Geology, 235(3), 249-263.

Ballegooy, S.V, Wentz, F., & Boulanger, R. W. (2015). Evaluation of CPT-based Liquefaction Procedures at Regional Scale. Soil Dynamics and Earthquake Engineering, 79, 315-334.

Bizhu, H. E., & Xiufu, Q. I. A. O. (2015). Advances and Overview of the Study on Paleo‐earthquake Events: A Review of Seismites. Acta Geologica Sinica (English Edition), 89(5), 1702-1746.

Bruce, J.G. (1978). Soils of Hamilton City. *N.Z. Soil Survey Report* 31.

Buol, S. W., Southard, R. J., Graham, R. C., & McDaniel, P. A. (2011). Soil genesis and classification. John Wiley & Sons.

Clayton, P. J., & Johnson, J. T. (2013). Liquefaction resistance and possible aging effects in selected Pleistocene soils of the Upper North Island. Paper presented at Proc. 19th NZGS Geotechnical Symposium. Queenstown, New Zealand.

Dargie, G. C., Lewis, S. L., Lawson, I. T., Mitchard, E. T., Page, S. E., Bocko, Y. E., & Ifo, S. A. (2017). Age, extent and carbon storage of the central Congo Basin peatland complex. Nature, 542(7639), 86-90.

Davoren A. [with McCraw, J.D., Thompson, K.] (1978). A survey of New Zealand peat resources. Ministry of Works, Water and Soil Technical Publication 14. 157 p. + maps.

De Magistris, F. S., Lanzano, G., Forte, G., & Fabbrocino, G. (2014). A peak acceleration threshold for soil liquefaction: lessons learned from the 2012 Emilia earthquake (Italy). Natural Hazards, 74(2), 1069-1094.

Donahue, J. L. (2007). The liquefaction susceptibility, resistance, and response of silty and clayey soils. ProQuest.

Edbrooke, S. (2005). Geology of the Waikato area. Scale 1: 250,000. Geological Map 4. IGNS, Lower Hutt. 68pp. + map 4.

Ettensohn, F. R., Rast, N., & Brett, C. E. (Eds.). (2002). Ancient seismites (Vol. 359). Geological Society of America.

Eslami, A., Mola-Abasi, H., & Shourijeh, P. T. (2014). A polynomial model for predicting liquefaction potential from cone penetration test data. Scientia Iranica. Transaction A, Civil Engineering, 21(1), 44.

Eurocode 8. (2004) EN 1998-5, design of structures for earthquake resistance—part 5: foundations, retaining structures and geotechnical aspects. CEN European Committee for Standardization, Bruxelles, Belgium.

Green, J.D., Lowe, D.J. (1985). Stratigraphy and development of c. 17 000 year old Lake Maratoto, North Island, New Zealand, with some inferences about postglacial climatic change. New Zealand Journal of Geology and Geophysics 28, 675-699.

Guo, T., & Prakash, S. (1999). Liquefaction of silts and silt-clay mixtures. Journal of Geotechnical and Geoenvironmental Engineering, 125(8), 706-710.

Haskell, J. J. M., Madabhushi, S. P. G., Cubrinovski, M., & Winkley, A. (2013). Lateral spreading-induced abutment rotation in the 2011 Christchurch earthquake: observations and analysis. Geotechnique, 63(15), 1310.

Heidari, T., & Andrus, R. D. (2010). Mapping liquefaction potential of aged soil deposits in Mount Pleasant, South Carolina. Engineering Geology, 112(1), 1- 12.

Huang, Y., & Yu, M. (2013). Review of soil liquefaction characteristics during major earthquakes of the twenty-first century. Natural hazards, 65(3), 2375-2384.

Hume, T. M., Sherwood, A. M., & Nelson, C. S. (1975). Alluvial sedimentology of the Upper Pleistocene Hinuera Formation, Hamilton Basin, New Zealand. Journal of the Royal Society of New Zealand, 5(4), 421-462.

Ibrahim, K. M. H. I. (2014). "Liquefaction analysis of alluvial soil deposits in Bedsa south west of Cairo." Ain Shams Engineering Journal 5(3): 647-655.

Jolly, R. J., & Lonergan, L. (2002). Mechanisms and controls on the formation of sand intrusions. Journal of the Geological Society, 159(5), 605-617.

Juang, C. H., Yuan, H., Lee, D. H., & Ku, C. S. (2002). Assessing CPT-based methods for liquefaction evaluation with emphasis on the cases from the Chi-Chi, Taiwan, earthquake. Soil Dynamics and Earthquake Engineering, 22(3), 241- 258

Kamp, P. J. J., & Lowe, D. J. (1981). Quaternary stratigraphy, landscape, and soils of the Hamilton Basin. In R. M. Briggs (Ed.), Geological Society of New Zealand Miscellaneous Publication, Vol. 29B (Tour Guides) (pp. 14–28). Hamilton, New Zealand: University of Waikato.

Kleyburg, M. A. (2015). Paleoliquefaction in Late Pleistocene alluvial sediments in the Hauraki and Hamilton basins. Proceedings, 12th Australia New Zealand Conference on Geomechanics (ANZ 2015), 22-25 February, 2015, Wellington, pp. 524-531.

Lai, S. Y., Chang, W. J., & Lin, P. S. (2006). Logistic regression model for evaluating soil liquefaction probability using CPT data. Journal of Geotechnical and Geoenvironmental Engineering, 132(6), 694-704.

Lee, D. H., Ku, C. S., & Yuan, H. (2004). A study of the liquefaction risk potential at Yuanlin, Taiwan. Engineering Geology, 71(1), 97-117.

Lees, J. J., Ballagh, R. H., Orense, R. P., & van Ballegooy, S. (2015). CPT-based analysis of liquefaction and re-liquefaction following the Canterbury earthquake sequence. Soil Dynamics and Earthquake Engineering, 79, 304-314.

Lowe, D.J. 2010. Introduction to the landscapes and soils of the Hamilton Basin. In: Lowe, D.J.; Neall, V.E., Hedley, M; Clothier, B.; Mackay, A. 2010. Guidebook for Pre-conference North Island, New Zealand „Volcanoes to Oceans" field tour (27- 30 July). 19th World Soils Congress, International Union of Soil Sciences, Brisbane. Soil and Earth Sciences Occasional Publication No. 3, Massey University, Palmerston North, pp. 1.24-1.61.

Luo, Q., Wang, C. Y., & Li, X. W. (2013). Experimental Study on Silt Liquefaction Characteristics of Different Fines Content. In Applied Mechanics and Materials (Vol. 353, pp. 2323-2326). Trans Tech Publications.

Manville, V. (2002). Sedimentary and geomorphic responses to ignimbrite emplacement: Readjustment of the Waikato River after the AD 181 Taupo eruption, New Zealand. The Journal of Geology, 110(5), 519-541.

Manville, V., Wilson, C. J. N. (2004). The 26.5 ka Oruanui eruption, New Zealand: a review of the roles of volcanism and climate in the post-eruptive sedimentary response. New Zealand Journal of Geology and Geophysics 47, 525-547.

Manville, V., White, J. D. L., Houghton, B. F. & Wilson, C. J. N. (1999). Paleohydrology and sedimentology of a post-1.8 ka breakout flood from intracaldera Lake Taupo, North Island, New Zealand. Geological Society of America Bulletin 111, 1435-1447.

Maurer, B. W., Green, R. A., & Taylor, O. D. S. (2015). Moving towards an improved index for assessing liquefaction hazard: lessons from historical data. Soils and Foundations, 55(4), 778-787.

Maurya, D. M., Goyal, B., Patidar, A. K., Mulchandani, N., Thakkar, M. G., & Chamyal, L. S. (2006). Ground Penetrating Radar imaging of two large sand blow craters related to the 2001 Bhuj earthquake, Kachchh, Western India. Journal of applied geophysics, 60(2), 142-152.

Mayne, P. W., Christopher, B. R., & DeJong, J. (2001). Manual on Subsurface Investigations. FHWA NHI-01-031. Washington DC, National Highway Institute.

McCraw, J. D. (1967). The surface features and soil patterns of the Hamilton Basin. Earth Science Journal, 1, 59-74.

McCraw, J. D. (2011). The Wandering River. Landforms and geological history of the Hamilton Basin. GSNZ Guidebook 16. Levin, New Zealand: Geoscience Society of New Zealand Guidebook.

Ministry of Business Innovation and Employment. (2017). New Zealand Geotechical Database. New Zealand.

Montenat, C., Barrier, P., & Hibsch, C. (2007). Seismites: An attempt at critical analysis and classification. Sedimentary Geology, 196(1), 5-30.

Moon, V. G., & de Lange, W. P. (2017). Potential shallow seismic sources in the Hamilton Basin: final report for EQC project No. 16/717 (5 July 2017). School of Science, UOW, Hamilton, 41 pp. Retrieved September 6, 2017.

Moretti, M., & Sabato, L. (2007). Recognition of trigger mechanisms for soft-sediment deformation in the Pleistocene lacustrine deposits of the Sant'Arcangelo Basin (Southern Italy): Seismic shock vs. overloading. Sedimentary Geology, 196(1), 31-45.

New Zealand Geotechnical Society INC (2016). Earthquake geotechinical engineering practice. Module 1: Overview of the guidelines.

New Zealand Standard. (2004). Structural Design Actions,. Part 5: Earthquake actions- New Zealand. New Zealand.

Nichols. G. (2009). Rivers and Alluvial Fans. Sedimentology and Stratigraphy, John Wiley & Sons,: 131-138.

NZ Transport Agency (2014). The NZ Transport Agency's Bridge manual. Site Stability, Foundations, Earthworks and Retaining Walls: 6-7.

Obermeier, S. F. (1996). Use of liquefaction-induced features for paleoseismic analysis—an overview of how seismic liquefaction features can be distinguished from other features and how their regional distribution and properties of source sediment can be used to infer the location and strength of Holocene paleo- earthquakes. Engineering Geology, 44(1), 1-76.

Obermeier, S. F. (2009). Using liquefaction-induced and other soft-sediment features for paleoseismic analysis. In McCalpin, J.P (Ed), International Geophysics: Paleoseismology. Amsterdam, US: Academic Press.

Obermeier, S. F., Jacobson, R. B., Smoot, J. P., Weems, R. E., Gohn, G. S., Powars, D. S., & Monroe, J. E. (1990). Earthquake-induced liquefaction features in the coastal setting of South Carolina and in the fluvial setting of the New Madrid seismic zone. United States Geological Survey, Professional Paper;(USA), 1504.

Obermeier, S. F., Olson, S. M., & Green, R. A. (2005). Field occurrences of liquefaction-induced features: a primer for engineering geologic analysis of paleoseismic shaking. Engineering Geology, 76(3–4), 209-234.

Opus (2013). Ruakura Development: Stage 1 Geotechnical Investigation. Tainui Group Holdings Limited Geotechnical Interpretive Report New Zealand.

Opus (2014). Ruakura Interchange, Assessment of Water Effects. Waikato Expressway: Hamilton Section: 10.

Orense, R. P., & Pender, M. J. (2013). Liquefaction characteristics of crushable pumice sand. Paper presented at Proc. of the 18th International Conference on Soil Mechanics and Geotechnical Engineering. Paris, France.

Owen, G., & Moretti, M. (2011). Identifying triggers for liquefaction-induced soft-sediment deformation in sands. Sedimentary Geology, 235(3), 141-147.

Persaud, M., Villamor, P., Berryman, K. R., Ries, W., Cousins, J., Litchfield, N., & Alloway, B. V. (2016). The Kerepehi Fault, Hauraki Rift, North Island, New Zealand: active fault characterisation and hazard. New Zealand Journal of Geology and Geophysics, 59(1), 117-135.

Petch, R., & Marshall, T. (1988). Ground water resources of the Tauranga group sediments in the Hamilton Basin, North Island, New Zealand. Journal of Hydrology (New Zealand), 81-98.

Rydelek, P. A., & Tuttle, M. (2004). Explosive craters and soil liquefaction. Nature, 427(6970), 115-6. Retrieved from http://ezproxy.waikato.ac.nz/login?url=http://search.proquest.com/docview/204545673?accountid=17287.

Rauch, A. F. (1997). EPOLLS: an empirical method for predicting surface displacements due to liquefaction-induced lateral spreading in earthquakes.

Robertson, P. K., & Wride, C. E. (1998). Evaluating cyclic liquefaction potential using the cone penetration test. Canadian Geotechnical Journal, 35(3), 442-459.

Robertson, P. K. (2009). Performance based earthquake design using the CPT. In Proceedings of IS-Tokyo 2009: International Conference on Performance-Based Design in Earthquake Geotechnical Engineering — From Case History to Practice, Tokyo, Japan, 15–18 June 2009. Edited by T. Kokusho, Y. Tsukamoto, and M. Yoshimine. CRC Press/Balkema, Leiden, the Netherlands. pp. 3–20.

Sağlam, S. (2015). A critical assessment on seismic liquefaction potential of fine-grained soils. Natural Hazards, 79(3), 1847-1865.

Schofield, J. (1965). The hinuera formation and associated quaternary events: With an Appendix on Experimental Alluviation. New Zealand journal of geology and geophysics, 8(5), 772-791.

Seed, H. B., & Idriss, I. M. (1971). Simplified procedure for evaluating soil liquefaction potential. Journal of Soil Mechanics & Foundations Div.

Seid-Karbasi, M., & Byrne, P. M. (2007). Seismic liquefaction, lateral spreading, and flow slides: a numerical investigation into void redistribution. Canadian Geotechnical Journal, 44(7), 873-890.

Selby, M. J., & Lowe, D. J. (1992). The middle Waikato Basin and hills. Pp. 233-255 in Soons, J.M.; Selby, M.J. (eds). *Landforms of New Zealand: Second Edition.* Longman Paul, Auckland.

Shen, M., Chen, Q., Zhang, J., Gong, W., & Juang, C. H. (2016). Predicting liquefaction probability based on shear wave velocity: an update. Bulletin of Engineering Geology and the Environment, 1-16

Sherwood, A. M. (1972). Sedimentary structures, texture and paleoenvironment of the Hinuera Formation (Doctoral dissertation, University of Waikato).

Statistics New Zealand. (2013). "2013 Census QuickStats about a place:Hamilton City." Population and dwellings Retrieved 28/06, 2017.

Sonmez, B., & Ulusay, R. (2008). Liquefaction potential at Izmit Bay: comparison of predicted and observed soil liquefaction during the Kocaeli earthquake. Bulletin of Engineering Geology and the Environment, 67(1), 1-9.

Thevanayagam, S. (2000). Liquefaction potential and undrained fragility of silty soils. Proceedings of the 12th World Conference Earthquake Engineering, New Zealand Society of Earthquake Engineering, Wellington, New Zealand.

Tonkin and Taylor. (2013). Liquefaction vulnerability study. Report prepared for:

Earthquake Commission.

Toprak, S., & Holzer, T. L. (2003). Liquefaction potential index: field assessment. Journal of Geotechnical and Geoenvironmental Engineering, 129(4), 315-322.

van Ballegooy, S., Green, R. A., Lees, J., Wentz, F., & Maurer, B. W. (2015). Assessment of various CPT based liquefaction severity index frameworks relative to the Ishihara (1985) H 1–H 2 boundary curves. Soil Dynamics and Earthquake Engineering, 79, 347-364.

Wallace, L. M., Hamling, I., Holden, C., Villamor, P., & Williams, C. (2016). Introduction to NZJGG special issue in honour of John Beavan's scientific contributions.

Webb, T. H., Lilburne, L. R. (2011). Criteria for defining the soil family and soil sibling − the fourth and fifth categories of the New Zealand Soil Classification. *Landcare Research Science Series* No. 3. 38pp.

Williams, P. W. (1991). Tectonic geomorphology, uplift rates and geomorphic response in New Zealand. Catena, 18(5), 439-452.

Youd, T. L., Idriss, I. M., Andrus, R. D., Arango, I., Castro, G., Christian, J. T., ... & Ishihara, K. (2001). Liquefaction resistance of soils: summary report from the 1996 NCEER and 1998 NCEER/NSF workshops on evaluation of liquefaction resistance of soils. Journal of geotechnical and geoenvironmental engineering, 127(10), 817-833.

Youd, T. L., & Perkins, D. M. (1978). Mapping liquefaction-induced ground failure potential. Journal of the Geotechnical Engineering Division, 104(4), 433-446.